

1 Supplementary information

2

3 Paleo-Eskimo genetic legacy across North America

4 Pavel Flegontov, N. Ezgi Altınışık, Piya Changmai, Nadin Rohland, Swapan Mallick, Nicole
5 Adamski, Deborah A. Bolnick, Nasreen Broomandkhoshbacht, Francesca Candilio, Brendan J.
6 Culleton, Olga Flegontova, T. Max Friesen, Choongwon Jeong, Thomas K. Harper, Denise
7 Keating, Douglas J. Kennett, Alexander M. Kim, Thiseas C. Lamnidis, Ann Marie Lawson, Iñigo
8 Olalde, Jonas Oppenheimer, Ben A. Potter, Jennifer Raff, Robert A. Sattler, Pontus Skoglund,
9 Kristin Stewardson, Edward J. Vajda, Sergey Vasilyev, Elizaveta Veselovskaya, M. Geoffrey
10 Hayes, Dennis H. O'Rourke, Johannes Krause, Ron Pinhasi, David Reich, Stephan Schiffels

11

12 CONTENTS

13	Supplementary tables	2
14	SI 1. Description of archaeological sites	4
15	SI 2. Radiocarbon dating	9
16	SI 3. Ancient DNA isolation and sequencing	12
17	SI 4. Principal component analysis and outlier removal	16
18	SI 5. Exhaustive analysis of ancestry streams in small population sets	18
19	SI 6. Haplotype sharing statistics	23
20	SI 7. Admixture inference with <i>GLOBETROTTER</i>	28
21	SI 8. Rare allele sharing statistics	33
22	SI 9. Demographic modeling with <i>Rarecoal</i>	41
23	SI 10. Admixture graph modeling using <i>qpGraph</i>	56
24	SI 11. Additional results on Aleutian population history	67
25	SI 12. Dating admixture events using <i>ALDER</i>	70
26	SI 13. Overview of the Dene-Yeniseian linguistic hypothesis	72
27	Supplementary Discussion	80

28

29 **Supplementary tables**

30

31 **Supplementary Table 1.** Summary of genome-wide data from 48 newly reported ancient
32 individuals.

33 Notes:

34 * based on being a father or son of I5319 at the same site who has a calibrated radiocarbon date

35 ** based on being a 2nd to 3rd degree relative of I5319 at the same site who has a calibrated radiocarbon date

36 *** context from 16 other dates at the same site

37

38 **Supplementary Table 2.** Reservoir-adjusted radiocarbon calibrations and stable isotope
39 data for 46 ancient skeletal samples analyzed in this study. Average calibrated ages (Cal BP,
40 μ) and their 95% confidence intervals are shown (CalBP, 2σ).

41

42 **Supplementary Table 3.** Information on newly genotyped present-day individuals.

43

44 **Supplementary Table 4.** Composition of the genomic and SNP array datasets used in this
45 study. Individual counts correspond to dataset versions after removal of outliers, relatives,
46 and ancient samples with a high percentage of missing data, but prior to a more stringent
47 filtering applied to the datasets used for f_4 -statistics, for *qpWave*, and for *qpAdm* analyses
48 (see the Methods). Meta-populations are abbreviated as follows: Paleo-Eskimos (P-E),
49 Eskimo-Aleut speakers and ancient Neo-Eskimos (E-A), Chukotko-Kamchatkan speakers (C-
50 K), proto-Paleo-Eskimos (PPE, i.e. groups having uncertain position within the C-K/E-A/P-E
51 clade), Na-Dene speakers (mostly Athabaskans, ATH), Northern First Peoples (NAM),
52 Southern First Peoples (SAM), Basal First Peoples (BAM), West Siberians (WSIB), East
53 Siberians (ESIB), Southeast Asians (SEA), Europeans (EUR), Africans (AFR). Shotgun
54 sequencing data were generated in this study for one ancient Aleut individual (I0719 or
55 378620) and one ancient Athabaskan individual (I5319 or MT-1) or taken from three
56 published sources: the Simons Genome Diversity Project (Mallick et al. 2016), Raghavan et
57 al. (2015), and Moreno-Mayar et al. (2018). Two SNP array datasets were used: based on
58 the HumanOrigins array and on Illumina arrays. HumanOrigins data were taken from
59 Mathieson et al. (2015) and Jeong et al. (2019, in press) or generated in this study for
60 Alaskan Iñupiat and West Siberians (Enets, Kets, Nganasans, and Selkups). Illumina data
61 were taken from the following sources: Li et al. 2008, Behar et al. 2010, Rasmussen et al.
62 2010, Fedorova et al. 2013, Raghavan et al. 2014a, 2014b, 2015, Verdu et al. 2014,
63 Kushniarevich et al. 2015. Genome-wide targeted enrichment data were generated in this
64 study using the 1240K SNP panel (Fu et al. 2015) for 48 ancient individuals (11 Aleuts, 3
65 Northern Athabaskans, 21 Neo-Eskimos of the Old Bering Sea culture, one Middle Dorset
66 Paleo-Eskimo, and 12 individuals from the Ust'-Belaya site on the Angara river), and merged
67 with both SNP array datasets. Before the merging step, the following low-coverage samples
68 were removed: 5 ancient Aleuts, 2 Neo-Eskimos (one from the Ekven and another from the
69 Uelen site), and 3 Ust'-Belaya Angara individuals. One ancient Athabaskan sample was
70 removed as a first-degree relative of another sample.

71 Notes:

72 * The Dakelh population was referred to as Athabaskan in Rasmussen et al. (2010) and as
73 'Northern Athabaskan 1' or simply Athabaskan in Raghavan et al. (2015).

74 ** The Caucasian (CAU), Middle Eastern (ME), South Asian (SAS), and Australo-Melanesian
75 (OCE) meta-populations were included in the HumanOrigins dataset, but were not used for
76 most analyses except for *ADMIXTURE*.

77

78 **Supplementary Table 5.** Details of datasets used in this study.

79 Notes:

80 * transitions were removed in this dataset version

81 ** all individuals had missing rates below the threshold, except for the Middle Dorset
82 individual having the missing rate of 0.89-0.90

83 *** rare variants occurring from 2 to 5 times in reference populations (AFR, EUR, SEA, SIB,
84 C-K)

85 ^ listing only segregating sites among the 9 populations analyzed with *Rarecoal*. The total
86 number of sites analyzed is 14,740,571, as in the rare allele sharing analysis

87 ^^ analyzed as 9 meta-populations and 3 ancient genomes mapped on the tree

88

89 **Supplementary Table 6.** Z-scores and site counts for f_4 -statistics ($American_i$, $Half A$, $American_j$;
90 $American_i$, $Half B$, Dai). Statistics were calculated for 6 datasets (HumanOrigins, 1240K,
91 Illumina, with or without transitions), and percentage of significantly positive f_4 -statistics (Z
92 > 3) is shown for each dataset version.

93

94 *References (for Supplementary tables)*

- 95 1000 Genomes Project Consortium. A global reference for human genetic variation. *Nature* **526**, 68–74 (2015).
96 Behar, D. M. *et al.* The genome-wide structure of the Jewish people. *Nature* **466**, 238–242 (2010).
97 Fedorova, S. A. *et al.* Autosomal and uniparental portraits of the native populations of Sakha (Yakutia):
98 implications for the peopling of Northeast Eurasia. *BMC Evol. Biol.* **13**, 127 (2013).
99 Fu, Q. *et al.* An early modern human from Romania with a recent Neanderthal ancestor. *Nature* **524**, 216–219
100 (2015).
101 Jeong, C. *et al.* Characterizing the genetic history of admixture across inner Eurasia. *Nature Ecology and*
102 *Evolution*, in press (2019).
103 Kushniarevich, A. *et al.* Genetic heritage of the Balto-Slavic speaking populations: A synthesis of autosomal,
104 mitochondrial and Y-chromosomal data. *PLoS ONE* **10**, e0135820 (2015).
105 Li, J. Z. *et al.* Worldwide human relationships inferred from genome-wide patterns of variation. *Science* **319**,
106 1100–1104 (2008).
107 Mallick, S. *et al.* The Simons Genome Diversity Project: 300 genomes from 142 diverse populations. *Nature*
108 **538**, 201–206 (2016).
109 Mathieson, I. *et al.* Genome-wide patterns of selection in 230 ancient Eurasians. *Nature* **528**, 499–503 (2015).
110 Moreno-Mayar, J. V. *et al.* Terminal Pleistocene Alaskan genome reveals first founding population of Native
111 Americans. *Nature* **553**, 203–207 (2018).
112 Raghavan, M. *et al.* The genetic prehistory of the New World Arctic. *Science* **345**, 1255832 (2014a).
113 Raghavan, M. *et al.* Upper Palaeolithic Siberian genome reveals dual ancestry of Native Americans. *Nature* **505**,
114 87–91 (2014b).
115 Raghavan, M. *et al.* Genomic evidence for the Pleistocene and recent population history of Native Americans.
116 *Science* **349**, 1–20 (2015).
117 Rasmussen, M. *et al.* Ancient human genome sequence of an extinct Palaeo-Eskimo. *Nature* **463**, 757–762
118 (2010).
119 Verdu, P. *et al.* Patterns of admixture and population structure in native populations of northwest North
120 America. *PLoS Genet.* **10**, e1004530 (2014).
121

122 **Supplementary Information section 1**

123 **Description of archaeological sites**

124

125 **1.1 Ancient Eastern Aleutian Islanders**

126 The skeletal samples from the eastern Aleutians were selected from curated collections at
127 the Smithsonian Institution by M. Geoffrey Hayes, who was gloved, sleeved, and masked at
128 all times to prevent self-contamination of the samples. All samples were small, fragmentary
129 ribs free of pathological lesions and were immediately placed in sterile ziplock bags (Hayes
130 2002) for transport to the lab for analysis.

131 The remains were excavated or collected by Aleš Hrdlička in the late 1930s. The
132 geographic locations of the material are burial caves on Shiprock Island (northeast of Umnak
133 Island), and Kagamil, one of the sacred Islands of the Four Mountains, immediately west of
134 Umnak (Extended Data Table 1). The third site providing samples for molecular analysis is
135 Chaluka, a deep midden site on Umnak adjacent to the contemporary village of Nikolski.

136 For the present study, the samples available for analysis included six individuals from
137 Kagamil, with three osteologically determined to be female, one as probably female (later
138 identified genetically as a male), and two as male. As reported by Brenner Coltrain et al.
139 (2006), these six Kagamil samples exhibit a calibrated age range of 479 – 596 years before
140 present (calBP). The single individual from Shiprock was identified as a male with an age of
141 749 calBP. Finally, four individuals from the Chaluka site at Nikolski (three males and one
142 female according to genetic data) exhibited an age range of 702 – 2,305 calBP. In this study,
143 the dates were recalibrated (Supplementary Table 1 and 2) using an updated marine
144 reservoir correction as described in Supplementary Information section 2.

145 Based on cranial metrics, Hrdlička (1945) postulated that the mummified remains
146 from the burial caves on Kagamil and Shiprock represented immediate ancestors of modern
147 Aleut people who had replaced an earlier population of ‘Pre-’ or ‘Paleo-Aleuts’ about a
148 millennium ago. He viewed the remains at Chaluka as representatives of this earlier
149 occupation of the Islands.

150 Although Hrdlička (1945) considered the ‘Paleo-Aleuts’ to be older than ‘Neo-Aleuts’,
151 with only the latter ancestral to modern Aleut people following a replacement event around
152 1,000 years ago, direct dating of the ancient remains (Brenner Coltrain, et al. 2006) clearly
153 established that while all individuals recovered from Chaluka were ‘Paleo-Aleuts’ by
154 Hrdlička’s cranial metric criteria, they coexisted with ‘Neo-Aleuts’ for several hundred years
155 following the appearance of the latter at about 1,000 calBP. Thus, the strict replacement
156 model of Hrdlička’s was untenable and the prehistory of peoples of the Aleutian chain, at
157 least in the east, proved to be more complex than previously thought (Smith et al. 2009).

158 Molecular characterization of the ancient Aleut individuals was conducted following
159 consultations with and permissions from local communities and authorities, including the
160 Chaluka Corporation, the Aleut Corporation, and the Aleutians Pribilof Islands Association.

161

162 *References (for this section)*

- 163 Brenner Coltrain, J. B., Hayes, M.G. & O’Rourke D.H. Hrdlička’s Aleutian population-replacement hypothesis. A
164 radiometric evaluation. *Curr. Anthropol.* **47**, 537–548 (2006).
165 Hayes, M. G. Paleogenetic assessments of human migration and population replacement in North American

166 Arctic prehistory. Doctoral Dissertation, University of Utah (2002).
167 Hrdlička, A. *The Aleutian and Commander Islands and their inhabitants*. Philadelphia: Wistar Institute of
168 Anatomy and Biology (1945).
169 Smith, S. *et al.* Inferring population continuity versus replacement with aDNA: A cautionary tale from the
170 Aleutian Islands. *Hum. Biol.* **81**, 19–38 (2009).

171

172 **1.2 Ancient Northern Athabaskans**

173 The ancient Athabaskan population in this study is derived from three individuals found
174 intermingled in a non-burial context in the riparian zone of the upper Kuskokwim river. Tochak
175 is the Athabaskan place-name for the area around the modern mixed ethnic community of
176 McGrath, southwest Interior Alaska. Known as the Tochak McGrath Discovery, the three
177 individuals were buried in overbank sediments that also feature unassociated buried organic
178 bands with terrestrial and aquatic fauna, hearth matrix, flaked stone and bone artifacts. The
179 human remains could not be linked stratigraphically to the surrounding cultural occupation
180 features. We genetically determined the three individuals to be successive generations of
181 consanguineous relatives: 30-40 year-old male (MT-1), 19-20 year-old male (MT-2), and 2-3
182 year old female (MT-3) (Extended Data Table 1). The genetic analysis indicates a father-son
183 relationship for MT-1 / MT-2, a grandfather-granddaughter relationship for MT-1 / MT-3, and
184 an uncle-niece relationship for MT-2 / MT-3. To reduce correlation in the genetic sequences,
185 only individuals MT-1 and MT-3 were selected for downstream genetic analyses. Nearly
186 complete skeletal representation and articulation pattern of all three individuals in massive
187 sand deposits suggest that these individuals died together of exposure and were buried by
188 overbank sedimentation.

189 Soon after the time of discovery, a tripartite agreement was reached for scientific
190 analysis between the McGrath Native Village Council (the federal recognized Alaska Native
191 tribe), MTNT Ltd. (consortium of Alaska Native Claims Settlement Act village corporations) and
192 Tanana Chiefs Conference (the regional non-profit consortium of 37 federally recognized
193 Athabaskan Tribes and Alaskan Native associations in the Yukon and Kuskokwim river basins in
194 Interior Alaska). R.A. Sattler has facilitated community-based research, collaboration with
195 academic institutions, tribal consultation, public outreach and further data recovery at the
196 Tochak discovery locale (Sattler *et al.* 2013).

197

198 *References (for this section)*

199 Sattler, R. A. *et al.* Tochak McGrath discovery: Precontact human remains in the Upper Kuskokwim River region of
200 interior Alaska. *Alaska J. Anthropol.* **11**, 185–186 (2013).

201

202 **1.3 Early Neo-Eskimos (Old Bering Sea culture)**

203 Four and 17 individuals buried at neighboring Uelen and Ekven cemeteries, respectively,
204 were sequenced in this study (Extended Data Table 1). These cemeteries of the Old Bering
205 Sea (Drevneberingomorskaya) culture are located on the Chukotka Peninsula. The Uelen
206 burial ground is separated by only 170 m from the present-day settlement Uelen on the
207 coast of the Chukchi Sea, and the Ekven burial ground is about 40 km away. The site was
208 discovered in 1955 by D. A. Sergeev, and its further excavation was carried out by the
209 Institute of Ethnography of the Academy of Sciences of the USSR (details are reported in
210 Levin & Sergeev 1964, Dikov 1967, Arutyunov & Sergeev 1969).

211 Both sites represent burial grounds of the Old Bering Sea culture of sea mammal
212 hunters and fishers of the Arctic zone of Siberia and North America. This culture is related to
213 others in the Bering Straits region that partially overlap in time (1,700-1,000 calBP): Okvik,
214 Punuk, and Birnik, collectively (with the later related Thule tradition) termed the Northern
215 Maritime tradition (Collins 1964). The Old Bering Sea stage is the earliest in development of
216 this cultural tradition and is dated to between ~2,300-1,300 calBP (Arutyunov and Sergeev
217 1975, Gerlach and Mason 1992) with evidence for continuity with the later Okvik, Punuk,
218 and Birnik cultures (Arutyunov and Sergeev 1969, Gerlach and Mason 1992, Bronshtein et
219 al. 2016, Mason 2016).

220 Mortuary behavior at the Ekven burial ground (189 burials) is more variable than
221 that in other cemeteries of this culture. The buried were laid not only in an extended
222 position, but also in a curled position, and there are numerous paired and group burials.
223 Human remains from the Uelen and Ekven burial grounds provide an important source of
224 data for the bioanthropology of Old Bering Sea culture individuals (Levin & Sergeev 1964,
225 Debets 1975). Odontological materials from the Ekven burial ground, and to a lesser extent
226 from Uelen, are very similar to those of present-day Eskimos (especially from Alaska) (Zubov
227 1969).

228 According to all cultural traits studied, the Ekven and Uelen ancient populations
229 were extremely similar. Which is quite natural, since the distance between the two sites
230 does not exceed 35-40 kilometers. Nevertheless, even with such a close neighborhood
231 between the two burial grounds, there are some differences.

232 This difference is observed, for example, in the ratio of the "x" and "y" harpoon tips.
233 According to the classification principles by H. Collins (Collins 1964), if the tip is equipped
234 with blades located in the same plane with a hole for the line, this is expressed by the letter
235 "x", and if the planes are perpendicular, then the letter "y" is used. In Uelen, "x" harpoon
236 tips prevail; in Ekven, on the contrary, the "y" series is more numerous. It was noted that
237 the type "x" has advantages over the supposedly earlier type "y" (Arutyunov and Sergeev,
238 1969).

239 Excavations in 1962-1967 at the Ekven cemetery, along with previously known
240 burials in an elongated position, revealed a new type of burial that had not previously been
241 found in ancient Eskimo burial grounds, namely, the appearance of skeletons in a crooked
242 position. A considerable number of paired and collective burials was found at the Ekven
243 cemetery. Some burials were disturbed by later graves (for example, burial 21). In some
244 tombs scattered bones of other individuals were found in addition to the main skeleton.
245 Presumably, such burials were made on the site of older burials, and the old skeletons were
246 destroyed and fell with a backfill into new burials.

247

248 *References (for this section)*

249 Arutyunov, S. A. & Sergeev, D. A. *Drevniye kul'tury aziaskih eskimosov: uelenskiy mogil'nik* [Ancient cultures of
250 *Asian Eskimos: the Uelen burial ground*]. Moscow: Nauka (1969).

251 Arutyunov, S. A. & Sergeev, D. A. *Problemy etnicheskoy istorii Beringomorya: ekvenskiy mogil'nik* [Problems of
252 *the ethnic history of the Bering Sea region: the Ekven burial ground*]. Moscow: Nauka (1975).

253 Bronshtein, M. M., Dneprovsky, K. A. & Savintsky, A. B. Ancient Eskimo cultures of Chukotka. *The Oxford*
254 *Handbook of the Prehistoric Arctic*, ed. Friesen, T. M., Mason, O. K. New York: Oxford University Press.
255 469-488 (2016).

256 Collins, H. B. The Arctic and Subarctic. *Prehistoric Man in the New World*, ed. Jennings, J. D. & Norbeck, E.
257 Chicago: University of Chicago Press. 85-114 (1964).

258 Debets, G. F. Paleontologicheskiye materialy iz drevneberingomorskih mogil'nikov Uelen i Ekven

259 [Paleoanthropological materials from the Old Bering Sea burial grounds Uelen and Ekven]. *Problemy*
260 *etnicheskoy istorii Beringomorya: ekvenskiy mogil'nik* [Problems of the ethnic history of the Bering Sea
261 *region: the Ekven burial ground*], ed. Arutyunov, S. A. & Sergeyev, D. A. Moscow: Nauka. 198 (1975).
262 Dikov, N. N. Uelenskiy mogil'nik po dannym raskopok 1956, 1958 i 1963 gg [The Uelen burial ground according
263 to excavations in 1956, 1958 and 1963]. *Istoriya i kul'tura narodov Severa Dal'nego Vostoka* [History and
264 *culture of the peoples of the northern Far East*], *Trudy SVKNII SO AN SSSR, vol. 17*. Moscow: Nauka (1967).
265 Gerlach, C. & Mason, O. K. Calibrated radiocarbon dates and cultural interaction in the Western Arctic. *Arctic*
266 *Anthropol.* **29**, 54–81 (1992).
267 Levin, M. G. & Sergeyev, D. A. Drevniye mogil'niki Chukotki i nekotorye aspekty eskimoskoy problemy
268 [Ancient burial grounds in Chukotka and some aspects of the Eskimo problem]. *Doklady na VII*
269 *Mezhdunarodnom kongresse antropologicheskikh i etnograficheskikh nauk*. Moscow (1964).
270 Mason, O. K. The Old Bering Sea florescence about Bering Strait. *The Oxford Handbook of the Prehistoric Arctic*,
271 ed. Friesen, T. M., Mason, O. K. New York: Oxford University Press. 417–442 (2016).
272 Zubov, A. A. Antropologicheskii analiz cherepykh seriy iz Ekvenskogo i Uelenskogo mogil'nikov
273 [Anthropological analysis of cranial series from the Ekven and Uelen burial grounds]. *Drevniye kul'tury*
274 *aziatskikh eskimosov: uelenskiy mogil'nik* [Ancient cultures of Asian Eskimos: the Uelen burial ground], ed.
275 Arutyunov, S. A. & Sergeyev, D. A. Moscow: Nauka (1969).

276

277 **1.4 The Ust'-Belaya site on the Angara river**

278 The Ust'-Belaya burial ground (Ust-Belaya II - Shumilikha) is located on the right bank of the
279 Belaya River at the confluence with the Angara River. This is burial ground is unique not only
280 for the Angara basin and the Baikal region, but also for Eastern Siberia because of burials in
281 a sitting position. Separate burials of such a type and small clusters of them are found
282 throughout Eastern Siberia, particularly in Transbaikalia and Mongolia, but such a large
283 necropolis has not been found anywhere. In addition, in an eroded floodplain burials of
284 another type were found: lying, in birch bark, and with partial cremation (Gerasimova
285 1981).

286

287 *References (for this section)*

288 Gerasimova, M. M. Cherepa iz II Ust'-Bel'skogo mogil'nika (Shumilikha) [Skulls from Ust'-Belaya II (Shumilikha)
289 burial ground]. *Bronzovy vek Priangarya* [The Bronze Age in the Angara basin]. Irkutsk (1981).

290

291 **1.5 The Dorset Period of the Paleo-Eskimo tradition**

292 The Dorset period of the Paleo-Inuit (Paleo-Eskimo) tradition in the Eastern North American
293 Arctic is represented by a sample (I10427, NiNg-1) from the Buchanan site near Cambridge Bay,
294 Victoria Island, Nunavut, Canada. Buchanan was originally excavated by Taylor (1967);
295 renewed excavation by Friesen in 2007 yielded the sample described here. It is an adult left
296 lower 3rd molar with heavy wear. This tooth was recovered from a depth of 15 cm below
297 surface level in a warm-season dwelling. Artifacts from this tent ring are consistent with the
298 Middle Dorset period, with no evidence of mixing or intrusive artifacts. The seven diagnostic
299 harpoon heads are all of the Middle Dorset Frobisher Grooved type. The sample was previously
300 subjected to shallow shotgun sequencing (0.004x coverage) and radiocarbon dating (Raghavan
301 et al. 2014). The radiocarbon date has been recalibrated in this study to 1,900 – 1,610 calBP
302 using a different marine reservoir correction (see section 2). The previously published
303 calibrated date was older: 2,182 – 2,123 calBP (Raghavan et al. 2014).

304 The Middle Dorset specimen was recovered as part of a collaborative project initiated
305 by the Kitikmeot Heritage Society (KHS) of Cambridge Bay, Nunavut. Sampling of the specimen
306 for DNA, AMS dating, and isotopic analysis was discussed with the KHS before the research

307 occurred, and specific permission for this analysis was received from the Nunavut Government
308 via a destructive analysis request. This latter permission involved consultation with the Inuit
309 Heritage Trust, a Nunavut-wide body dedicated to the preservation, enrichment, and
310 protection of Inuit Cultural Heritage.

311

312 *References (for this section)*

313 Raghavan, M. *et al.* The genetic prehistory of the New World Arctic. *Science* **345**, 1255832 (2014).

314 Taylor, W. E. Summary of archaeological field work on Banks and Victoria Islands, Arctic Canada, 1965. *Arctic*
315 *Anth.* **4**, 221–243 (1967).

316

317 **1.6 Alaskan Iñupiat**

318 Iñupiat samples in this study were collected, along with genealogical records and participant
319 surveys, by M. Geoffrey Hayes and Jennifer A. Raff from the communities of Atqasuk,
320 Anaktuvuk Pass, Utqiagvik (formerly known as Barrow), Kaktovik, Nuiqsut, Point Hope, Point
321 Lay, and Wainwright between 2008-2010 as described in Raff *et al.* (2015). This project was
322 begun at the suggestion of an Elder in Utqiagvik to complement ancient DNA work on burial
323 populations in the region, and was approved by Northwestern University's Institutional
324 Review Board, after consultation with the Ukpeagvik Iñupiat Corporation, the Native Village
325 of Barrow, and Senior Advisory Council of Barrow (Elders). Of the 181 samples collected, 35
326 individuals who consented to have their DNA used for ancestry research were selected for
327 inclusion in this study to represent a diversity of mitochondrial haplogroups and geographic
328 origins (reported in Raff *et al.* 2015) and to represent both sexes in as close to equal
329 proportions as possible. During the outlier removal procedure described in the Methods
330 section, 20 individuals with minimal admixture from outside populations were selected for
331 downstream analyses.

332

333 *References (for this section)*

334 Raff, J. A. *et al.* Mitochondrial diversity of Iñupiat people from the Alaskan North Slope provides evidence for the
335 origins of the Paleo- and Neo-Eskimo peoples. *Am. J. Phys. Anthropol.* **157**, 603–614 (2015).

336

337 **Supplementary Information section 2**

338 **Radiocarbon dating**

339

340 We report 11 new direct AMS ^{14}C bone dates from the Penn State Accelerator Mass
341 Spectrometer laboratory (PSUAMS) and recalibrate 13 previously published radiocarbon
342 dates from three other AMS radiocarbon laboratories (Arizona [AA]: 11; Beta Analytic
343 [Beta]: 1; UC Irvine [UCIAMS]: 1; see Supplementary Table 2 and Fig. S2.1). Bone preparation
344 and quality control methods for the AA and Beta samples are described elsewhere (Brenner
345 Coltrain et al. 2006, Halffman et al. 2015).

346

347 **2.1 Old Bering Sea and Ust'-Belaya Angara samples**

348 At PSUAMS and UCIAMS, bone collagen for ^{14}C and stable isotope analyses and was
349 extracted and purified using a modified Longin method with ultrafiltration (Kennett et al.
350 2017). Bones were initially cleaned of adhering sediment and the exposed surfaces were
351 removed with an X-acto blade. Samples (200–400 mg) were demineralized for 24–36 h in
352 0.5N HCl at 5 °C followed by a brief (<1 h) alkali bath in 0.1N NaOH at room temperature to
353 remove humates. The residue was rinsed to neutrality in multiple changes of Nanopure H_2O ,
354 and then gelatinized for 12 h at 60 °C in 0.01N HCl. The resulting gelatin was lyophilized and
355 weighed to determine percent yield as a first evaluation of the degree of bone collagen
356 preservation. Rehydrated gelatin solution was pipetted into pre-cleaned Centriprep
357 (McClure et al. 2010) ultrafilters (retaining 430 kDa molecular weight gelatin) and
358 centrifuged 3 times for 20 min, diluted with Nanopure H_2O and centrifuged 3 more times for
359 20 min to desalt the solution. Carbon and nitrogen concentrations and stable isotope ratios
360 were measured at the Yale Analytical and Stable Isotope Center with a Costech elemental
361 analyzer (ECS 4010) and Thermo DeltaPlus analyzer. Sample quality was evaluated by %
362 crude gelatin yield, %C, %N and C/N ratios before AMS ^{14}C dating. C/N ratios for all 11
363 samples fell between 3.14 and 3.32, indicating good collagen preservation (Van Klinken
364 1999).

365 Collagen samples (~2.1 mg) were combusted for 3 h at 900 °C in vacuum-sealed
366 quartz tubes with CuO and Ag wires. Sample CO_2 was reduced to graphite at 550 °C using H_2
367 and a Fe catalyst, with reaction water drawn off with $\text{Mg}(\text{ClO}_4)_2$ (Santos et al. 2004).
368 Graphite samples were pressed into targets in Al cathodes and loaded on the target wheel
369 for AMS analysis. The ^{14}C ages were corrected for mass-dependent fractionation with
370 measured $\delta^{13}\text{C}$ values (Stuiver and Polach 1977) and compared with samples of Pleistocene
371 whale bone (backgrounds, 48,000 ^{14}C BP), late Holocene bison bone (~1,850 ^{14}C BP), late AD
372 1800s cow bone and OX-2 oxalic acid standards for calibration.

373

374 **2.2 Northern Athabaskan (Tochak McGrath) samples**

375 Collagen removed from the femur of MT-1 (I5319; the eldest individual) yielded a radiocarbon
376 age of 1170 ± 30 BP (AMS lab code Beta-337194). This age estimate provides an older limiting
377 age on the time of death of the Tochak family. Isotopic analysis has determined relatively high
378 carbon and nitrogen values on all three individuals that suggest a strong marine component to
379 their diet (i.e., anadromous salmon) (Halffman et al. 2015).

380 The isotopic values suggest that the radiocarbon age on human collagen may over-

381 estimate the actual time of death, and the date was calibrated as described below. Given the
382 direct age on MT-1 as a maximum limiting age, charcoal dates from matrix of two spatially
383 separate hearths at the Tochak site provide a younger limiting age of around 350 years before
384 present: 320 ± 30 BP (465-300 calBP; AMS lab code Beta-333837) and 380 ± 30 BP (505-320
385 calBP; AMS lab code Beta-343499).

386

387 **2.3 Middle Dorset sample**

388 The Middle Dorset tooth from the Buchanan site yielded a direct AMS date of $2,325 \pm 15$ BP
389 (UCIAMS 86237). When assuming 90% marine contribution to diet, and using the
390 geographically closest ΔR of 232 ± 30 , from Bathurst Inlet (Coulthard et al 2010), the date
391 calibrates to 1,900-1,610 calBP (95.4% confidence). Two radiocarbon dates have also been
392 obtained for caribou bone from the same feature: $1,790 \pm 15$ BP (1,809-1,627 calBP, 95.4%
393 confidence, UCIAMS 76625), and $1,725 \pm 15$ BP (1,696-1,568 calBP, 95.4% confidence,
394 UCIAMS 76626). These radiocarbon dates are consistent with the direct tooth date, and
395 with other Middle Dorset dates from the region (Friesen 2016).

396

397 **2.4 Calibration of radiocarbon dates**

398 All ^{14}C ages were calibrated with OxCal version 4.2.3 (Bronk Ramsey 2013) using mixtures
399 of the northern hemisphere terrestrial calibration curve (IntCal13) and the marine curve
400 (Marine13; Reimer et al. 2013). Marine contribution was estimated using stable carbon and
401 nitrogen isotopes and was assigned values of 0% for far inland contexts (Ust'-Belaya
402 Angara), 50% for inland samples influenced by anadromous salmon (Tochak McGrath), and
403 90% for coastal samples (all other sites). The geographical context of sites is reflected in the
404 reported $\delta^{15}\text{N}$ measurements, which range from 11.0 to 15.7‰ (Ust'-Belaya), 15.2‰
405 (Tochak McGrath), and 18.3 to 22.3‰ (coastal sites).

406 For dates from Alaska and Chukotka we used a ΔR of 455 ± 81 (Misarti and Maschner
407 2015), which is based on an average for this region (Reimer and Reimer 2001). For a single
408 date from Victoria Island in Nunavut (UCIAMS-86237) the nearest ΔR value (Bathurst Inlet,
409 232 ± 30) was used (Coulthard et al. 2010). The reservoir-corrected dates are presented in
410 Supplementary Table 2 and Fig. S2.1.

411

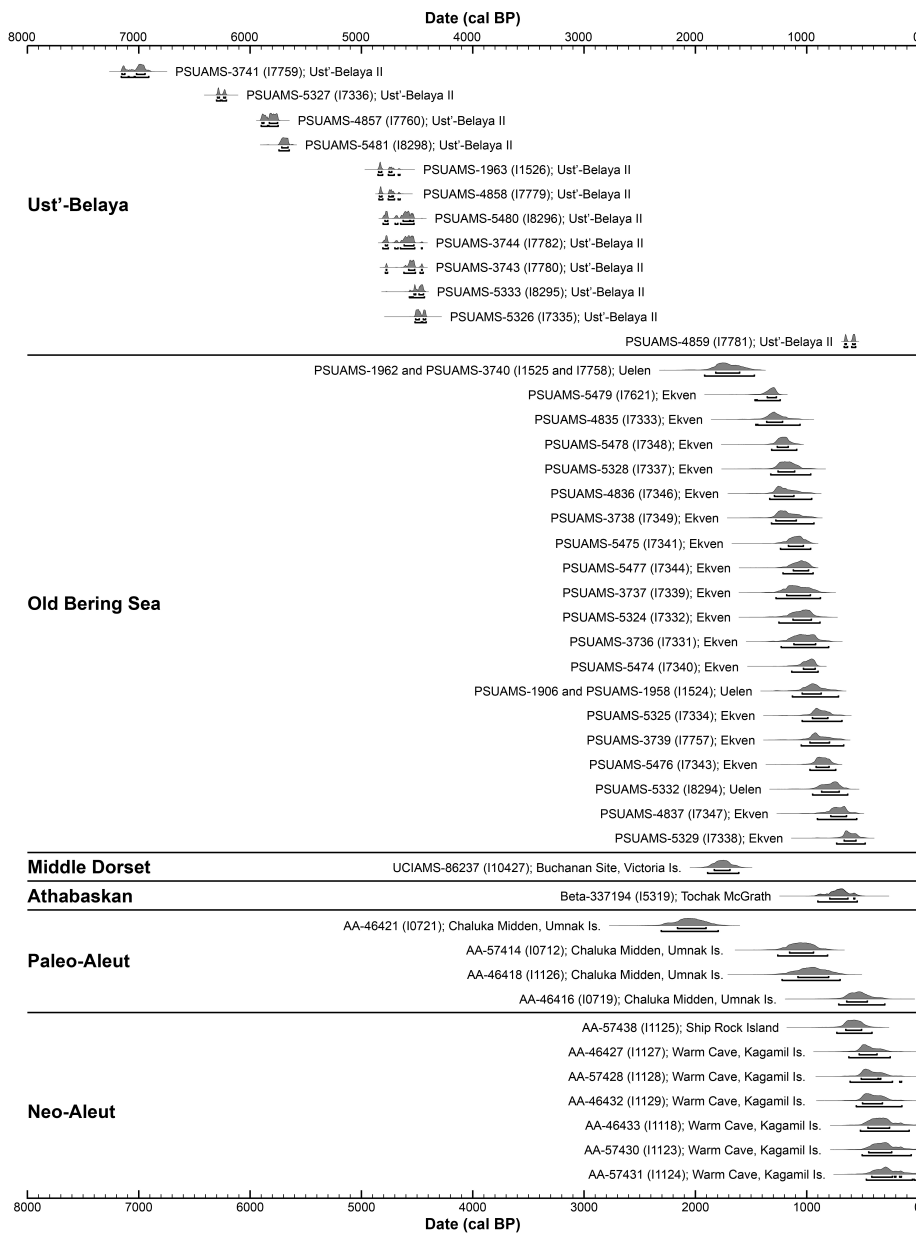
412 *References (for this section)*

- 413 Brenner Coltrain, J., et al. Hrdlička's Aleutian population-replacement hypothesis. A radiometric evaluation.
414 *Curr. Anthropol.* **47**, 537–548 (2006).
- 415 Bronk Ramsey, C. OxCal 4.23 Online Manual https://c14.arch.ox.ac.uk/oxcalhelp/hlp_contents.html (2013).
- 416 Byers D. A. et al. 2011. Stable isotope chemistry, population histories and Late Prehistoric subsistence change
417 in the Aleutian Islands. *J. Archaeol. Sci.* **38**, 183–196 (2011).
- 418 Coulthard, R. D. et al. New marine ΔR values for Arctic Canada. *Quat. Geochronol.* **5**, 419–434 (2010).
- 419 Friesen, T. M. Middle Dorset communal structures on Victoria Island. *Open Arch.* **2**, 194–208 (2016).
- 420 Kennett, D. J. et al. Archaeogenomic evidence reveals prehistoric matrilineal dynasty. *Nat. Commun.* **8**, 14115
421 (2017).
- 422 Halfman, C. M., Sattler, R. & Clark, J. L. Bone collagen stable isotope analysis of three late Holocene humans from
423 Interior Alaska. *Am. J. Phys. Anthropol.* **156** (S60), 157 (2015).
- 424 McClure, S. B., García Puchol, O. & Culleton, B. J. AMS Dating of Human Bone from Cova De La Pastora: New
425 Evidence of Ritual Continuity in the Prehistory of Eastern Spain. *Radiocarbon* **52**, 25–32 (2010).
- 426 Misarti, N. & Maschner, H. D. G. The Paleo-Aleut to Neo-Aleut transition revisited. *J. Anthropol. Archaeol.* **37**,
427 67–84 (2015).

428 Raghavan, M. *et al.* The genetic prehistory of the New World Arctic. *Science* **345**, 1255832 (2014).
 429 Reimer, P. J. *et al.* Intcal13 and Marine13 radiocarbon age calibration curves 0-50,000 years Cal Bp.
 430 *Radiocarbon* **55**, 1869–1887 (2013).
 431 Reimer, P. J. & Reimer, R. W. A marine reservoir correction database and on-line interface. *Radiocarbon* **43**,
 432 461–463 (2001).
 433 Santos, G. M. *et al.* Magnesium perchlorate as an alternative water trap in AMS graphite sample preparation:
 434 A report on sample preparation at KCCAMS at the University of California, Irvine. *Radiocarbon* **46**, 165–
 435 173 (2004).
 436 Stuiver, M. & Polach, H. A. Reporting of C-14 Data-Discussion. *Radiocarbon* **19**, 355–363 (1977).
 437 Van Klinken, G. J. Bone collagen quality indicators for palaeodietary and radiocarbon measurements. *J.*
 438 *Archaeol. Sci.* **26**, 687–695 (1999).

439

440 **Fig. S2.1.** Plot of probability distributions for new AMS ¹⁴C dates (PSUAMS results) and previously published
 441 regional radiocarbon data (Brenner Coltrain *et al.* 2006; Byers *et al.* 2011; Halffman *et al.* 2015; Raghavan *et al.*
 442 2014) with marine reservoir correction. Alaska and Chukotka $\Delta R = 455 \pm 81$ (Misarti and Maschner 2015);
 443 Victoria Island $\Delta R = 232 \pm 30$ (Coulthard *et al.* 2010). No marine reservoir correction was applied to the Ust'-
 444 Belaya Angara samples located in the Baikal region. The brackets below the calibrated distributions are the
 445 68.2% (upper bracket) and 95.4% (lower bracket) credible intervals of the calibrated range.



446

447 **Supplementary Information section 3**

448 **Ancient DNA isolation and sequencing**

449

450 **3.1 Ancient DNA isolation**

451 Powder from skeletal remains was prepared in dedicated clean room facilities either at
452 University College Dublin in Dublin Ireland (the samples from Siberia), or Harvard Medical
453 School in Boston USA (the samples from North America). All subsequent DNA extraction,
454 library preparation, target capture enrichment and Illumina sequencing was performed at
455 Harvard Medical School in Boston (USA) (Table S3.1).

456 For tooth samples, after surface cleaning by fine sandblasting, the dentine area of roots
457 and crowns was milled to obtain fine powder. For petrous samples or the cochlear region of
458 the inner ear was extracted by sandblasting and subsequently milled into fine powder,
459 respectively. In the case of the rib bones from the Aleutian Islanders, bones were cleaned at
460 the surface with a sanding disk and fine powder was collected for DNA extraction by drilling
461 into the cleaned area.

462 About 75 mg (+/- 9 mg) of powder was then used for DNA extraction following an
463 established protocol by Dabney *et al.* (2013), with modifications as in Korlević *et al.* (2015);
464 that is, the MinElute/Zymo funnel assembly was replaced by the funnel-column assembly from
465 the Roche High Pure Viral Nucleic Acid Large Volume Kit. The final volume of DNA extract was
466 90 µl.

467 A double-stranded barcoded Illumina library was prepared for each sample using the
468 'partial UDG treatment' protocol (Rohland *et al.* 2015). For 3 libraries the settings were
469 identical to the original publication, and for the remaining 55 libraries updated setting were
470 used (see notes to Table S3.1).

471 After cleanup of the amplified libraries, we performed a screening step: a capture
472 enrichment targeting the mitochondrial genome and additional nuclear loci (manuscript in
473 preparation) following the procedure described in Maricic *et al.* (2010). After unique
474 identification indices were added to each enriched library, we then sequenced the enrichment
475 product together with the original libraries (also after addition of a unique index pair to each
476 library) – shotgun, on an Illumina NextSeq 500 instrument for 2x 76 cycles and 2x 7cycles.

477 Nuclear data were produced by enriching the original short libraries for 1.24 million
478 SNP loci following the protocol by Fu *et al.* 2015 (SNP information in Haak *et al.* 2015,
479 Mathieson *et al.* 2015). For 3 libraries, enrichment reactions were performed on two separate
480 bait pools with 390 thousand and 840 thousand targeted SNPs each. For the rest of the
481 libraries, the two arrays were combined into a single pool targeting 1.24 million SNPs.
482 Sequencing was performed on an Illumina NextSeq 500 instrument for 2x 76 cycles and 2x
483 7cycles.

484 Samples I0719 (an ancient Aleutian Islander) and I5319 (an ancient Athabaskan) were
485 both shotgun sequenced on a NextSeq 500 instrument for 2x76 cycles.

486

487 *References (for this section)*

488 Dabney, J. *et al.* Complete mitochondrial genome sequence of a Middle Pleistocene cave bear reconstructed from
489 ultrashort DNA fragments. *Proc. Natl. Acad. Sci. U. S. A.* **110**, 15758–15763 (2013).
490 Fu, Q. An early modern human from Romania with a recent Neanderthal ancestor. *Nature* **524**, 216–219 (2015).

491 Haak, W. *et al.* Massive migration from the steppe was a source for Indo-European languages in Europe. *Nature*
 492 **522**, 207–211 (2015).
 493 Korlević, P. *et al.* Reducing microbial and human contamination in DNA extractions from ancient bones and teeth.
 494 *Biotechniques* **59**, 87–93 (2015).
 495 Maricic, T., Whitten, M. & Pääbo, S. Multiplexed DNA sequence capture of mitochondrial genomes using PCR
 496 products. *PLoS One* **5**, e14004 (2010).
 497 Mathieson, I. *et al.* Genome-wide patterns of selection in 230 ancient Eurasians. *Nature* **528**, 499–503 (2015).
 498 Rohland, N. *et al.* Partial uracil-DNA-glycosylase treatment for screening of ancient DNA. *Philos. Trans. R. Soc.*
 499 *Lond. B Biol. Sci.* **370**, 20130624 (2015).

500

501 **Table S3.1.** DNA extraction, library preparation and nuclear targeted enrichment. For most individuals, one library
 502 per individuals was prepared and we here use the individual ID to identify the library as well.

503 ^a Dabney *et al.* 2013 with the addition of the funnel-column assembly from the Roche kit as in Korlević *et al.*
 504 (2015), elution in 2x 45 µl.

505 ^b Dabney *et al.* 2013 using a smaller portion of lysate with a silica bead cleanup instead of silica based columns,
 506 elution in 2x 15 µl.

507 ¹ Rohland *et al.* (2015) with the following modifications: 1) the elution volume after the MinElute cleanup of the
 508 ligation reaction was reduced from 20 µl to 16 µl; 2) the Fill-in reaction volume was reduced from 40 µl to 25 µl; 3)
 509 the ThermoPol buffer was replaced by the Isothermal amplification buffer; 4) *Bst* polymerase, large fragment
 510 (New England Biolabs), was replaced by *Bst* 2.0 Polymerase, large fragment (New England Biolabs); 5) PCR volume
 511 was reduced from 400 µl to 100 µl.

512 ² Rohland *et al.* (2015) with the following modifications: 1) the elution volume after the ligation reaction cleanup
 513 was reduced from 20 µl to 16 µl; 2) the Fill-in reaction volume was reduced from 40 µl to 25 µl; 3) the ThermoPol
 514 buffer was replaced by the Isothermal amplification buffer; 4) *Bst* polymerase, large fragment (New England
 515 Biolabs), was replaced by *Bst* 2.0 Polymerase, large fragment (New England Biolabs); 5) PCR volume was reduced
 516 from 400 µl to 100 µl; 5) the MinElute column cleanups were replaced with silica bead cleanups.

517

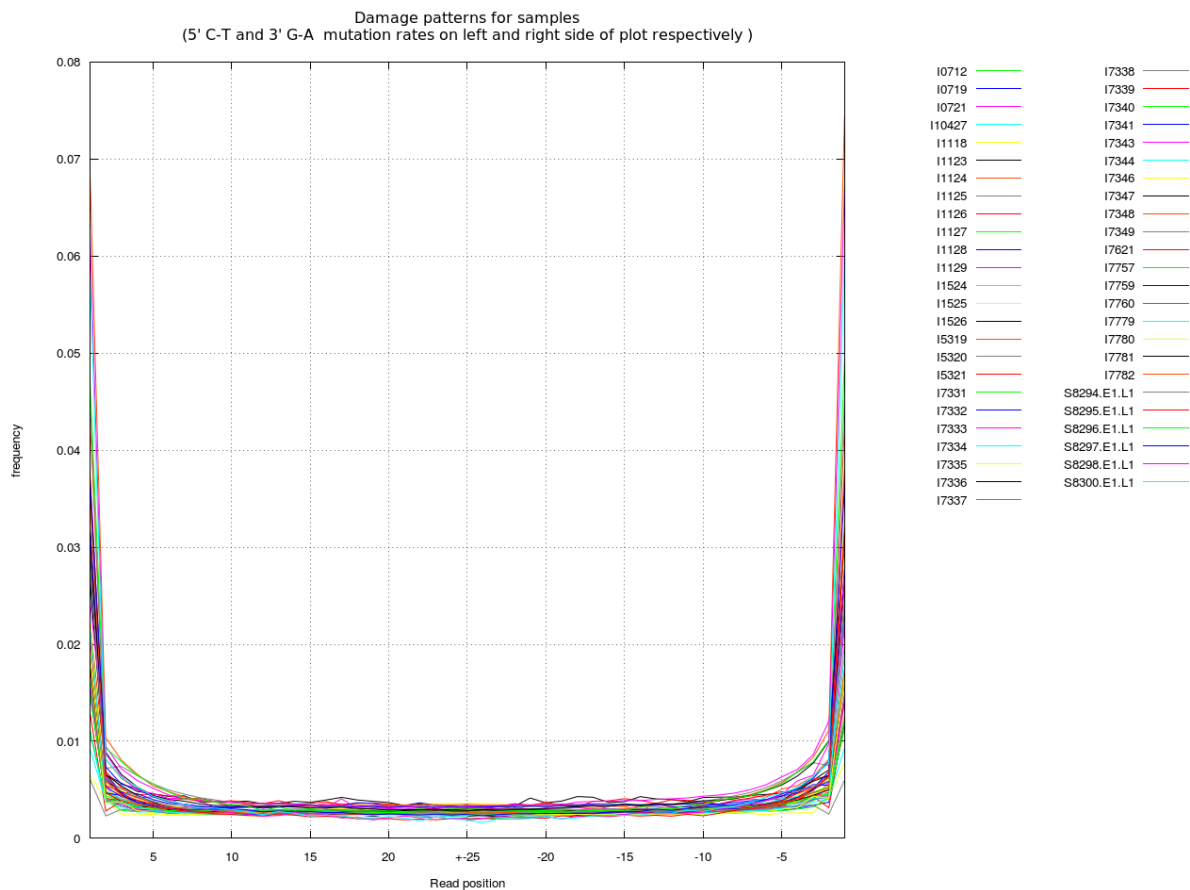
Analysis ID	library components	sample type	powder produced in	powder used for extraction, mg	extraction protocol	extract used for library preparation, µl	library preparation	damage rate in the final nucleotide	nuclear capture protocol
I0712	S0712.E1.L1	bone (rib)	Boston	74	Dabney <i>et al.</i> 2013 ^a	30	Rohland <i>et al.</i> 2015	1.5%	390k + 840k
I0719	S0719.E1.L1	bone (rib)	Boston	68	Dabney <i>et al.</i> 2013 ^a	30	Rohland <i>et al.</i> 2015	1.4%	390k + 840k
I0721	S0721.E1.L1	bone (rib)	Boston	74	Dabney <i>et al.</i> 2013 ^a	30	Rohland <i>et al.</i> 2015	2.5%	390k + 840k
I1118	S1118.E1.L1	bone (rib)	Boston	67	Dabney <i>et al.</i> 2013 ^a	30	Rohland <i>et al.</i> 2015 ¹	0.7%	1240k
I1123	S1123.E1.L1	bone (rib)	Boston	76	Dabney <i>et al.</i> 2013 ^a	30	Rohland <i>et al.</i> 2015 ¹	2.7%	1240k
I1124	S1124.E1.L1	bone (rib)	Boston	75	Dabney <i>et al.</i> 2013 ^a	30	Rohland <i>et al.</i> 2015 ¹	4.3%	1240k
I1125	S1125.E1.L1	bone (rib)	Boston	74	Dabney <i>et al.</i> 2013 ^a	30	Rohland <i>et al.</i> 2015 ¹	2.0%	1240k
I1126	S1126.E1.L2	bone (rib)	Boston	74	Dabney <i>et al.</i> 2013 ^a	3	Rohland <i>et al.</i> 2015 ²	2.4%	1240k
I1127	S1127.E1.L1	bone (rib)	Boston	73	Dabney <i>et al.</i> 2013 ^a	30	Rohland <i>et al.</i> 2015 ¹	1.5%	1240k
I1128	S1128.E1.L1	bone (rib)	Boston	73	Dabney <i>et al.</i> 2013 ^a	30	Rohland <i>et al.</i> 2015 ¹	2.7%	1240k
I1129	S1129.E1.L1	bone (rib)	Boston	73	Dabney <i>et al.</i> 2013 ^a	30	Rohland <i>et al.</i> 2015 ¹	2.1%	1240k
I1524	S1524.E1.L1	molar	Dublin	68	Dabney <i>et al.</i> 2013 ^a	30	Rohland <i>et al.</i> 2015 ¹	1.9%	1240k
I1525	S1525.E1.L1	molar	Dublin	72	Dabney <i>et al.</i> 2013 ^a	30	Rohland <i>et al.</i> 2015 ¹	2.2%	1240k
	S7758.E1.L1	tooth	Dublin	67	Dabney <i>et al.</i> 2013 ^a	10	Rohland <i>et al.</i> 2015 ²	1.6%	1240k
I1526	S1526.E1.L1	molar	Dublin	71	Dabney <i>et al.</i> 2013 ^a	30	Rohland <i>et al.</i> 2015 ¹	3.8%	1240k
	S7778.E1.L1	tooth	Dublin	71	Dabney <i>et al.</i> 2013 ^a	10	Rohland <i>et al.</i> 2015 ²	2.4%	1240k
I5319	S5319.E1.L1	petrous	Boston	83	Dabney <i>et al.</i> 2013 ^a	10	Rohland <i>et al.</i> 2015 ²	6.4%	1240k
	S5319.E2.L1	petrous	Boston	28	Dabney <i>et al.</i> 2013 ^b	10	Rohland <i>et al.</i> 2015 ²	7.3%	1240k

	S5319.E2.L2	petrous	Boston	28	Dabney <i>et al.</i> 2013 ^b	30	Rohland <i>et al.</i> 2015 ²	8.0%	1240k
I5320	S5320.E1.L1	petrous	Boston	75	Dabney <i>et al.</i> 2013 ^a	10	Rohland <i>et al.</i> 2015 ²	4.0%	1240k
	S5320.E2.L1	petrous	Boston	16	Dabney <i>et al.</i> 2013 ^b	10	Rohland <i>et al.</i> 2015 ²	4.6%	1240k
	S5320.E2.L2	petrous	Boston	16	Dabney <i>et al.</i> 2013 ^b	30	Rohland <i>et al.</i> 2015 ²	5.0%	1240k
I5321	S5321.E1.L1	petrous	Boston	66	Dabney <i>et al.</i> 2013 ^a	10	Rohland <i>et al.</i> 2015 ²	1.0%	1240k
	S5321.E2.L1	petrous	Boston	22	Dabney <i>et al.</i> 2013 ^b	10	Rohland <i>et al.</i> 2015 ²	1.2%	1240k
	S5321.E2.L2	petrous	Boston	22	Dabney <i>et al.</i> 2013 ^b	30	Rohland <i>et al.</i> 2015 ²	1.5%	1240k
I7331	S7331.E1.L1	molar	Dublin	75	Dabney <i>et al.</i> 2013 ^a	10	Rohland <i>et al.</i> 2015 ²	1.5%	1240k
I7332	S7332.E1.L1	molar	Dublin	75	Dabney <i>et al.</i> 2013 ^a	10	Rohland <i>et al.</i> 2015 ²	2.1%	1240k
I7333	S7333.E1.L1	molar	Dublin	75	Dabney <i>et al.</i> 2013 ^a	10	Rohland <i>et al.</i> 2015 ²	1.4%	1240k
I7334	S7334.E1.L1	molar	Dublin	68	Dabney <i>et al.</i> 2013 ^a	10	Rohland <i>et al.</i> 2015 ²	0.9%	1240k
I7335	S7335.E1.L1	molar	Dublin	64	Dabney <i>et al.</i> 2013 ^a	10	Rohland <i>et al.</i> 2015 ²	3.2%	1240k
I7336	S7336.E1.L1	molar	Dublin	57	Dabney <i>et al.</i> 2013 ^a	10	Rohland <i>et al.</i> 2015 ²	3.4%	1240k
I7337	S7337.E1.L1	molar	Dublin	58	Dabney <i>et al.</i> 2013 ^a	10	Rohland <i>et al.</i> 2015 ²	1.2%	1240k
I7338	S7338.E1.L1	molar	Dublin	74	Dabney <i>et al.</i> 2013 ^a	10	Rohland <i>et al.</i> 2015 ²	0.6%	1240k
I7339	S7339.E1.L1	molar	Dublin	75	Dabney <i>et al.</i> 2013 ^a	10	Rohland <i>et al.</i> 2015 ²	1.6%	1240k
I7340	S7340.E1.L1	molar	Dublin	75	Dabney <i>et al.</i> 2013 ^a	10	Rohland <i>et al.</i> 2015 ²	1.1%	1240k
I7341	S7341.E1.L1	molar	Dublin	75	Dabney <i>et al.</i> 2013 ^a	10	Rohland <i>et al.</i> 2015 ²	1.8%	1240k
I7342_d	S7342.E1.L1	molar	Dublin	70	Dabney <i>et al.</i> 2013 ^a	10	Rohland <i>et al.</i> 2015 ²	1.3%	1240k
I7343	S7343.E1.L1	molar	Dublin	70	Dabney <i>et al.</i> 2013 ^a	10	Rohland <i>et al.</i> 2015 ²	1.5%	1240k
I7344	S7344.E1.L1	molar	Dublin	72	Dabney <i>et al.</i> 2013 ^a	10	Rohland <i>et al.</i> 2015 ²	1.2%	1240k
I7346	S7346.E1.L1	molar	Dublin	80	Dabney <i>et al.</i> 2013 ^a	10	Rohland <i>et al.</i> 2015 ²	1.8%	1240k
I7347	S7347.E1.L1	molar	Dublin	55	Dabney <i>et al.</i> 2013 ^a	10	Rohland <i>et al.</i> 2015 ²	1.7%	1240k
I7348	S7348.E1.L1	molar	Dublin	57	Dabney <i>et al.</i> 2013 ^a	10	Rohland <i>et al.</i> 2015 ²	1.9%	1240k
I7349	S7349.E1.L1	molar	Dublin	70	Dabney <i>et al.</i> 2013 ^a	10	Rohland <i>et al.</i> 2015 ²	1.5%	1240k
I7621	S7621.E1.L1	bone	Dublin	63	Dabney <i>et al.</i> 2013 ^a	10	Rohland <i>et al.</i> 2015 ²	3.5%	1240k
I7757	S7757.E1.L1	molar	Dublin	62	Dabney <i>et al.</i> 2013 ^a	10	Rohland <i>et al.</i> 2015 ²	1.4%	1240k
I7759	S7759.E1.L1	molar	Dublin	82	Dabney <i>et al.</i> 2013 ^a	10	Rohland <i>et al.</i> 2015 ²	3.0%	1240k
I7760	S7760.E1.L1	molar	Dublin	70	Dabney <i>et al.</i> 2013 ^a	10	Rohland <i>et al.</i> 2015 ²	2.6%	1240k
I7779	S7779.E1.L1	bone (cranial)	Dublin	63	Dabney <i>et al.</i> 2013 ^a	10	Rohland <i>et al.</i> 2015 ²	2.3%	1240k
I7780	S7780.E1.L1	molar	Dublin	67	Dabney <i>et al.</i> 2013 ^a	10	Rohland <i>et al.</i> 2015 ²	1.8%	1240k
I7781	S7781.E1.L1	molar	Dublin	66	Dabney <i>et al.</i> 2013 ^a	10	Rohland <i>et al.</i> 2015 ²	3.0%	1240k
I7782	S7782.E1.L1	molar	Dublin	62	Dabney <i>et al.</i> 2013 ^a	10	Rohland <i>et al.</i> 2015 ²	3.3%	1240k
I8294	S8294.E1.L1	bone (phalanx)	Dublin	75	Dabney <i>et al.</i> 2013 ^a	10	Rohland <i>et al.</i> 2015 ²	2.6%	1240k
I8295	S8295.E1.L1	bone (cranial)	Dublin	71	Dabney <i>et al.</i> 2013 ^a	10	Rohland <i>et al.</i> 2015 ²	3.5%	1240k
I8296	S8296.E1.L1	bone (cranial)	Dublin	68	Dabney <i>et al.</i> 2013 ^a	10	Rohland <i>et al.</i> 2015 ²	4.8%	1240k
	S8297.E1.L1	bone (cranial)	Dublin	68	Dabney <i>et al.</i> 2013 ^a	10	Rohland <i>et al.</i> 2015 ²	3.7%	1240k
I8298	S8298.E1.L1	bone (cranial)	Dublin	75	Dabney <i>et al.</i> 2013 ^a	10	Rohland <i>et al.</i> 2015 ²	6.5%	1240k
	S8300.E1.L1	bone (cranial)	Dublin	75	Dabney <i>et al.</i> 2013 ^a	10	Rohland <i>et al.</i> 2015 ²	5.9%	1240k
I10427	S10427.E1.L2	molar	Boston	73	Dabney <i>et al.</i> 2013 ^a	10	Rohland <i>et al.</i> 2015 ²	3.1%	1240k

519 3.2 Bioinformatic processing

520 Raw sequencing data was generated on an Illumina NextSeq 500 instrument. For libraries
521 captured against the set of 1.24 million nuclear SNPs, sample-identifying sequences (barcodes)
522 were trimmed. Adapters were stripped and read pairs with at least 15 bp overlap were merged
523 into a single sequence (allowing for 1 mismatch) at least 30 bp in length, using a modified form
524 of the SeqPrep tool (<https://github.com/jstjohn/SeqPrep>) which retains the highest quality
525 base in the overlap region. Autosomal sequences were aligned to the human reference
526 genome hg19 (1000 genomes version, downloaded at
527 http://ftp.1000genomes.ebi.ac.uk/vol1/ftp/technical/reference/human_g1k_v37.fasta.gz)
528 using *bwa* v.0.6.1 with the *samse* command (Li and Durbin 2009). Following alignment, clusters
529 of duplicate reads were identified based on start and end position, and orientation; for each
530 cluster of reads, the highest quality representative was used.

531 For libraries with mitochondrial DNA enrichment, the same procedure was used, except
532 that the mitochondrial sequences were treated separately and aligned to the RSRs reference
533 genome (Behar et al. 2012) rather than hg19. We measured damage rates on both ends of
534 mapped reads to assess their authenticity, as summarized in Table S3.1 and in Fig. S3.1.



535

536 **Fig. S3.1:** Damage rates (5' C->T, 3' A->G) obtained from mapped reads of all samples.

537

538 *References (for this section)*

539 Behar, D. M. *et al.* A 'Copernican' reassessment of the human mitochondrial DNA tree from its root. *Am. J. Hum.*
540 *Genet.* **90**, 675–684 (2012).

541 Li, H. & Durbin, R. Fast and accurate short read alignment with Burrows-Wheeler Transform. *Bioinformatics* **25**,
542 1754–1760 (2009).

543 **Supplementary Information section 4**

544 **Principal component analysis and outlier removal**

545

546 The first round of outlier removal (prior to *ChromoPainter v.1* and *v.2*, *fineSTRUCTURE*, HSS,
547 *GLOBETROTTER* analyses and the *ADMIXTURE* analyses presented in Extended Data Fig. 8) is
548 illustrated in Tables S4.1 and S4.2. These spreadsheets display unsupervised *ADMIXTURE*
549 results (K=14 and K=11 in the case of the HumanOrigins and Illumina datasets, respectively),
550 average weighted Euclidean distances, PC1 vs. PC2 plots, and outcomes of the outlier
551 removal procedure for each American and Siberian population composed of 3 or more
552 individuals and having at least one outlier. We note that outliers were removed from all
553 populations, and the above-mentioned populations were selected to illustrate our approach
554 and at the same time to keep the size of the spreadsheets reasonably small. The procedure
555 itself is explained in the Methods section.

556 Individuals having outlying average weighted Euclidean distances (vs. all other
557 individuals in a population) were identified using the established definition of an outlier: $>$
558 $[3^{\text{rd}} \text{ quartile} + 1.5 \times (3^{\text{rd}} \text{ quartile} - 1^{\text{st}} \text{ quartile})]$. Manual removal of outliers based on
559 *ADMIXTURE* profiles, i.e. on outstanding proportions of European and other non-typical
560 ancestry components, was prioritized, and some individuals identified as outliers based on
561 average weighted Euclidean distances were kept if they had a typical *ADMIXTURE* profile
562 (see examples for the Ket, Nganasan, Tubalar, and Yup'ik Chaplin/Sireniki populations in the
563 HumanOrigins dataset, Table S4.1). If a majority of individuals in a population had colonial
564 admixture, we removed only those having the most extreme admixture proportions, in
565 order to keep the final population size reasonably large (see examples for the Splatsin,
566 Stswecem'c, Tlingit and other groups in the Illumina dataset, Table S4.2). Removal of
567 outliers based on average weighted Euclidean distances was prioritized if all individuals had
568 a uniform *ADMIXTURE* profile (see examples for the Karitiana, Mansi, Surui, Xavante, and
569 Zapotec populations in the HumanOrigins dataset, Table S4.1).

570 To illustrate the effects of the second round of outlier removal (prior to *qpWave*,
571 *qpAdm*, *qpGraph*, *ALDER*, and f_4 -statistic analyses), we performed principal component
572 analysis (PCA) on the datasets without transitions used for the above-listed analyses (Fig.
573 S4.1). Native American individuals (i.e. those belonging to the First Peoples, Na-Dene, and
574 Eskimo-Aleut meta-populations) having $>1\%$ European, African, or Southeast Asian ancestry
575 according to *ADMIXTURE* were removed, as well as Chukotkan and Kamchatkan individuals
576 with $>1\%$ European ancestry. PCA plots for original datasets prior to any outlier removal are
577 shown in Fig. 1a and Extended Data Fig. 2.

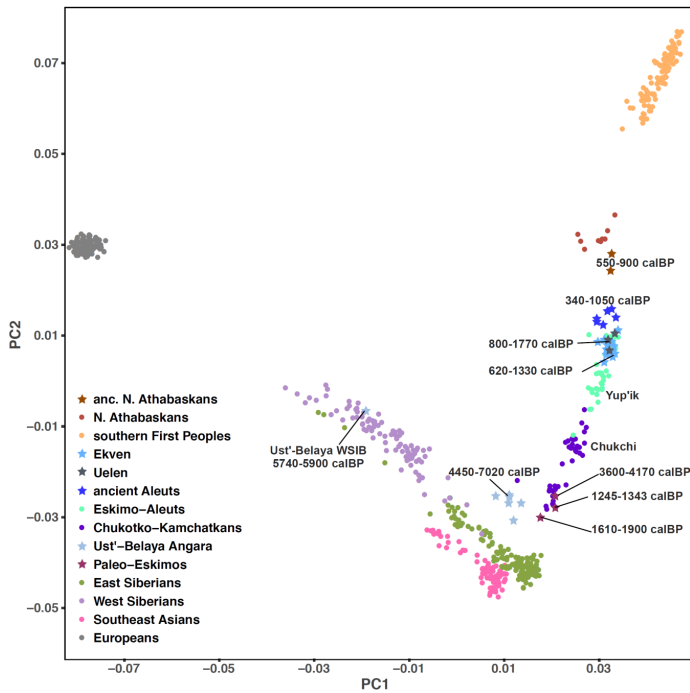
578 We dated 12 burials at the Ust'-Belaya site at the confluence of the Belaya and
579 Angara Rivers: seven burials were dated to ca. 4,500 – 4,800 calBP, four burials were dated
580 to an earlier period between ca. 5,700 and 7,000 calBP, and a medieval burial was dated to
581 ca. 600 calBP (Supplementary Table 2). We generated genome-wide data for all 12
582 individuals (Supplementary Table 1). Among these samples, 3 were removed due to a high
583 percentage of missing data (Supplementary Table 1), and all but one remaining samples
584 form a tight cluster positioned between the C-K/P-E and Siberian clusters in the space of
585 two principal components (PC1 and PC2, Fig. 1a, Extended Data Fig. 2). Remarkably, an
586 individual I7760 (Mos85) buried at Ust'-Belaya and dated to 5740 – 5900 calBP
587 (Supplementary Table 2) is a genetic outlier demonstrating the typical West Siberian genetic

588 profile (Fig. 1a, Extended Data Fig. 2).

589

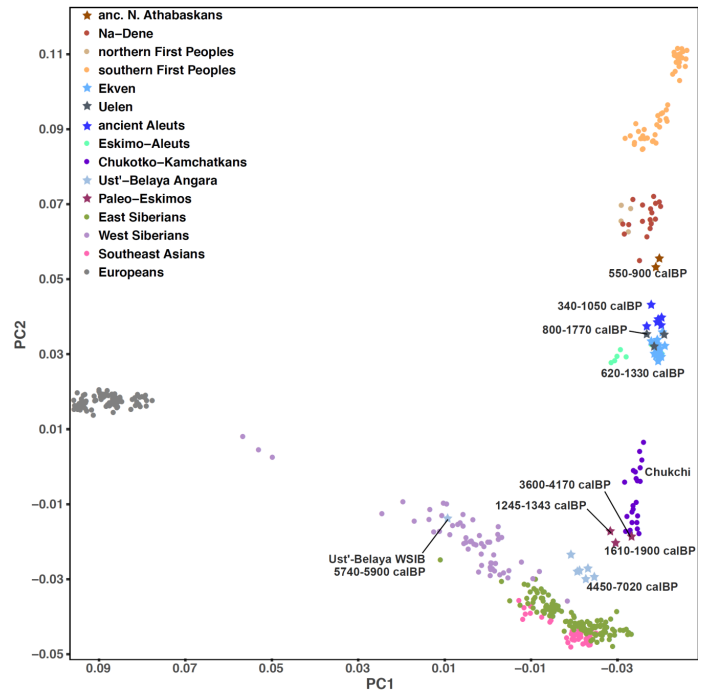
590 **Fig. S4.1.** PCA based on the HumanOrigins (a) and Illumina (b) datasets without transitions used for the
591 *qpWave/qpAdm* and *ALDER* analyses. The datasets have undergone a stringent outlier removal procedure, as
592 described in the Methods section. The analyses are based on 649 (a) or 472 (b) individuals and 111,147 (a) or
593 96,155 (b) loci. Plots of two principal components (PC1 vs. PC2) are shown (linkage disequilibrium pruning was
594 not applied). The following meta-populations most relevant for our study are plotted: present-day Eskimo-
595 Aleut and Chukotko-Kamchatkan speakers, ancient Chukotkan Neo-Eskimos (Ekven and Uelen sites), ancient
596 Aleuts, Paleo-Eskimos (the Saqqaq, Middle Dorset and Late Dorset individuals), ancient Northern Athabaskans,
597 present-day Na-Dene speakers, Northern and Southern First Peoples, West and East Siberians, the Ust'-Belaya
598 Angara ancient Siberian population, Southeast Asians, and Europeans. Calibrated radiocarbon dates in years
599 before present are shown for ancient samples. For individuals, 95% confidence intervals are shown, and for
600 populations, minimal and maximal median dates among individuals are shown.

601 a



602

b



603 **Supplementary Information section 5**

604 **Exhaustive analysis of ancestry streams in small population sets**

605

606 We performed testing of two- and three-way admixture models in groups of three and four
607 populations (triplets and quadruplets) using *qpAdm* (Haak et al. 2015) and *qpWave* (Reich et
608 al. 2012): closely related tools that in conjunction allow testing whether two- or multi-
609 component admixture models fit the data, and allow inferring admixture proportions
610 (*qpAdm*) without assuming a particular tree topology. This class of methods relies on allele
611 frequencies in populations, and thus requires careful definition of population groups and
612 outlier pruning. The *qpWave* tool is used to infer how many independent lines of ancestry
613 relate a set of test populations to a set of outgroups. *qpWave* relies on a matrix of statistics
614 $f_4(\text{test}_1, \text{test}_i; \text{outgroup}_1, \text{outgroup}_x)$. Usually, few test populations from a certain region and
615 a diverse worldwide set of outgroups (having no recent gene flow from the region of
616 interest) are co-analyzed (Haak et al. 2015, Lazaridis et al. 2016, Skoglund et al. 2015), and a
617 statistical test is performed to determine whether allele frequencies in the test populations
618 can be explained by one, two, or more streams of ancestry derived from the outgroups. If a
619 group of three populations, a triplet, is derived from two ancestry streams according to a
620 *qpWave* test, and any pair of the constituent populations shows the same result, it follows
621 that one of the populations can be modelled as having ancestry from the other two using
622 *qpAdm*. If a set of outgroups includes populations closely related to at least one of the
623 admixture partners, the power to distinguish alternative admixture models is increased.

624 The following sets of outgroup populations were used for analyses on the
625 HumanOrigins dataset: 1) "OG19", 19 outgroups from five broad geographical regions:
626 Mbuti, Taa, Yoruba (Africans), Nganasan, Tuvinian, Ulchi, Yakut (East Siberians), Altaian, Ket,
627 Selkup, Tubalar (West Siberians), Czech, English, French, North Italian (Europeans), Dai,
628 Miao, She, Thai (Southeast Asians); 2) "OG19_UB1526", OG19 and an ancient Siberian
629 individual I1526 (the highest-coverage individual at the Ust'-Belaya Angara site) that is
630 distinct from the other Siberians according to our PCA analyses (section 4) and thus might
631 increase the diversity of Siberian outgroups and the resolution of the method; 3) "OGA", 8
632 diverse Siberian populations (Nganasan, Tuvinian, Ulchi, Yakut, Even, Ket, Selkup, Tubalar)
633 and a Southeast Asian population (Dai); 4) "OGA_Koryak", OGA and Koryak, a C-K group that
634 supposedly provides higher resolution since it is closely related to the putative PPE
635 admixture partners (section 10); 5) "OGA_UB1526", OGA and the Ust'-Belaya Angara
636 individual I1526.

637 Similar sets of outgroup populations were used for analyses based on the Illumina
638 dataset: 1) "OG20": Bantu (Kenya), Mandenka, Mbuti, Yoruba (Africans), Buryat, Evenk,
639 Nganasan, Tuvinian, Yakut (East Siberians), Altaian, Khakas, Selkup (West Siberians), Basque,
640 Sardinian, Slovak, Spanish (Europeans), Dai, Lahu, Miao, She (Southeast Asians); 2)
641 "OG20_UB1526", OG20 and the highest-coverage Ust'-Belaya Angara individual I1526; 3)
642 "OGA", 9 Siberian populations (Buryat, Dolgan, Evenk, Nganasan, Tuvinian, Yakut, Altaian,
643 Khakas, Selkup) and Dai; 4) "OGA_Koryak", OGA and Koryak; 5) "OGA_UB1526", OGA and
644 the Ust'-Belaya Angara individual I1526. Population triplets and quadruplets were tested
645 using both the HumanOrigins and Illumina SNP array datasets, with or without transition
646 polymorphisms, and using these five alternative outgroup sets. Paleo-Eskimos (P-E) were
647 represented by the Saqqaq (ca. 3,900 calBP), or Middle Dorset (ca. 1,750 calBP), or Late
648 Dorset individuals (ca. 750 calBP), widely separated in space and time, and two types of SNP

649 calls were tested for the Saqqaq individual: published diploid calls (Raghavan et al. 2014)
650 with 50-58% missing rates in various dataset versions, and pseudo-haploid calls with much
651 lower missing rates of 4-11% (in various dataset versions) generated by us and also used for
652 *qpGraph* model fitting (section 10). Missing rates for the Middle and Late Dorset samples
653 were as follows: 89-90% and 70-75% in various dataset versions, respectively. Chukotko-
654 Kamchatkan speakers (C-K) served as an alternative PPE source, and were represented by
655 Chukchi, Koryak, and Itelmen (the HumanOrigins dataset), and by Chukchi and Koryak in the
656 case of the Illumina dataset.

657 For the *qpWave/qpAdm* analyses, any American individuals with >1% European,
658 African, or Southeast Asian ancestry according to the *ADMIXTURE* analysis (Extended Data
659 Fig. 8) were removed, as well as Chukotkan and Kamchatkan individuals with >1% European
660 ancestry. Some additional Chipewyan and West Greenlandic Inuit individuals were removed
661 since European ancestry undetectable with *ADMIXTURE* was revealed in them using *D*-
662 statistics (Yoruba or Dai, Icelander; Chipewyan individual, Karitiana) and (Yoruba or Dai,
663 Slovak; West Greenlandic Inuit individual, Karitiana). Any individual with any of the two
664 absolute Z-scores >3 was removed.

665 First, we tested if essentially all present-day and ancient American and Chukotkan
666 populations can be modelled as a mixture of two sources: selected First Peoples (FAM) and
667 mostly unadmixed representatives of the PPE clade: P-E or C-K. To this end, we exhaustively
668 tested the following population triplets using *qpAdm*, for four dataset versions and five
669 outgroup sets: 1/ C-K, FAM, PPE; 2/ E-A, FAM, PPE; 3/ Na-Dene (N-D), FAM, PPE; 4/ P-E,
670 FAM, PPE; 5/ SAM, FAM, PPE; 6/ NAM, FAM, PPE. The FAM group was represented by three
671 alternative sources in the case of the HumanOrigins dataset: relatively large SAM
672 populations with no signs of colonial admixture (Guarani, 17 ind.; Karitiana, 12 ind.; Mixe, 10
673 ind.). In the case of the Illumina dataset, a NAM source with no signs of P-E admixture
674 (Extended Data Figs. 3 and 4) was also added, and the full list of alternative FAM sources
675 was as follows: Pima (SAM, 13 ind.), Karitiana (SAM, 13 ind.), Mixtec (SAM, 7 ind.), Nisga'a
676 (NAM, 3 ind.). A C-K outgroup (Koryak in the "OGA_Koryak" outgroup sets) was not tested
677 for population triplets/quadruplets including a C-K group since such models are expected to
678 be non-fitting by default.

679 Here we summarize the results for the HumanOrigins transversion-only dataset
680 (Table S5.1). First, C-K (represented by Koryak or Itelmen) does not make a good PPE source
681 for E-A populations since most 2-way admixture models "E-A = FAM + C-K" are non-fitting
682 even at the 0.01 *p*-value threshold (5 or 6 of 18 models fit). This result holds for all outgroup
683 sets tested. However, models including Chukchi as a PPE source fit much better, probably
684 because of an elevated E-A admixture in Chukchi (see Fig. 1a, Extended Data Figs. 2 and 8,
685 sections 5, 8). Notably, the models generally work for ancient Aleuts and the Old Bering Sea
686 group from Uelen, and the former group has no C-K admixture according to our *qpGraph*,
687 *Rarecoal*, and RASS analyses (sections 8, 9, 10). This result can be interpreted in the
688 following way: two-way admixture models "FAM + C-K" do not fit for ancient Neo-Eskimos
689 (Ekven) and for present-day Iñupiat and Yup'ik since two distinct PPE sources contributed to
690 these groups, i.e. the original PPE source and C-K during the later bidirectional gene flow
691 event. Moreover, according to all fitting *qpGraph* models (Fig. S10.3), C-K groups are rather
692 distant from the PPE source in E-A (here named "PPE_{E-A}"), which is much closer to the
693 Saqqaq Paleo-Eskimo.

694 In line with these phylogenetic models, P-E make a perfect source for ancient and
695 present-day E-A: 332 of 360 models "E-A = FAM + P-E" are fitting at the 0.05 *p*-value

696 threshold. Here we counted all five alternative outgroup sets and four alternative P-E
697 sources (Saqqaq diploid calls, Saqqaq pseudo-haploid calls, the Middle Dorset individual and
698 the Late Dorset individual). Most non-fitting models are of the following type: “Yup'ik = FAM
699 + P-E”, with the “OGA_Koryak” outgroup set. Due to a high level of C-K admixture in Yup'ik
700 (see Extended Data Fig. 8, sections 5, 8), an assumption of the method, i.e. absence of gene
701 flow from ingroups to outgroups, is violated, and the models become non-fitting.

702 Second, both P-E and C-K make good proxies for PPE ancestry in ancient and
703 present-day N-D (Table S5.1): 72 of 108 models “N-D = FAM + C-K” (or 67% of models) are
704 fitting at the 0.05 p -value threshold; 126 of 144 models “N-D = FAM + P-E” (or 88% of
705 models) are fitting at the 0.05 p -value threshold (here we counted four alternative outgroup
706 sets, three alternative C-K sources, and four alternative P-E sources). These results agree
707 with the best-fitting admixture graph (Fig. S10.5) since PPE_{C-K} and PPE_{P-E} split points are
708 approximately equidistant from the PPE_{N-D} split point, and thus C-K and P-E may serve
709 equally well as proxies for PPE_{N-D} .

710 Third, most admixture models for 19 SAM populations are consistent with 0% PPE
711 ancestry (Extended Data Fig. 3a-e, Table S5.1. We observe that estimates of PPE ancestry
712 proportions in other populations are highly dependent on the PPE proxies used (Table S5.1):
713 the lowest for the Late Dorset individual, and the highest for Saqqaq pseudo-haploid calls.
714 We refrain from judging which estimates are closer to reality, although ranking of
715 populations according to the PPE ancestry proportion remains relatively stable across
716 various proxies and outgroup sets (Fig. 1b, Extended Data Figs. 3 and 4). Here we ranked
717 populations according to increasing percentage of PPE ancestry (Fig. 1b): 1/ SAM, 2/
718 Chipewyans and Dakelh, 3/ ancient Athabaskans, 4/ ancient Aleuts, 5/ Iñupiat, Ekven, and
719 Uelen having almost equal percentages, 6/ Yup'ik Naukan, 7/ Yup'ik Chaplin/Sireniki, 8/ C-K
720 and P-E. This ranking is in line with our migration model (see the Discussion and Fig. 3).
721 Gene flow from neighboring NAM groups most likely continued after the initial NAM/P-E
722 admixture event in Na-Dene ancestors, so the percentage of PPE ancestry went down
723 gradually over time. Ancient Aleuts remained in Alaska and never experienced the later
724 pulse of C-K admixture (section 10), which is shared by Ekven, Uelen (ancient Chukotkan
725 Neo-Eskimos of the Old Bering Sea culture), and Iñupiat (present-day Alaskans whose
726 ancestors migrated from Chukotka according to archaeological evidence, Jensen 2016,
727 Mason 2016). Unlike Iñupiat and other Inuit, Yup'ik have remained in Chukotka since their
728 initial backward migration from Alaska (Fig. 3), and had much more time for interacting with
729 local C-K; thus the elevated PPE ancestry proportion in Yup'ik is not unexpected. The C-K/E-
730 A admixture was bidirectional (section 10), and E-A ancestry proportion is also non-uniform
731 among C-K.

732 The results remain virtually the same for the full HumanOrigins dataset (Table S5.2).
733 Even fewer models “E-A = FAM + Koryak/Itelmen” fit the data: 8 models of 144 at the p -
734 value threshold of 0.05, namely the models “ancient Aleuts = FAM + Koryak/Itelmen” with
735 the OGA and OG19 outgroup sets. In contrast, most models “E-A = FAM + P-E” remain
736 fitting: 284 of 360 models at the 0.05 p -value threshold. Here we counted all five alternative
737 outgroup sets and four alternative P-E sources. Most non-fitting models are those with the
738 “OGA_Koryak” outgroup, and that result reflects C-K admixture in the ancestors of
739 Yup'ik/Inuit. The results also remain unchanged for Na-Dene speakers: both P-E and C-K
740 make good proxies for PPE ancestry in ancient and present-day N-D (Table S5.2): 71 of 108
741 models “N-D = FAM + C-K” (or 66% of models) are fitting at the 0.05 p -value threshold; 107
742 of 144 models “N-D = FAM + P-E” (or 74% of models) are fitting at the 0.05 p -value

743 threshold (here we counted four alternative outgroup sets, three alternative C-K sources,
744 and four alternative P-E sources). The ranking of populations by PPE ancestry proportions
745 also remains unchanged (Extended Data Fig. 4a-e, Table S5.2).

746 Next, we repeated the same analyses for the Illumina dataset. An advantage of this
747 dataset is that it includes a wider diversity of Na-Dene speakers (Tlingit and Southern
748 Athabaskans, in addition to Northern Athabaskans) and FAM populations (NAM in addition
749 to SAM). The results of admixture model testing with *qpAdm* are generally similar for the
750 Illumina and HumanOrigins datasets, with the following notable differences. First, for both
751 the transversions-only (Table S5.3) and full datasets (Table S5.4), C-K and P-E represent
752 equally fitting ancestry sources for E-A: 1/ models “E-A = FAM + C-K”, 138 (72%, Table S5.3)
753 or 126 (66%, Table S5.4) of 192 models fit the data at the *p*-value threshold of 0.05; 2/
754 models “E-A = FAM + P-E”, 330 (86%, Table S5.3) or 244 (64%, Table S5.4) of 384 models fit
755 the data at the *p*-value threshold of 0.05. Here we counted four alternative outgroup sets
756 and four alternative P-E sources (Saqqaq diploid calls, Saqqaq pseudo-haploid calls, Middle
757 Dorset, and Late Dorset). As expected, the models “E-A = FAM + P-E” with the
758 “OGA_Koryak” outgroup set are non-fitting for all E-A except for ancient Aleuts (Table S5.3).
759 This result reflects C-K admixture in the ancestors of Yup’ik/Inuit.

760 Another important finding is that PPE ancestry, with a proportion comparable to that
761 found in Na-Dene speakers, was detected in one NAM population, Splatsin, while in Nisga’a,
762 Haida, and in SAM populations it was consistent with 0% (Extended Data Figs. 3f-j and 4f-j,
763 Tables S5.3, S5.4). Here we ranked populations according to increasing percentage of PPE
764 ancestry (Extended Data Figs 3, 4): 1/ SAM, Nisga’a, and Haida, 2/ Southern Athabaskans, 3/
765 Tlingit, 4/ three Northern Athabaskan groups and Splatsin (NAM), 5/ West Greenlandic Inuit,
766 6/ ancient Athabaskans, 7/ Alaskan and East Greenlandic Inuit, ancient Aleuts, 8/ Ekven, and
767 Uelen, 9/ C-K and P-E.

768 We also analyzed other types of population triplets and quadruplets using *qpWave*.
769 To keep the number of tests reasonably low, here we excluded the lowest-coverage Paleo-
770 Eskimo individual, i.e. Middle Dorset. In total, we ran 54,948 *qpWave* tests. The quadruplets
771 tested had the following composition: SAM or NAM + N-D + E-A + P-E or C-K. The triplets
772 tested had the following composition: SAM or NAM or N-D + E-A + P-E or C-K. Below we
773 summarize results for the HumanOrigins dataset: the full and transversion-only versions,
774 with the 0.01 and 0.05 *p*-value thresholds (Tables S5.5 – S5.8). Quadruplets “SAM + N-D + E-
775 A + P-E” and triplets “SAM or N-D + E-A + P-E” were generally consistent with two migration
776 waves (Table S5.5), except for models “SAM + N-D + Yup’ik + P-E” and “SAM or N-D + Yup’ik
777 + P-E” with the “OGA_Koryak” outgroup set. As discussed above, this result reflects the third
778 genetic stream, i.e. the C-K admixture, easily detectable in Yup’ik having a high proportion
779 of C-K ancestry (Extended Data Fig. 8, section 8). Overall, the results are consistent with P-E
780 contributing genetically to both N-D and E-A, and the picture remains the same for the full
781 dataset at both *p*-value thresholds, although it becomes noisier (Tables S5.7, S5.8). When P-
782 E groups in the triplets and quadruplets were replaced by C-K groups, three or rarely even
783 four, but not two migration streams fitted the data in most cases (3,290 vs. 1,270 triplets
784 and quadruplets including Ekven, Inupiat, and Yup’ik), except for population sets including
785 ancient Aleuts (Tables S5.5 – S5.8) and Uelen Neo-Eskimos (Tables S5.5 – S5.7). This pattern
786 was observed for all outgroup sets, except for “OGA_Koryak”, which is expected to increase
787 the f_4 matrix rank for any C-K-containing population set: data for 211 vs. 929 triplets and
788 quadruplets fitted 2-stream vs. 3- or 4-stream models, respectively (Table S5.5). Taken
789 together, these results are again consistent with two PPE gene flow events in the E-A

790 history: the first event in Alaska, and another gene flow from C-K to Yup'ik/Inuit ancestors in
791 Chukotka. Ancient Aleuts had remained in Alaska and were not influenced by the latter
792 event. The result observed for Uelen is more difficult to interpret, but it is possibly explained
793 by the fact that Uelen is the smallest E-A group composed of just 3 pseudo-haploid
794 individuals (cf. 6 ancient Aleuts, 16 Ekven Neo-Eskimos, 9 Yup'ik Naukan, 15 Yup'ik
795 Chaplin/Sireniki, 20 Iñupiat, see Supplementary Table 4).

796 The Illumina dataset allowed us to explore population sets including NAM groups. In
797 the case of the transversion-only dataset and the p -value threshold of 0.01 (Table S5.9),
798 *qpWave* results were not influenced by the PPE proxy used: almost all triplets “SAM or NAM
799 or N-D + E-A + P-E or C-K” and quadruplets “SAM or NAM + N-D + E-A + P-E or C-K” were
800 consistent with two migration streams derived from the outgroups. The results were similar
801 for NAM- and SAM-containing population sets (Table S5.9). The C-K admixture in E-A
802 becomes apparent only if an outgroup very close to C-K is used, i.e. Koryak in the
803 “OGA_Koryak” outgroup set. In this case most quadruplets and triplets including P-E were
804 consistent with three migration streams, except for those including ancient Aleuts, as
805 expected (Table S5.9).

806 However, most triplets and quadruplets including C-K instead of P-E with the
807 “OGA_Koryak” outgroup set were consistent with two migration streams (344 vs. 36
808 models, Table S5.9), except for those including ancient Aleuts. The latter sets were mostly
809 consistent with three migration streams (18 models consistent with two streams vs. 58
810 models consistent with three streams, Table S5.9). This somewhat unexpected result may
811 be interpreted in the following way. If the method cannot easily resolve the PPE_{C-K} and PPE_{P-E}
812 ancestry sources, any population having ancestry from both sources (e.g., Yup'ik and Inuit)
813 might fit the two-stream model due to an apparent lack of resolution, as well as any
814 population having a low-level contribution from any of these sources (e.g., Na-Dene
815 speakers). However, (ancient) Aleuts under our model have a substantial ancestry
816 proportion (ca. 40-50%) derived from PPE_{P-E} only, thus a population group “SAM or NAM or
817 N-D + ancient Aleuts + C-K” is not expected to fit the two-stream model. Overall, the
818 *qpWave* results are noisier for the Illumina dataset (Tables S5.9 – S5.12), as compared to the
819 HumanOrigins dataset (Tables S5.5 – S5.8).

820

821 *References (for this section)*

- 822 Haak, W. *et al.* Massive migration from the steppe was a source for Indo-European languages in Europe.
823 *Nature* **522**, 207–211 (2015).
- 824 Jensen, A. M. Archaeology of the Late Western Thule/Iñupiat in North Alaska (A.D. 1300–1750). *The Oxford*
825 *Handbook of the Prehistoric Arctic*, ed. Friesen, T. M., Mason, O. K. New York: Oxford University Press.
826 513–536 (2016).
- 827 Lazaridis, I. *et al.* Genomic insights into the origin of farming in the ancient Near East. *Nature* **536**, 419–424
828 (2016).
- 829 Mason, O. K. Thule Origins in the Old Bering Sea Culture: The Interrelationship of Punuk and Birnirk Cultures.
830 *The Oxford Handbook of the Prehistoric Arctic*, ed. Friesen, T. M., Mason, O. K. New York: Oxford
831 University Press. 489–512 (2016).
- 832 Raghavan, M. *et al.* The genetic prehistory of the New World Arctic. *Science* **345**, 1255832 (2014).
- 833 Reich, D. *et al.* Reconstructing Native American population history. *Nature* **488**, 370–374 (2012).
- 834 Skoglund, P. *et al.* Genetic evidence for two founding populations of the Americas. *Nature* **525**, 104–108
835 (2015).
- 836

837 **Supplementary Information section 6**

838 **Haplotype sharing statistics**

839

840 To investigate Paleo-Eskimo ancestry in Native Americans in a hypothesis-free way, we
841 considered haplotypes shared between Native Americans and the ancient Saqqaq
842 individual. Cumulative lengths of shared autosomal haplotypes were produced with
843 *ChromoPainter v.1* for pairs of individuals, in the form of all vs. all “coancestry matrices”
844 (Lawson et al. 2012). First, for each American individual we considered the length of
845 haplotypes shared with Saqqaq in both the donor-to-recipient and recipient-to-donor
846 directions (in cM), which we refer to as Saqqaq haplotype sharing statistic or HSS. In the
847 same way we estimated haplotype sharing between each American individual and Africans,
848 Europeans, Siberians, and Arctic (Chukotko-Kamchatkan- and Eskimo-Aleut-speaking)
849 groups by averaging HSS across individuals of a given meta-population. To normalize for
850 coverage differences and other biases, we divided the Saqqaq HSS by the African HSS, and
851 termed the resulting statistic “relative HSS.” Alternatively, we used Siberian HSS as a
852 normalizer. To visually assess correlation of haplotype sharing with Saqqaq and with closely
853 related Chukotko-Kamchatkan- and Eskimo-Aleut-speaking populations, here collectively
854 termed Arctic, we combined relative Saqqaq HSSs and relative Arctic HSS on two-
855 dimensional plots. We analyzed both the HumanOrigins (Fig. S6.1) and the Illumina (Fig.
856 S6.2) datasets with a more diverse collection of Na-Dene-speaking individuals.

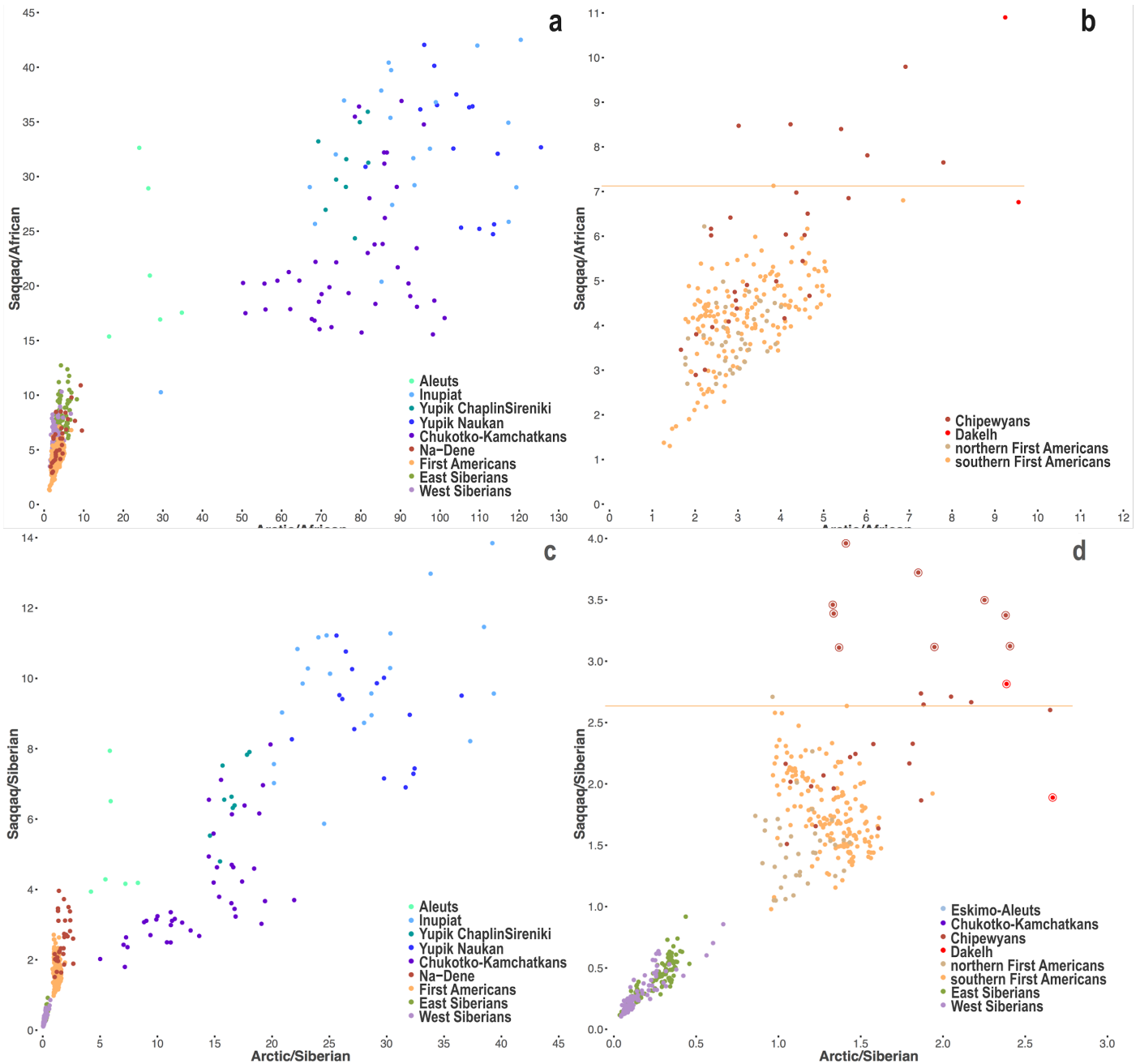
857 Since the ancient Saqqaq individual has demonstrable genetic affinities to both
858 Arctic and Siberian meta-populations (Rasmussen et al. 2010, Raghavan et al. 2014, 2015,
859 Flegontov et al. 2016, see also ADMIXTURE profiles in Extended Data Fig. 8), we also
860 scrutinized relative Arctic and Siberian HSSs (Figs. S6.3, S6.4). We observe that each meta-
861 population is scattered along a line on the Arctic vs. Siberian two-dimensional HSS plot,
862 which reflects similar ratios of the Siberian and Arctic haplotype sharing among its
863 members. The position of a population along the line depends on the presence of other
864 ancestry components. For example, Aleuts, who have a high level of European admixture
865 (Raghavan et al. 2014, 2015) (see also Extended Data Fig. 8), lie much closer to zero on both
866 axes as compared to other Eskimo-Aleut-speaking groups (Fig. S6.3a,c). While First Peoples
867 form a tight cluster, the Athabaskan-speaking Dakelh and some Chipewyans are shifted
868 considerably towards the Saqqaq individual (Fig. S6.3a,c). Since haplotype sharing statistics
869 behave linearly under recent admixture, we used linear combinations to calculate expected
870 HSSs for mixtures of First Peoples with Saqqaq or with Eskimo-Aleut-speaking populations.
871 We find that HSSs for two Dakelh (Fig. S6.3b,d) and for several Northern Athabaskan,
872 Southern Athabaskan, and Tlingit individuals (Fig. S6.4b,d) are inconsistent with a recent
873 Inuit or Yup'ik admixture event, but consistent with Saqqaq admixture. However, these
874 simple simulations do not rule out an ancient admixture event with a Neo-Eskimo group
875 since subsequent drift in Siberians or Arctic groups could have skewed the HSSs.

876

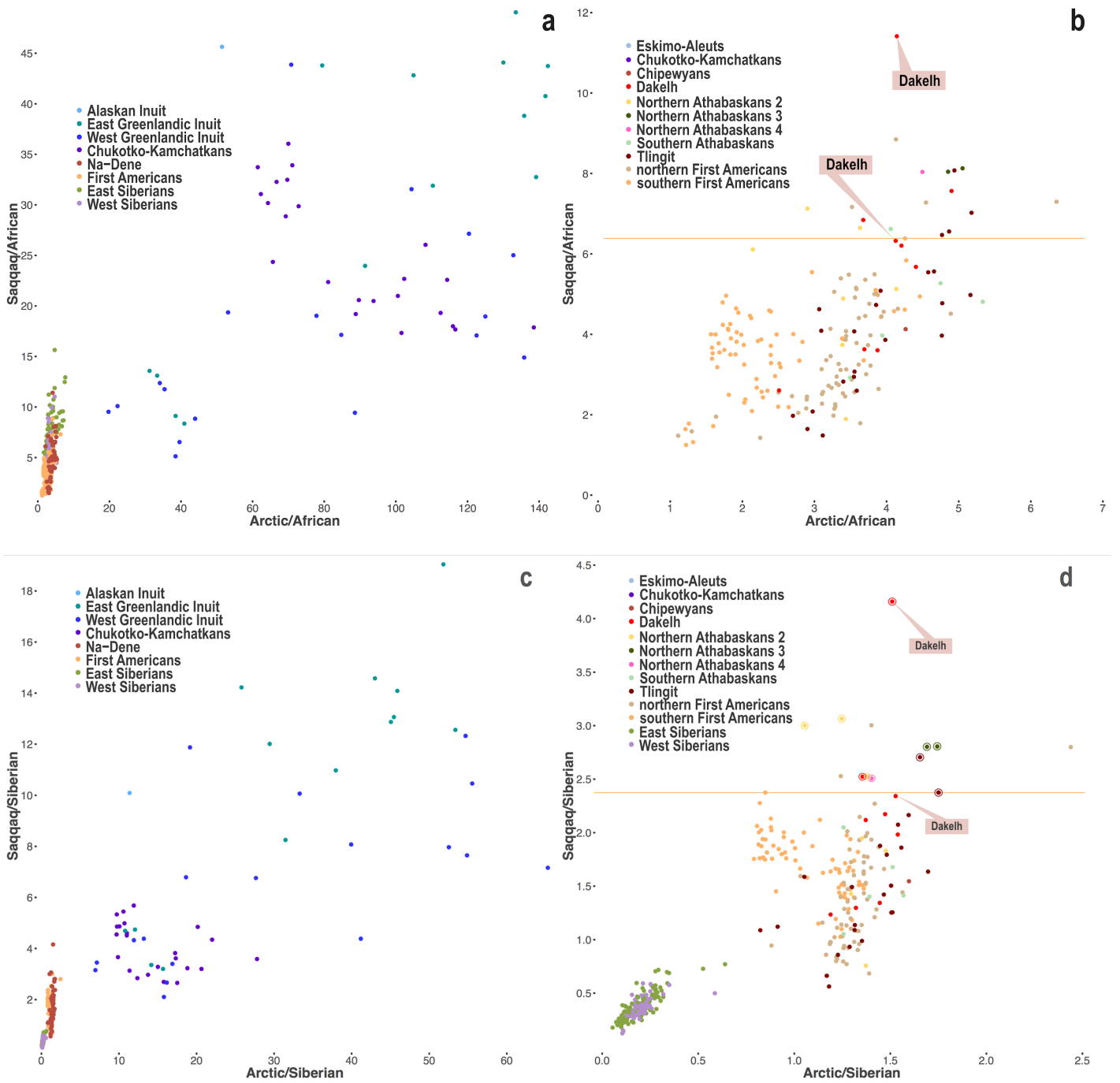
877

878 **Fig. S6.1.** Two-dimensional plots of Arctic and Saqqaq haplotype sharing statistics normalized using the African
 879 (a, b) or Siberian (c, d) meta-populations and based on the HumanOrigins SNP array dataset. a, c, Plots
 880 showing statistics for individuals of all relevant populations and meta-populations (color-coded according to
 881 the legend). b, d, Enlarged plots showing statistics for individuals of primarily First Peoples ancestry. The
 882 highest Saqqaq haplotype sharing statistics among Southern First Peoples is marked by the horizontal line.
 883 Northern Athabaskan-speaking individuals (outliers on the Arctic and/or Saqqaq axes) selected for the
 884 GLOBETROTTER analysis are marked with circles in panel d.

885

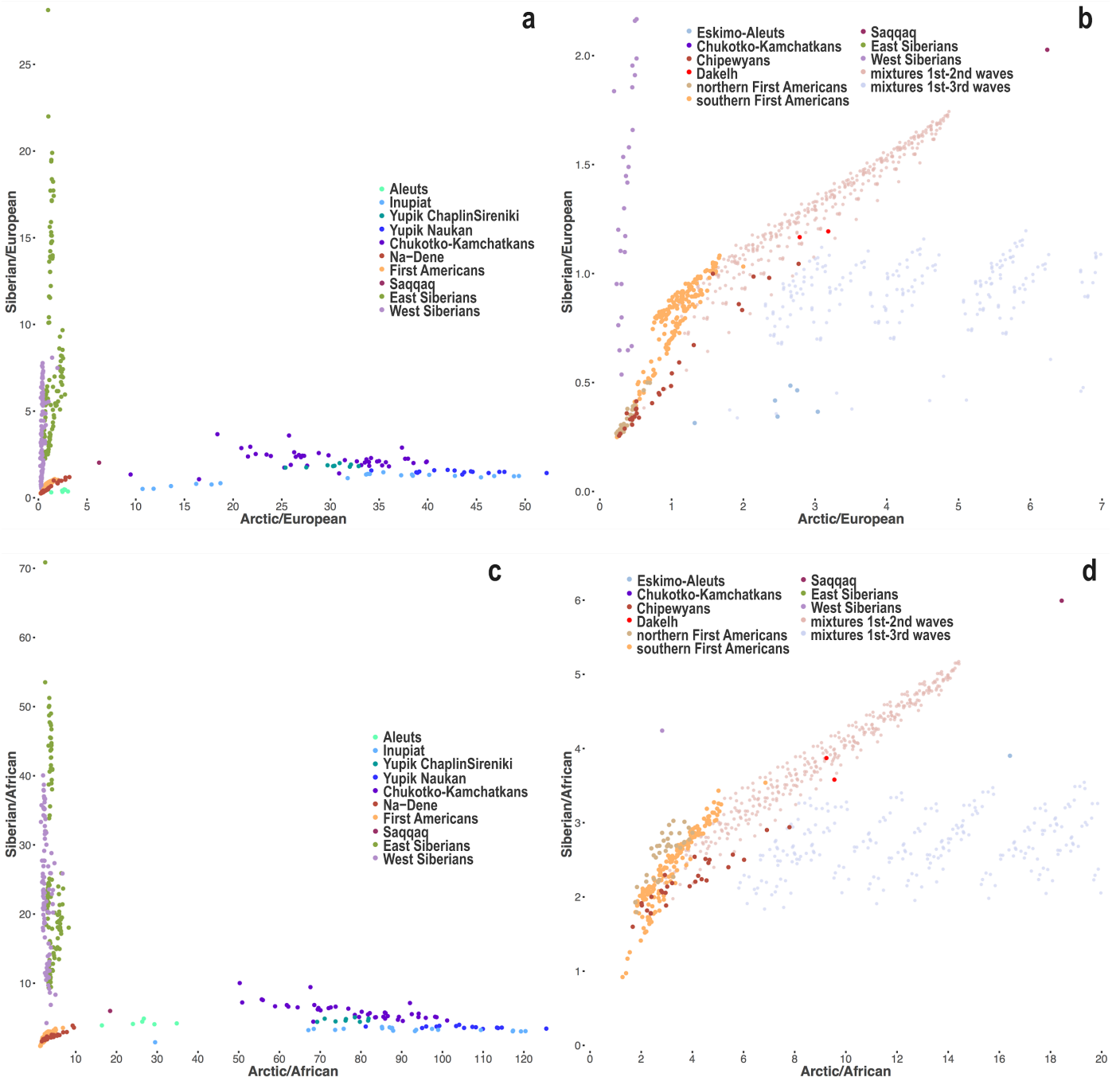


886 **Fig. S6.2.** The same results as in Fig. S6.1, but based on the Illumina SNP array dataset. Northern Athabaskan-
 887 and Tlingit-speaking individuals (outliers on the Arctic and/or Saqqaq axes) selected for the *GLOBETROTTER*
 888 analysis are marked with circles in panel **d**. Two Athabaskan-speaking Dakelh individuals with shotgun
 889 sequencing data, also included into the HumanOrigins and whole genome datasets, are marked with callouts.



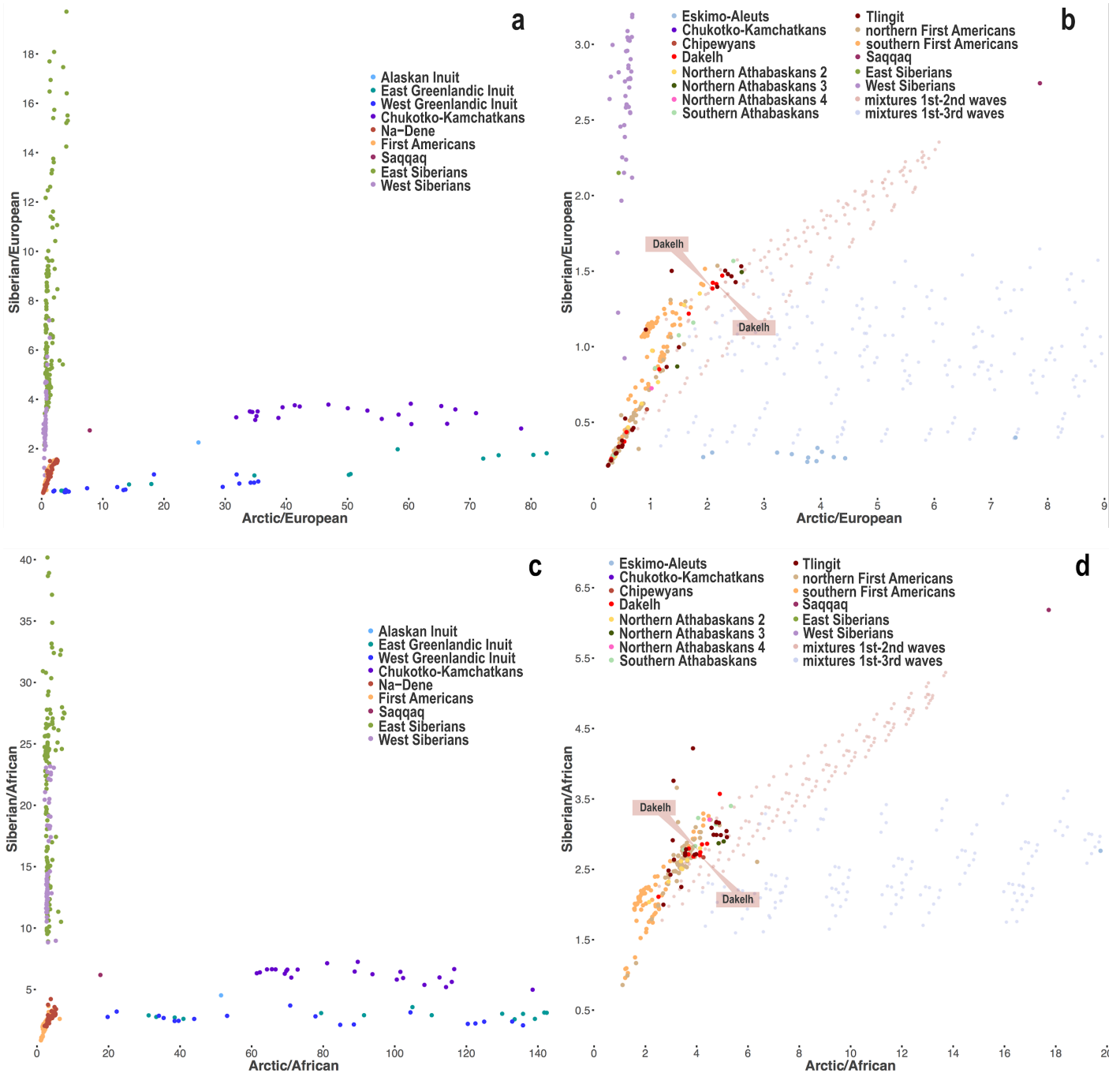
890
 891

892 **Fig. S6.3.** Two-dimensional plots of Arctic and Siberian haplotype sharing statistics normalized using the
 893 European (**a, b**) or African (**c, d**) meta-populations and based on the HumanOrigins SNP array dataset. **a, c,**
 894 Plots showing statistics for individuals of all relevant populations and meta-populations (color-coded according
 895 to the legend). **b, d,** Enlarged areas of the plots showing statistics for First Peoples individuals and simulated
 896 mixtures of any present-day southern First Peoples population and the Saqqaq individual (from 5% to 70%,
 897 with 5% increments), and similar mixtures with Eskimo-Aleut-speaking populations (>5% of Iñupiat or Yup'ik
 898 ancestry). Average values of the statistics in populations were used to calculate the simulated statistics.



899
 900

901 **Fig. S6.4.** The same results as in Fig. S6.3, but based on the Illumina SNP array dataset. For calculating
 902 simulated mixtures, the following Eskimo-Aleut-speaking populations were used: Alaskan Inuit, East or West
 903 Greenlandic Inuit. Various Na-Dene-speaking populations are color-coded, and two Athabaskan-speaking
 904 Dakelh individuals with shotgun sequencing data, also included into the HumanOrigins and whole genome
 905 datasets, are marked with callouts.



906 *References (for this section)*

907 Flegontov, P. *et al.* Genomic study of the Ket: A Paleo-Eskimo-related ethnic group with significant ancient
 908 North Eurasian ancestry. *Sci. Rep.* **6**, 20768 (2016).
 909 Lawson, D. J *et al.* Inference of population structure using dense haplotype data. *PLoS Genet.* **8**, 11–17 (2012).
 910 Raghavan, M. *et al.* The genetic prehistory of the New World Arctic. *Science* **345**, 125832 (2014).
 911 Raghavan, M. *et al.* Genomic evidence for the Pleistocene and recent population history of Native Americans.
 912 *Science* **349**, 1–20 (2015).
 913 Rasmussen, M. *et al.* Ancient human genome sequence of an extinct Palaeo-Eskimo. *Nature* **463**, 757–762
 914 (2010).

915 **Supplementary Information section 7**

916 **Admixture inference with *GLOBETROTTER***

917

918 To interpret haplotype sharing in a more quantitative way, we analyzed putative admixture
 919 events in Na-Dene using *GLOBETROTTER* (Hellenthal et al. 2014). *GLOBETROTTER* operates
 920 on coancestry curves, generated from *ChromoPainter v.2* results (Hellenthal et al. 2014),
 921 finds the best proxies of admixture partners in a dataset, determines admixture ratios and
 922 dates up to two distinct admixture events. To make a complex mixture history of Na-Dene
 923 amenable to *GLOBETROTTER* analysis, we pre-selected individuals based on low European
 924 admixture and high Saqqaq HSS (selected individuals are marked on two-dimensional HSS
 925 plots in Figs. S6.1d and S6.2d). Meta-populations or separate populations were alternatively
 926 used as haplotype donors in the *ChromoPainter v.2* analyses. Substantiating our preliminary
 927 conclusions, Saqqaq and First Peoples were determined to be the most likely admixture
 928 partners for Na-Dene speakers, with the Saqqaq contribution ranging from 7% to 51%,
 929 depending on the dataset and *GLOBETROTTER* set-up. Admixture dates were estimated as
 930 follows: 479 – 1,534 ya (95% confidence interval), if meta-populations were used as
 931 haplotype donors, and 1,073 – 2,202 ya, if populations were used as haplotype donors
 932 (Table S7.1, Fig. S7.1). Although the Paleo-Eskimo admixture in Na-Dene speakers was
 933 revealed by *GLOBETROTTER*, in line with other methods used in this study, the admixture
 934 dates estimated by *GLOBETROTTER* are much later than those estimated by *Rarecoal*
 935 (~4,400 – ~5,000 ya, Table S9.2).

936

		dataset	HumanOrigins	Illumina	HumanOrigins	HumanOrigins
<i>p</i>-value for any admixture event	haplotype donors		9 meta-populations ^{a)}	9 meta-populations ^{a,b)}	67 populations ^{c)}	67 populations ^{c,d)}
	target population		Northern Athabaskans (2 Dakelh, 9 Chipewyans) ^{e)}	2 Tlingit, 8 Northern Athabaskans ^{e)}	Northern Athabaskans (2 Dakelh, 9 Chipewyans) ^{e)}	Northern Athabaskans (2 Dakelh, 9 Chipewyans) ^{e)}
	GLOBETROTTER conclusion		0	0	0.005	0.005
			multiple dates	one-date multiway	uncertain	uncertain
coancestry curves	max. goodness-of-fit ^{g)}		0.987	0.503	0.908	0.695
	max. fit improvement for two-date curves ^{g)}		0.297	0.148	0.276	0.186
two dates, admixture event 1	inferred date, ya		144	522	139	67
	95% confidence interval, ya		92 – 178	315 – 898	29 – 249	29 – 153
	source 1		27% NAM	47% NAM	32% Cree (NAM)	36% Ojibwa (NAM)
	source 2		73% SAM	53% NAM	68% Nahua (SAM)	64% Nahua (SAM)
two dates, admixture event 2	inferred date, ya		916	522	1,335	1,574
	95% confidence interval, ya		479 – 1,534	N/A	739 – 3,487	1,073 – 2,202
	source 1		28% Saqqaq	7% Saqqaq	39% Iñupiat (E-A)	51% Saqqaq
	source 2		72% SAM	93% NAM	61% Cree (NAM)	49% Cree (NAM)

937 **Table S7.1.** The table shows fit statistics for *GLOBETROTTER* coancestry curves, as well as inferred mixture
938 partners, mixture proportions, dates and their 95% confidence intervals. The following abbreviations are used
939 for meta-populations: Eskimo-Aleut speakers, E-A; Northern First Peoples, NAM; Southern First Peoples, SAM.

940 ^{a)} The following non-overlapping meta-populations were used: 1/ the Saqqaq ancient genome and 2/ related
941 Chukotko-Kamchatkan-speaking groups (abbreviated as C-K); 3/ Eskimo-Aleut speakers (Aleuts, Inuit, Iñupiat,
942 Yup'ik, abbreviated as E-A); 4/ Northern First Peoples (NAM); 5/ Southern First Peoples (SAM); 6/ West
943 Siberians (WSIB); 7/ East Siberians (ESIB); 8/ Southeast Asians (SEA); 9/ Europeans (EUR).

944 ^{b)} Individuals with >15% West Eurasian admixture components (Extended Data Fig. 8) were removed from the
945 NAM meta-population.

946 ^{c)} Individuals with >15% West Eurasian admixture components (Extended Data Fig. 8) were removed from
947 NAM populations, and the remaining NAM individuals were merged into one population.

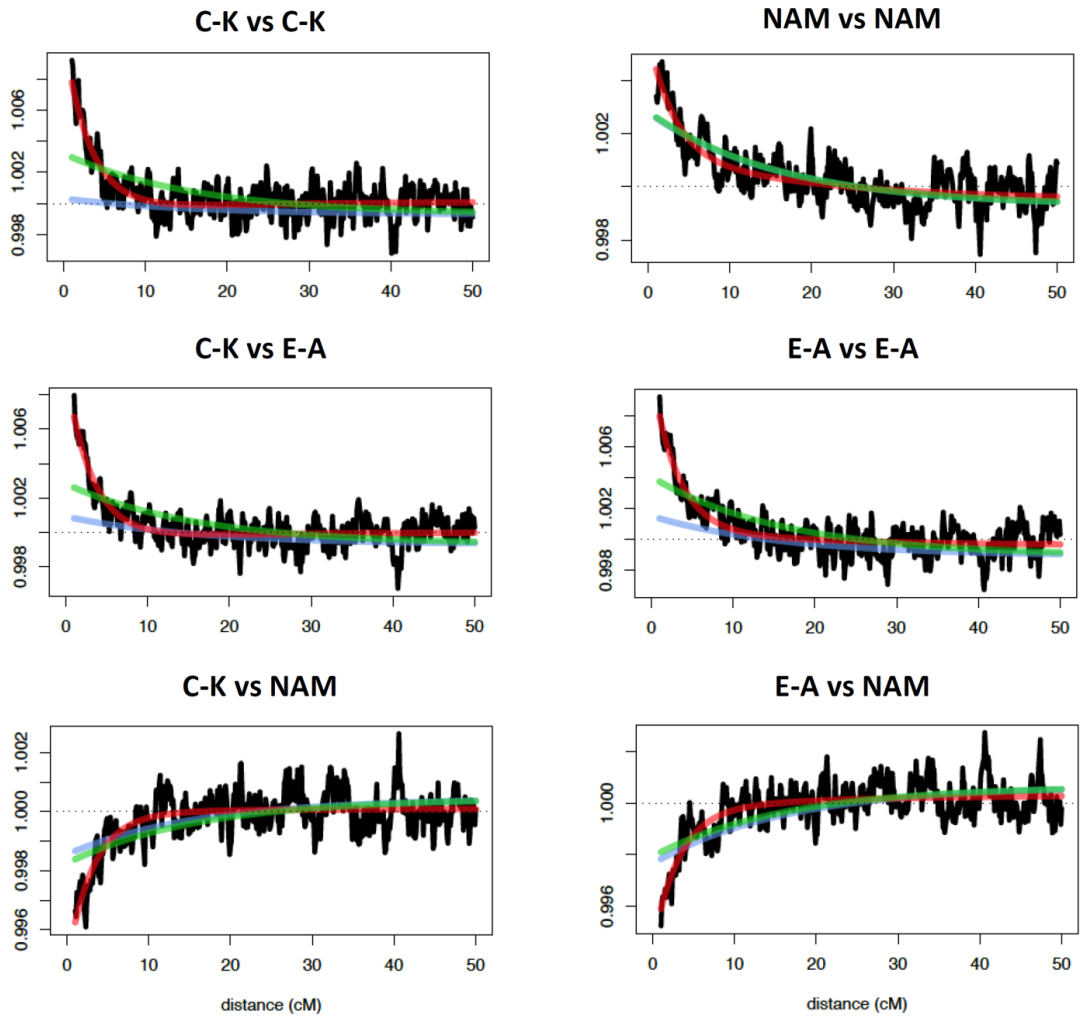
948 ^{d)} Standardizing by a “null” individual was performed to test for consistency, as recommended by the
949 *GLOBETROTTER* manual. This setting might be appropriate if the target population has undergone a
950 bottleneck.

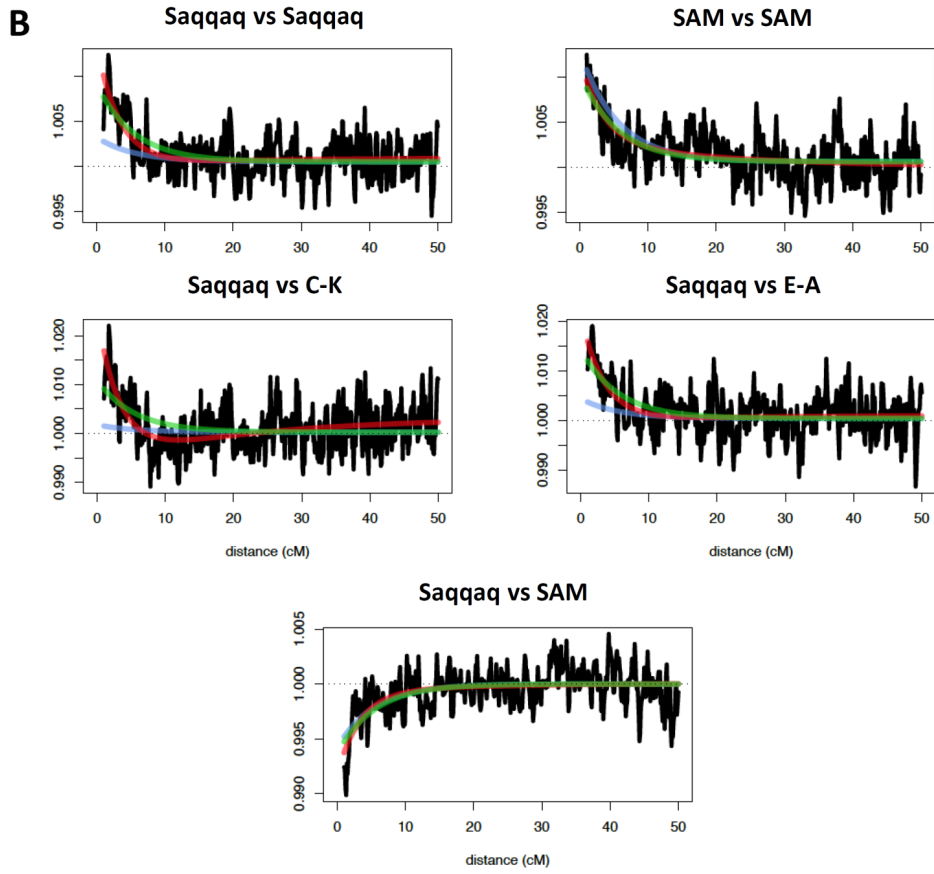
951 ^{e)} To make admixture history of the target population less complex and amenable to *GLOBETROTTER* analysis,
952 only Na-Dene-speaking individuals with prior evidence of elevated Paleo-Eskimo ancestry (Figs. S6.1d, S6.2d)
953 and with <10% West Eurasian ancestry estimated with *ADMIXTURE* (Extended Data Fig. 8) were used.

954 ^{f)} A maximal fit value across all curves is shown: two-date curves were considered if the overall conclusion was
955 “multiple dates”, and one-date curves were considered in other cases. Most relevant coancestry curves
956 illustrating the inferred admixture events are shown in Fig. S7.1.

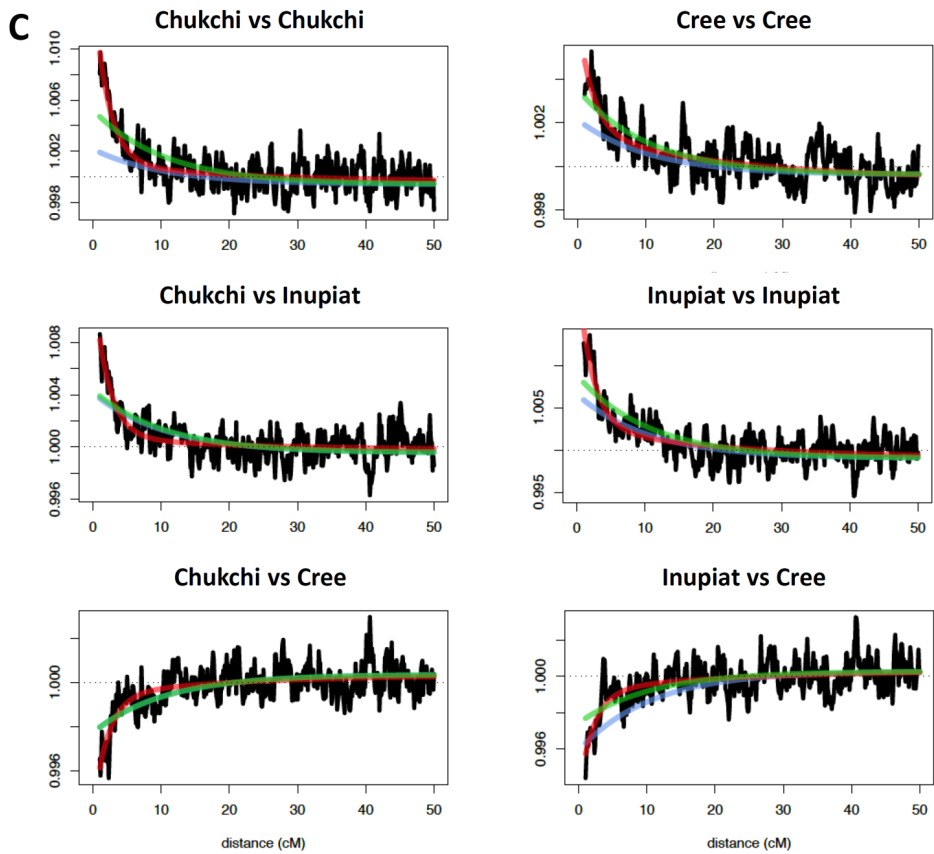
957

958 **Fig. S7.1.** Coancestry curves: relative probability of jointly copying two genomic chunks from a pair of donors
959 (y-axis) vs. genetic distance between the chunks in cM (x-axis). Several representative curves are shown for
960 each model: those with the best fit and those involving admixture partners inferred with *GLOBETROTTER* or
961 their closest proxies. Only curves reflecting the older Paleo-Eskimo/First Peoples admixture event are shown.
962 Here is a list of *GLOBETROTTER* set-ups we explored: Northern Athabaskan speakers with meta-populations (a)
963 or populations (c) as haplotype donors (the HumanOrigins dataset); Na-Dene speakers with meta-populations
964 as haplotype donors (the Illumina dataset) (b). Results under an alternative setting (normalization by a ‘null
965 individual’) are also shown for populations as haplotype donors (d). Original data are shown in black, and
966 curves approximating two admixture events with different dates – in red, two events with a single date – in
967 green, and one event – in blue. Composition of target Na-Dene populations is given in Table S7.1, and Figs.
968 S6.1d, S6.2d. The following meta-populations were used as haplotype donors: 1/ Saqqaq, 2/ related Chukotko-
969 Kamchatkan speakers (abbreviated as C-K); 3/ Eskimo-Aleut speakers (E-A); 4/ Northern First Peoples (NAM);
970 5/ Southern First Peoples (SAM); 6/ West Siberians (WSIB); 7/ East Siberians (ESIB), 8/ Southeast Asians (SEA);
971 9/ Europeans (EUR).

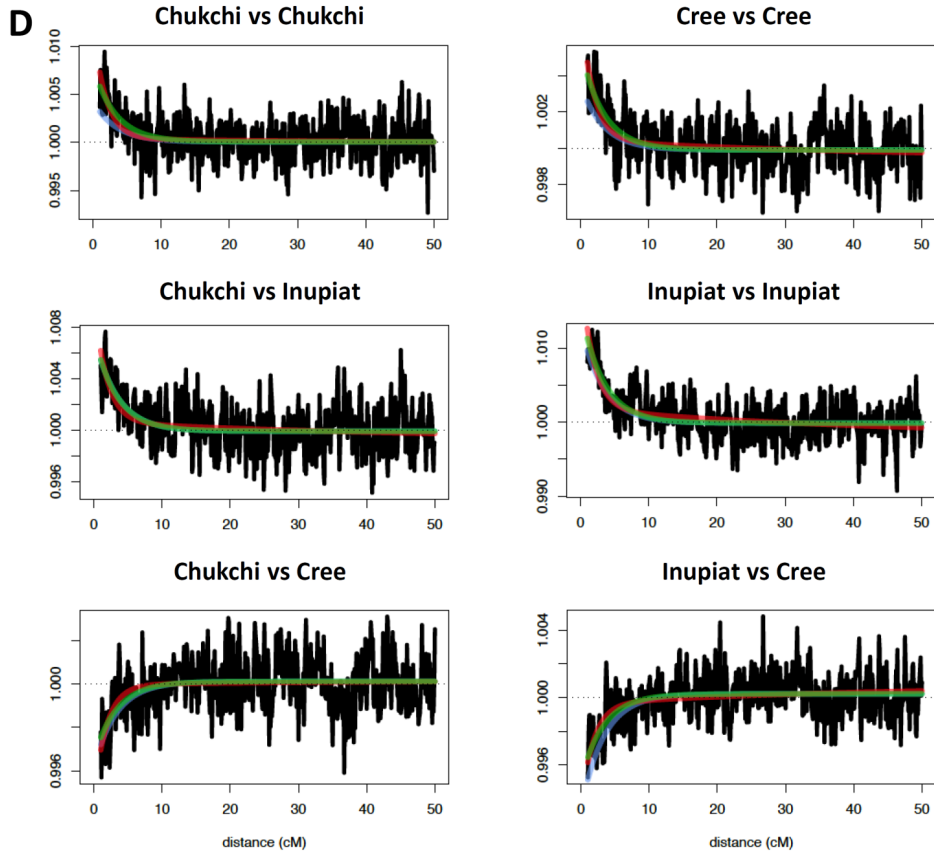
A



973



974



975

976

977 *References (for this section)*

978 Hellenthal, G. *et al.* A genetic atlas of human admixture. *Science* **343**, 747–751 (2014).

979

980 **Supplementary Information section 8**

981 **Rare allele sharing statistics**

982

983 To explore PPE ancestry in American and Beringian populations in a model-free way, we
 984 used rare allele sharing statistics. For this analysis, we used all segregating sites in the
 985 Simons Genome Diversity panel (Mallick et al. 2016) as well as in the present-day data from
 986 Raghavan et al. (2015), restricting to those sites at which at least 90% of individuals in both
 987 datasets independently have non-missing data. We also filtered out sites based on genome
 988 mappability, as defined in the PSMC pipeline (Li and Durbin 2011). This resulted in a dataset
 989 of 14,740,572 segregating sites in the combined dataset. The population composition of the
 990 dataset is summarized in Table S8.1.

991

Abb.	Full Name	Populations ¹⁾	Nr of samples
AFR	Africans	Bantu Herero, Bantu Kenya, Bantu Tswana, Biaka, Dinka, Esan, Gambian, Ju 'hoan North, Khomani San, Luhya, Luo, Mandenka, Masai, Mbuti, Mende, Somali, Yoruba	39
EUR	Europeans	Basque, Bergamo, Bulgarian, Crete, Czech, English, Estonian, French, Greek, Hungarian, Norwegian, Orcadian, Polish, Sardinian, Spanish, Tuscan	33
SEA	Southeast Asians	Ami, Atayal, Burmese, Cambodian, Dai, Kinh, Lahu, Miao, She, Thai	21
SIB	Core Siberians	Nivkh, Altaian, Buryat, Even, Ket, Mansi, Tubalar, Ulchi, Yakut	22
C-K	Chukotko-Kamchatkan speakers	Itelmen, Koryak, Chukchi	4
P-E	Paleo-Eskimo	Saqqaq	1
ALE	ancient Aleut	ancient Aleut	1
ESK	Eskimo speakers	Yup'ik from Chukotka, East and West Greenlandic Inuit	9
ATH	Northern Athabaskan speakers	Dakelh, Chipewyan, ancient Athabaskan	5
SAM	Southern First Peoples	Aymara, Chane, Huichol, Karitiana, Mayan, Mixe, Mixtec, Piapoco, Pima, Quechua, Surui, Yukpa, Zapotec	29
Total			164

992 **Table S8.1:** A table listing all modern samples and groups used in the rare allele sharing analysis. Data is from
 993 the two sources: Raghavan et al. (2015) and the Simons Genome Diversity Project data set (Mallick et al.
 994 2016), as indicated in Supplementary Table 4.

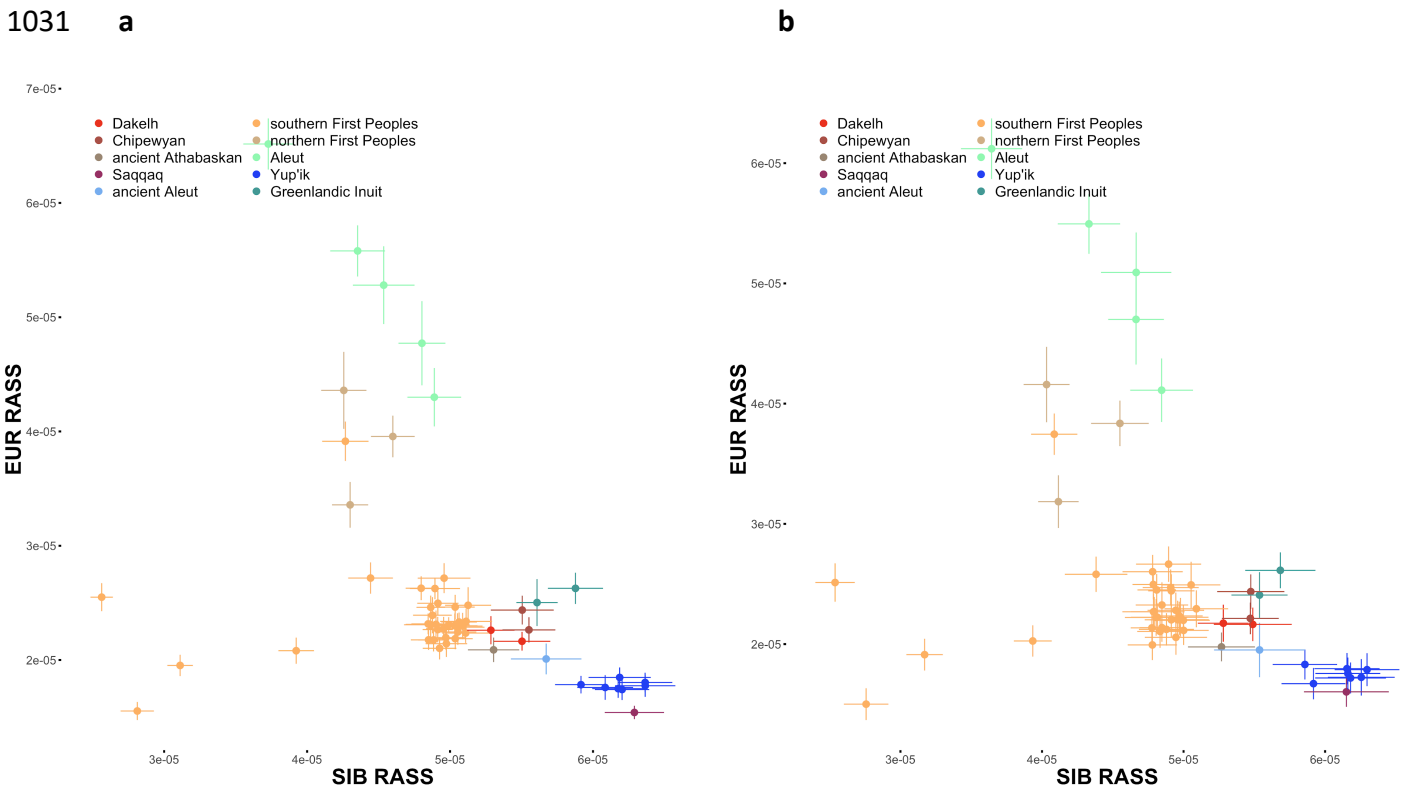
995 We then sampled pseudo-haploid genotypes on three ancient shotgun genomes
 996 (Saqqaq, I0719 called “Ancient Aleut” and I5319 called “Ancient Athabaskan”), the latter
 997 two of which are described in this study for the first time. Here, we used a pseudo-haploid
 998 calling method and i) required a minimum of 3 reads at each site, ii) restricted to biallelic
 999 sites, iii) called the allele that was supported by the majority of reads at that site. Since this
 1000 method is subtly dependent on coverage (high-coverage positions will have a stronger
 1001 reference bias than low-coverage positions), we first downsampled all query positions to
 1002 the required minimum coverage of 3, respectively.

1003 To quantify rare allele sharing, we developed the rare allele sharing statistics (RASS).
 1004 Essentially, RASS is similar to an outgroup- f_3 -statistic, but ascertained on rare derived alleles
 1005 in a set of reference populations. Specifically, we define

1006
$$RASS(x, y; \{\text{References, Outgroup}\}) = \frac{1}{L} \sum_i x_i y_i$$

1007 where the sum runs over all sites with derived allele count below some cutoff (say 5 or less)
 1008 within the *Reference* and *Outgroup* populations, x_i is the derived allele frequency in the test
 1009 individual, y_i is the derived allele frequency in the reference population, and L is the
 1010 number of sites in the sum (excluding missing data). Here, the *Outgroup* (Africans) is used to
 1011 polarize derived vs. ancestral alleles – that is, we look at the outgroup population, and take
 1012 the majority allele in that outgroup population to specify which should be the majority allele
 1013 for the ascertainment. If the majority of outgroup chromosomes have the non-reference
 1014 allele, then the ascertainment is done on the reference allele being rare (instead of the non-
 1015 reference allele).

1016 The following outgroup and reference meta-populations were used (Table S8.1):
 1017 Africans (39 ind.), Europeans (33 ind.), Southeast Asians (21 ind.), Siberians (22 ind.),
 1018 Chukotko-Kamchatkan (C-K) speakers (4 ind. including one Chukchi ind.). Importantly, the
 1019 ascertainment on allele frequency is done only within the reference and outgroup
 1020 populations, not within the test individuals. Here, reference populations included non-
 1021 American populations only, while test populations included American populations and
 1022 Chukotkan Yup'ik, closely related to American Inuit. Because of this ascertainment rule,
 1023 RASS between test individuals and reference populations is not affected by genetic drift
 1024 within the test individuals since putative admixture events, and we can therefore formally
 1025 test for admixture models within the test samples based on RASS (see below). For present-
 1026 day and ancient First Peoples, Athabaskan speakers, Paleo-Eskimos (P-E), and Eskimo-Aleut
 1027 (E-A) speakers we estimated RASS vs. Siberian and C-K reference meta-populations. Since
 1028 among C-K groups Chukchi demonstrate the highest level of E-A admixture (Fig. 1a,
 1029 Extended Data Figs. 2 and 8, sections 5, 10), for some analyses we excluded the Chukchi
 1030 individual.



1032

1033 **Fig. S8.1.** Two-dimensional plots of European (EUR) and Siberian (SIB) rare allele sharing statistics (RASS). Rare
 1034 alleles occurring from 2 to 10 times in the reference set of 238 haploid genomes (0.8-4.2% frequency)

1035 contributed to the statistics; the full **(a)** and transversion-only **(b)** datasets were used. The sample size for this
1036 analysis equals 238 + 2 haploid genomes in a target individual since individuals were analyzed separately.
1037 Standard deviations were calculated using a jackknife approach with chromosomes used as resampling blocks.
1038 Single standard error intervals and means are plotted. Populations and meta-populations are color-coded
1039 according to the legend.

1040

1041 We first removed all test individuals with substantial European admixture. To this
1042 end, we looked at RASS with SIB vs. EUR (see Fig. S8.1) and identified individuals with higher
1043 than expected EUR RASS, as compared to the bulk of Native American individuals. After
1044 inspection of Fig. S8.1, we used $>3 \times 10^{-5}$ as the RASS cutoff to mark individuals as admixed.
1045 In addition, we removed Native American individuals that were outliers according to the SIB
1046 RASS as they might have a low degree of African admixture (we used $<4.5 \times 10^{-5}$ as the cutoff
1047 to mark individuals as admixed). Since the African meta-population was used as an outgroup
1048 for RASS calculation, we could not measure African RASS directly.

1049 We then investigated RASS with C-K vs. RASS with SIB for the transversion-only
1050 dataset, as shown in Fig. S8.2. First, we observe that all Athabaskans (four present-day and
1051 one ancient individual), are shifted away from the cluster of First Peoples, towards the
1052 ancient Saqqaq individual. To explicitly test admixture scenarios, we simulated admixture
1053 points of 5%, 10%, ..., 75% Saqqaq admixture in Native Americans. The simulated points are
1054 simply linear combinations of the positions on the plot of various First Peoples individuals
1055 and Saqqaq. Importantly, RASS of Athabaskans matches admixture points between 29% and
1056 38%. The ancient Athabaskan is consistent with a slightly higher level of Saqqaq admixture
1057 of 42%, in agreement with other analyses (Fig. 1, Extended Data Figs. 2-4). Both C-K and
1058 Siberian RASS for the ancient Aleut individual I0719 sequenced by the shotgun approach
1059 (2.3x average coverage, Extended Data Table 1) are also perfectly consistent with a First
1060 Peoples/Paleo-Eskimo admixture (~65% Saqqaq admixture). In contrast, Inuit and especially
1061 Yup'ik individuals are shifted to the right on the x-axis, i.e. they demonstrate elevated C-K
1062 RASS not expected under the simple First Peoples/Paleo-Eskimo admixture scenario.

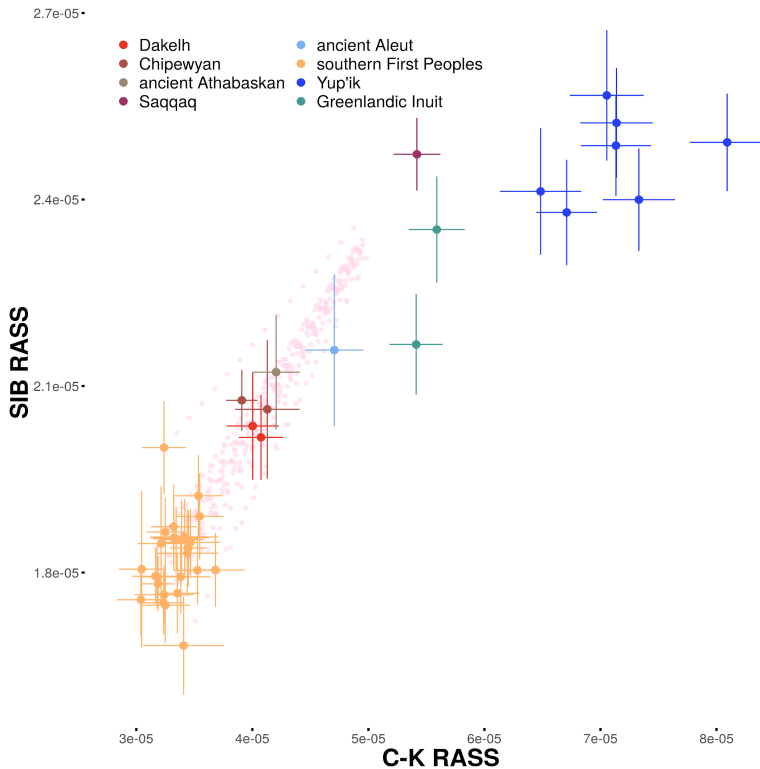


Fig. S8.2. Two-dimensional plot of Chukotko-Kamchatkan (C-K) and Siberian (SIB) rare allele sharing statistics (RASS). Rare alleles occurring from 2 to 5 times in the reference set of 238 haploid genomes (0.8-2.1% frequency) contributed to the statistics; the Chukchi individual was dropped from the C-K group, and the transversion-only dataset was used. The sample size for this analysis equals 238 + 2 haploid genomes in a target individual since individuals were analyzed separately. Standard deviations were calculated using a jackknife approach with chromosomes used as resampling blocks. Single standard error intervals and means are plotted. Populations and meta-populations are color-coded according to the legend. RASS for simulated mixtures of any present-day southern Native American individual and the Saqqaq individual (from 5% to 75% Saqqaq ancestry, with 5% increments) are plotted as semi-transparent pink circles.

1088

1089 E-A admixture found in all C-K populations (section 10), but especially high in
 1090 Chukchi (Fig. 1a, Extended Data Figs. 2 and 8, section 5), influences RASS for the ancient
 1091 Aleut individual. This effect is observed when the Chukchi individual is included into the C-K
 1092 reference group (Fig. S8.3b,c), especially in the case of the 2 to 5 allele count range (Figs.
 1093 S8.2 and S8.3c). The fact that E-A admixture in C-K influences results strongly when only the
 1094 rarest alleles are considered is not surprising since the bidirectional E-A/C-K admixture has
 1095 been dated to 1,700-2,300 ya using *Rarecoal* (Table. S9.2), and it is expected to post-date
 1096 the emergence of the first Neo-Eskimo archaeological culture on the Chukotkan side of
 1097 Bering Strait ca. 2200 calBP (see the Discussion). In contrast, the P-E admixture events in E-A
 1098 and Na-Dene have both been dated to roughly 4,400-4,900 ya using *Rarecoal* (Table S9.2)
 1099 and to 2,700-4,900 ya using the *ALDER* method (Table S12.1). Therefore, the signal of the
 1100 most recent event becomes stronger when the rarest alleles (reflecting recent mutations in
 1101 most cases) are considered.

1102 The C-K reference group can be replaced by the Saqqaq individual (SNP genotypes
 1103 called as described above), see Fig. S8.4. This approach does not allow analysis of low-
 1104 coverage ancient samples, but the signal of P-E admixture in Na-Dene speakers remains.

1105 Using the same genomic dataset, we also calculated outgroup f_3 -statistics:

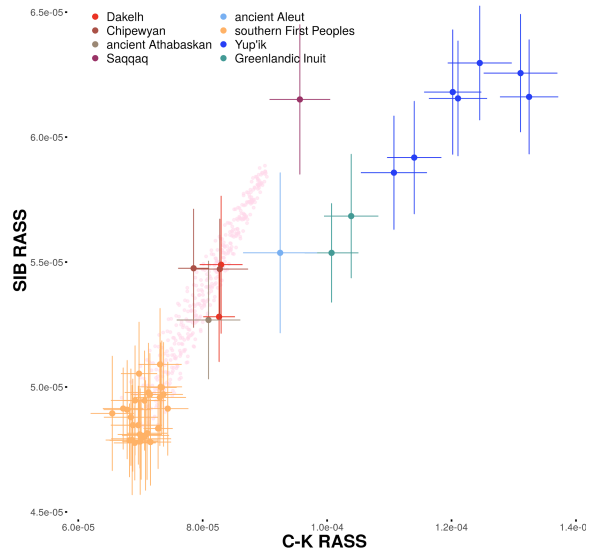
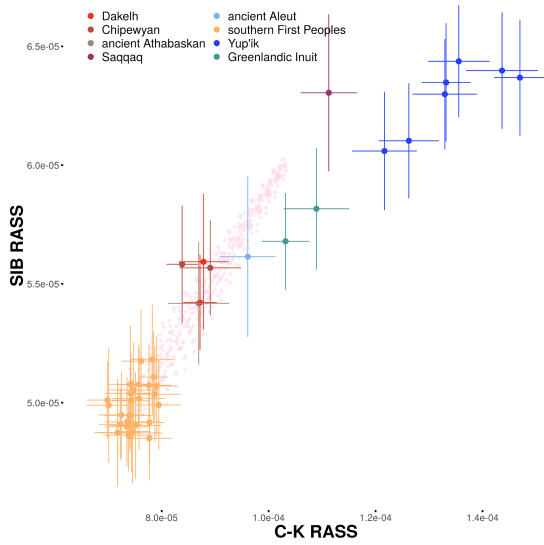
$$1106 \quad f_3(x, y; O) = \frac{1}{L} \sum_i (o - x_i)(o - y_i)$$

1107 where x_i is the allele frequency in the test population, y_i is the allele frequency in the
 1108 reference population, and o_i is the allele frequency in the outgroup (the African meta-
 1109 population). Again, L is the number of sites in the sum. This statistic takes into account all
 1110 sites, not only rare ones. It is clear that the resolution provided by C-K, Saqqaq and Siberian

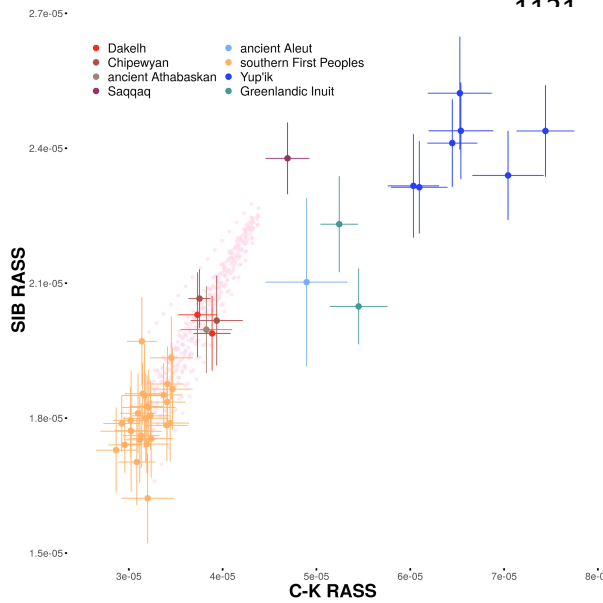
1111 RASS is much higher than that of outgroup statistics f_3 (Africans; C-K, an American/E-A/P-E
1112 individual), f_3 (Africans; Saqqaq, an American/E-A/P-E individual), and f_3 (Africans; Siberians,
1113 an American/E-A/P-E individual) (Fig. S8.5). Chipewyans and Dakelh are not distinguishable
1114 from First Peoples using outgroup f_3 -statistics, but are distinguishable using RASS.

1115 RASS and outgroup f_3 -statistics are correlated, especially if the rare allele count
1116 range from 2 to 10 is used (Fig. S8.6).

1117



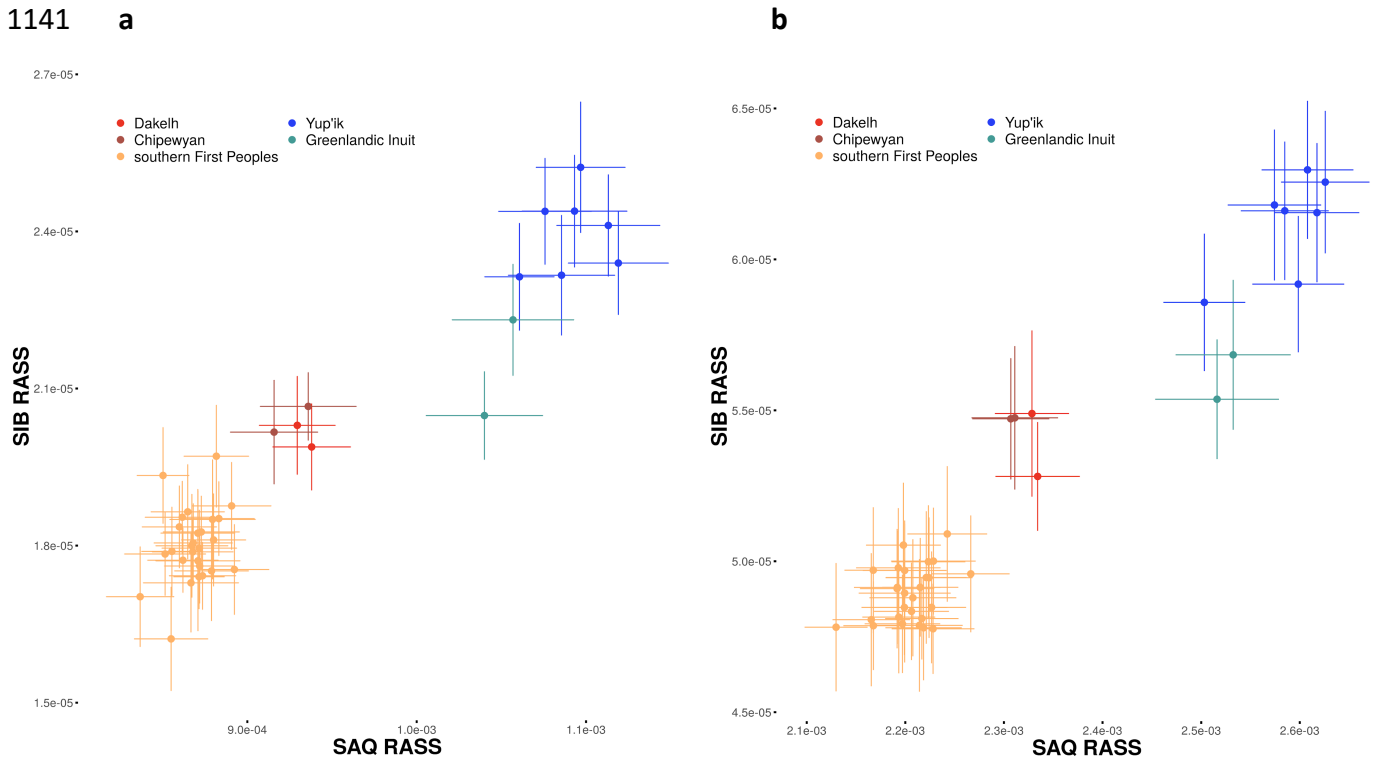
1119



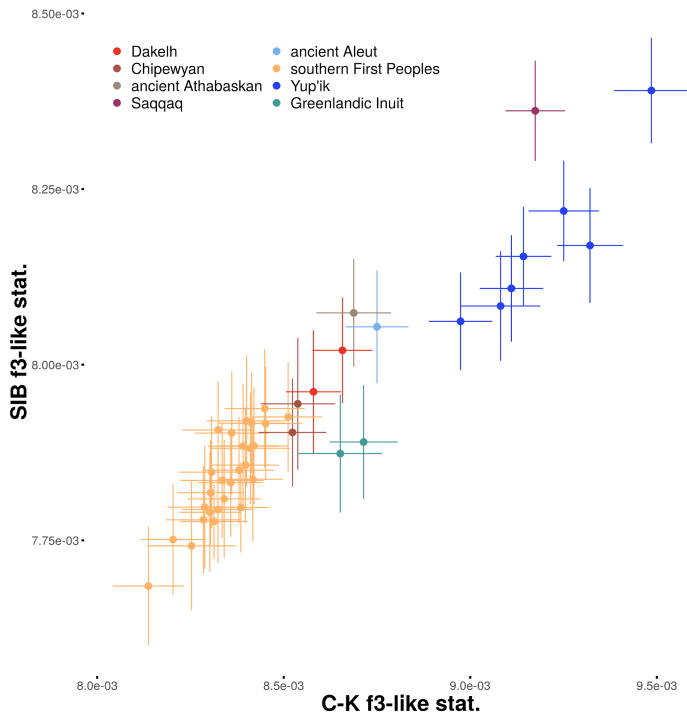
1121

1140

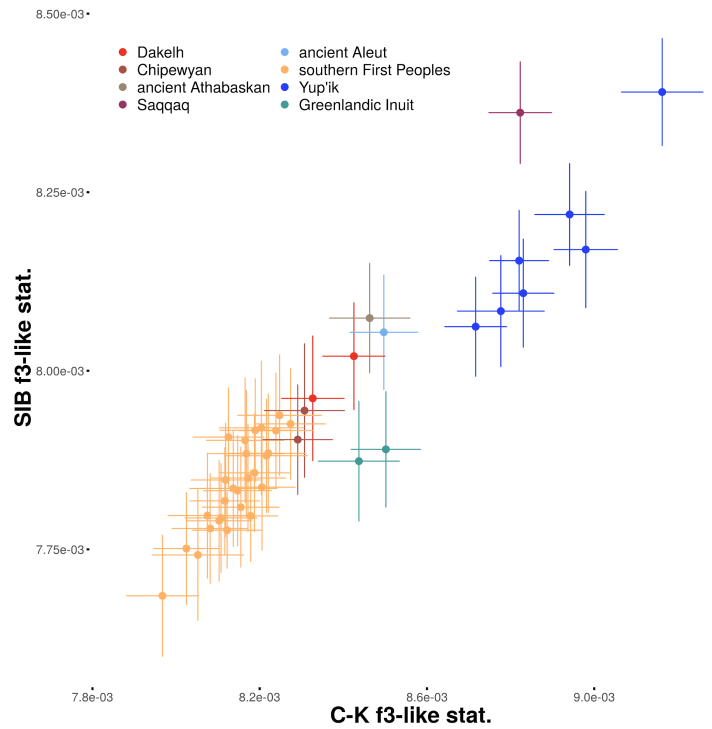
Fig. S8.3. Two-dimensional plots of Chukotko-Kamchatkan (C-K) and Siberian (SIB) rare allele sharing statistics (RASS). Rare alleles occurring from 2 to 10 (**a**, **b**) or 5 times (**c**) in the set of reference populations contributed to the statistics; the transversion-only dataset was used. The Chukchi individual was alternatively included into the C-K reference group (**b**, **c**) or dropped (**a**). The sample size for this analysis equals 238 + 2 haploid genomes in a target individual since individuals were analyzed separately. Standard deviations were calculated using a jackknife approach with chromosomes used as resampling blocks. Single standard error intervals and means are plotted. Populations and meta-populations are color-coded according to the legend. RASS for simulated mixtures of any present-day southern Native American individual and the Saqqaq individual (from 5% to 75% Saqqaq ancestry, with 5% increments) are plotted as semi-transparent pink circles.



1150 **a**



b



1151 **c**

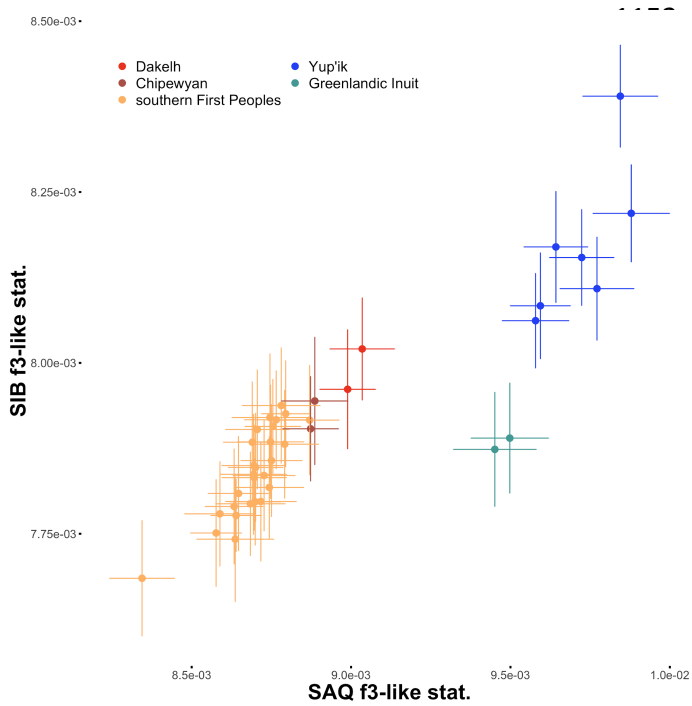
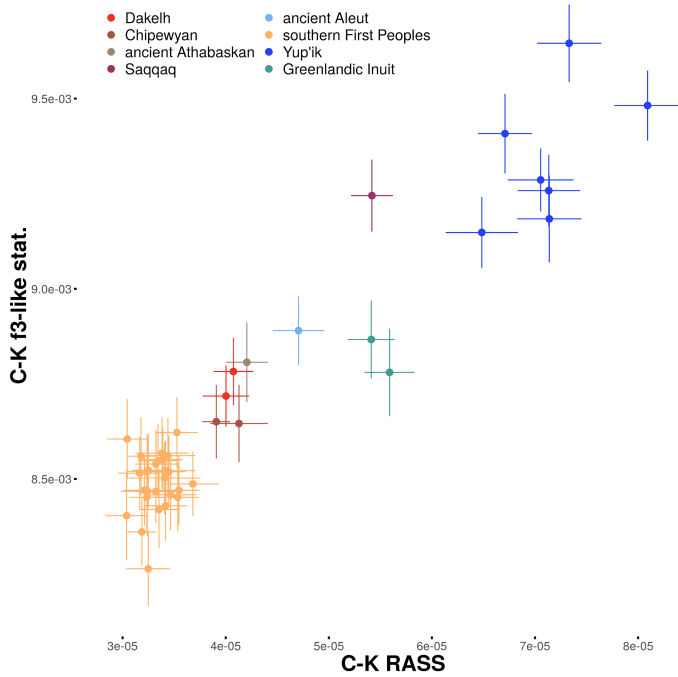


Fig. S8.5. Two-dimensional plots of Chukotko-Kamchatkan (C-K) and Siberian (SIB) (**a, b**) or Saqqaq (SAQ) and Siberian (SIB) (**c**) outgroup f_3 -statistics. The Chukchi individual was alternatively included into the C-K reference group (**b**) or dropped (**a**); the transversion-only dataset was used. The sample size for this analysis equals 238 + 2 haploid genomes in a target individual since individuals were analyzed separately. Standard deviations were calculated using a jackknife approach with chromosomes used as resampling blocks. Single standard error intervals and means are plotted. Populations and meta-populations are color-coded according to the legend.

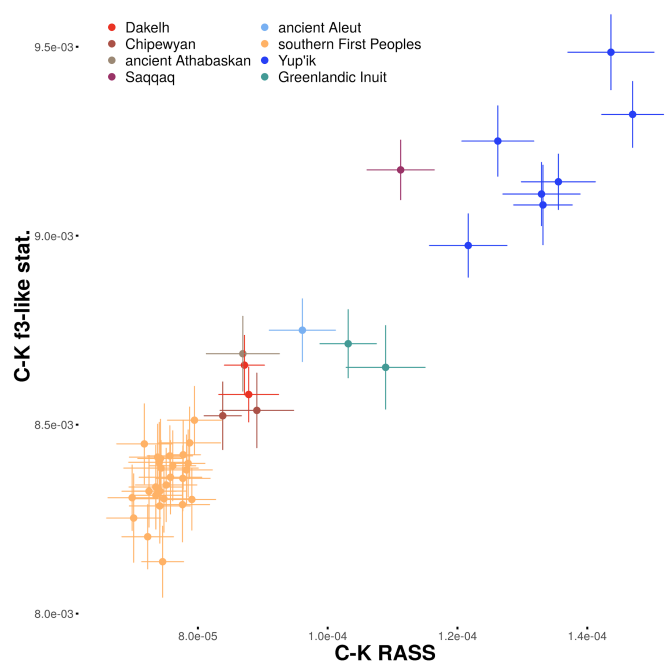
1170

1171

a



b



1173

1174 **Fig. S8.6.** Two-dimensional plots of Chukotko-Kamchatkan (C-K) rare allele sharing statistics vs. outgroup f_3 -
 1175 statistics. Rare alleles occurring from 2 to 5 (a) or 10 times (b) in the set of reference populations contributed
 1176 to RASS; the transversion-only dataset was used. The Chukchi individual was not included into the C-K
 1177 reference group. The sample size for this analysis equals 238 + 2 haploid genomes in a target individual since
 1178 individuals were analyzed separately. Standard deviations were calculated using a jackknife approach with
 1179 chromosomes used as resampling blocks. Single standard error intervals and means are plotted. Populations
 1180 and meta-populations are color-coded according to the legend.

1181

1182 *References (for this section)*

- 1183 Li, H. & Durbin, R. Inference of human population history from individual whole-genome sequences. *Nature*
 1184 **475**, 493–496 (2011).
 1185 Mallick, S. *et al.* The Simons Genome Diversity Project: 300 genomes from 142 diverse populations. *Nature*
 1186 **538**, 201–206 (2016).
 1187 Raghavan, M. *et al.* Genomic evidence for the Pleistocene and recent population history of Native Americans.
 1188 *Science* **349**, 1–20 (2015).
 1189

1190 **Supplementary Information section 9**

1191 **Demographic modeling with *Rarecoal***

1192

1193 **Rarecoal**

1194 *Rarecoal* is a software that implements a fast algorithm to estimate the joint site frequency
1195 spectrum for rare alleles (Schiffels et al. 2016). Since the initial report in Schiffels et al. 2016,
1196 we have improved the software substantially: We have added pulse-like admixture events
1197 to be able to model admixture graphs, and we have significantly optimized crucial parts of
1198 the program. The updated mathematical derivations of the model are included as a PDF
1199 document in the repository: <https://github.com/stschiff/rarecoal>. We also built in a
1200 regularization for population size changes, which penalizes large changes of the population
1201 size and helps to avoid overfitting.

1202

1203 **Data**

1204 In the following analysis, we will use the abbreviations for meta-populations shown in Table
1205 S9.1.

1206

Abb.	Full Name	Populations	Nr of samples
EUR	Europeans	Basque, Bergamo, Bulgarian, Crete, Czech, English, Estonian, French, Greek, Hungarian, Norwegian, Orcadian, Polish, Sardinian, Spanish, Tuscan	33
SEA	Southeast Asians	Ami, Atayal, Burmese, Cambodian, Dai, Kinh, Lahu, Miao, She, Thai	21
SIB	Core Siberians	Nivkh, Altaian, Buryat, Even, Ket, Mansi, Tubalar, Ulchi, Yakut	22
C-K	Chukotko-Kamchatkan speakers	Itelmen, Koryak	3
ALE	Aleuts	Aleut	5
ESK	Eskimo speakers	Yup'ik from Chukotka, East and West Greenlandic Inuit	9
ATH	Northern Athabaskan speakers	Dakelh, Chipewyan	4
NAM	Northern First Peoples	Cree, Tsimshian	3
SAM	Southern First Peoples	Aymara, Mixe, Mixtec, Piapoco, Quechua, Yukpa, Zapotec	14
Total			114

1207 **Table S9.1:** A table listing all modern samples and groups used in the *Rarecoal* analysis. Data is from the two
1208 sources: Raghavan et al. (2015) and the Simons Genome Diversity Project data set (Mallick et al. 2016), as
1209 indicated in Supplementary Table 4.

1210

1211 In the following model fits, we use “rarecoal maxl” to obtain maximum likelihood fits. For
1212 our final models, we also use “rarecoal mcmc” to obtain credibility intervals for parameters.
1213 We fit rare allele sharing histograms with maximum allele count of 4 in all modeled
1214 populations (corresponding to a maximum allele frequency of 1.7% in the full data set). This
1215 corresponds to 66% of all mutations in the full data set, i.e. much higher than the allele
1216 frequency due to the strong skew of the allele frequency spectrum towards rare alleles.

1217 In order to check model fits, we use the Rare Allele Sharing statistics (RASS) as

1218 defined in the Methods section. RASS between two populations X and Y is defined as

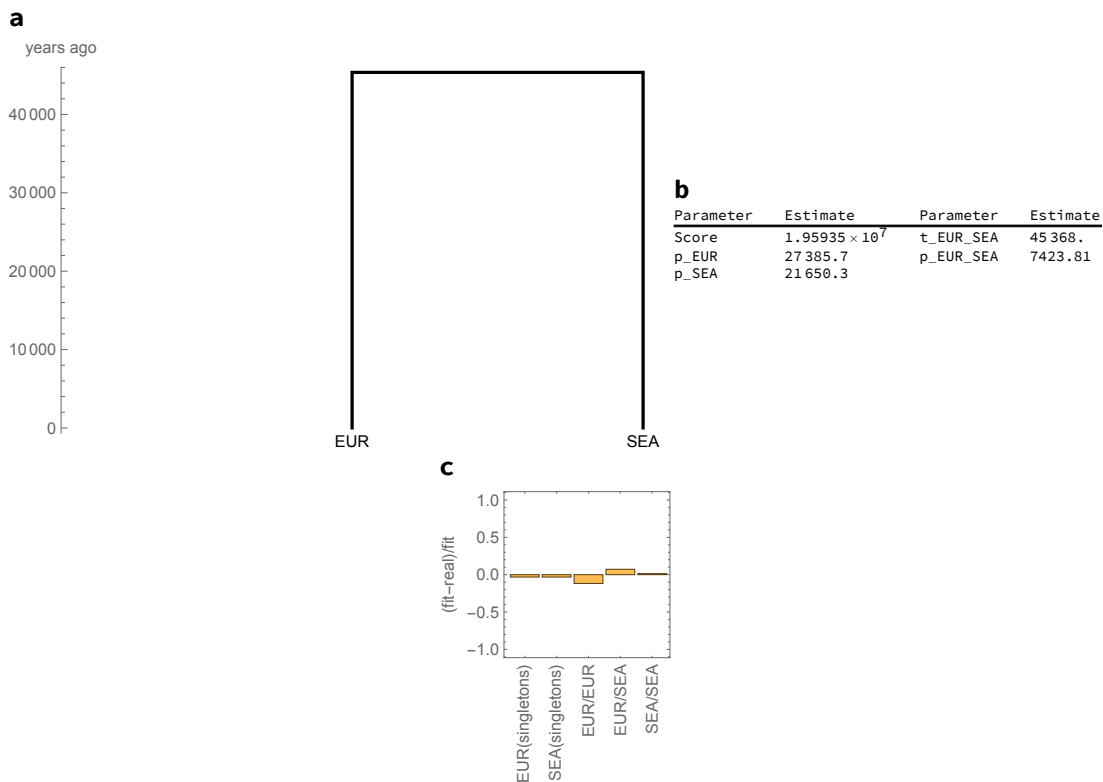
1219
$$RASS(X, Y) = \frac{1}{L} \sum_i x_i y_i,$$

1220 where x_i and y_i are the derived allele frequencies in populations X and Y, respectively. The
 1221 sum runs over all sites with total allele count less than or equal to 4 in the entire dataset
 1222 considered in the fit, and L is the number of those sites. Note that RASS can be computed
 1223 also with X=Y, in which case it describes rare allele sharing between individuals from the
 1224 same population. In addition, we also consider the rate of singletons per population as a
 1225 statistic to compare fits with data (see panels c in figures below).

1226

1227 **Fitting a simple split model for Europeans and Southeast Asians**

1228 We started with only two populations, Europeans (EUR) and Southeast Asians (SEA), and
 1229 fitted a simple model with 4 parameters (a single split time, two population sizes in the two
 1230 extant branches, and one population size in the ancestral branch). The result yields –
 1231 unsurprisingly – a very good fit with a split time of around 45,000 years ago (ya) (Fig. S9.1).



1232

1233 **Fig. S9.1.** A model connecting Europeans (EUR) and Southeast Asians (SEA). A schematic indicating the tree (a),
 1234 the parameters (b) and the fit deviation between the model and the data (c).

1235

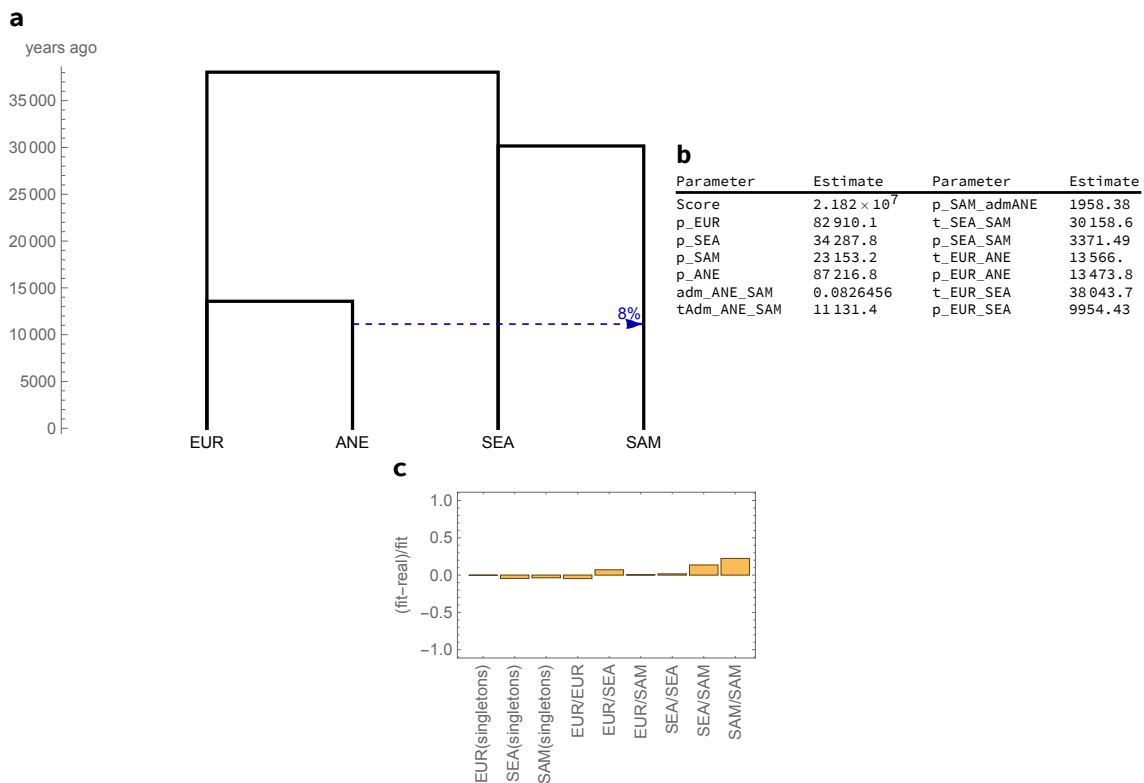
1236 As shown in Fig. S9.1, we summarize models using a schematic (a), a table with the
 1237 parameters (b), and the relative deviation between the model and the data in terms of rare
 1238 allele sharing statistics (RASS, see above and the Methods). Here, the statistics
 1239 EUR(singletons) and SEA(singletons) indicate simply the deviation of the fit in terms of
 1240 frequency of singletons in both populations. EUR/EUR and SEA/SEA indicate deviations
 1241 between the data and the model for mutations shared within each group, and EUR/SEA
 1242 indicates the fit deviation for allele sharing across groups.

1243 Parameter names (Fig. S9.1b) starting with “p” denote population sizes, and those
 1244 starting with “t” denote split times. By “Score” we denote the negative log-likelihood: the
 1245 lower this number, the better the fit. The inferred population sizes and split times are scaled
 1246 to real time and size using a mutation rate of 1.25×10^{-8} (Scally and Durbin 2012) and a
 1247 generation time of 29 years (Fenner 2005, Scally and Durbin 2012).

1248

1249 **Adding Native Americans**

1250 We next added Southern First Peoples (SAM) onto the tree. From our *qpGraph* analysis (see
 1251 section 10), we know that First Peoples inherit a separate Eurasian lineage, which from
 1252 previous publications is known as *Ancient North Eurasian* (ANE) (Patterson et al. 2012,
 1253 Raghavan et al. 2014a). We model this lineage as a “ghost” population that split off from the
 1254 EUR branch. The inferred model fits well (Fig. S9.2), although the inferred ANE contribution
 1255 to Native Americans (here 8%) is far below the estimates in our *qpGraph* models, which are
 1256 around 40% (Fig. S10.5). We believe this may be due to the lack of the Late Pleistocene
 1257 Native American bottleneck, which we will add further below when adding other Native
 1258 American populations. The EUR/ANE split time at 13.6 kya is also unrealistically late. Most
 1259 likely this effect is observed because instead of ancient genomes we used high-coverage
 1260 genomes of present-day Europeans having substantial ANE-related admixture (Haak et al.
 1261 2015).



1262

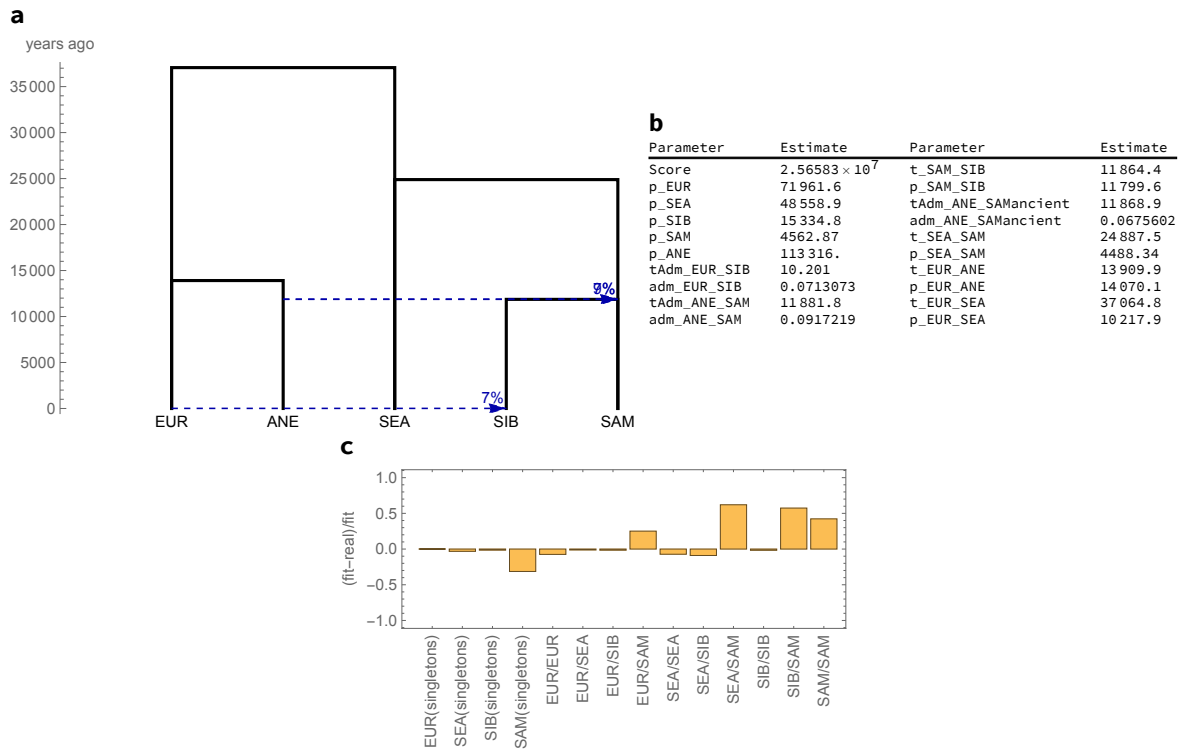
1263 **Fig. S9.2.** Adding Southern First Peoples onto the EUR/SEA tree, with a ghost population ANE.

1264

1265 **Adding Siberians**

1266 We then added Siberians (SIB) to the tree. According to our *qpGraph* models, they can be
 1267 modeled as a sister clade to Native Americans, with extra European and East Asian
 1268 contributions. We here omitted the East Asian contribution to check whether a simpler

1269 model with only European contribution also fits. Also, we now split the ANE contribution
 1270 into two admixture events, one into the ancestral SIB/SAM branch, and one into the SAM
 1271 branch (Fig. S9.3), as in the *qpGraph* models. The resulting fit shows substantial
 1272 overestimation of SEA/SAM allele sharing, which is likely due to the lack of the American
 1273 Pleistocene bottleneck, as well as the lack of additional Asian admixture in SIB, which
 1274 “drags” the SEA split time close to SIB and SAM, leading to the overestimation. We
 1275 therefore added SEA admixture in the next model with Chukotko-Kamchatkan speakers
 1276 below.



1277
 1278 **Fig. S9.3.** Adding Siberians onto the EUR/SEA/SAM tree. As indicated in panel c, RASS between SEA and SAM is
 1279 overestimated by 50% in this model.

1280

1281 Adding Kamchatkan populations

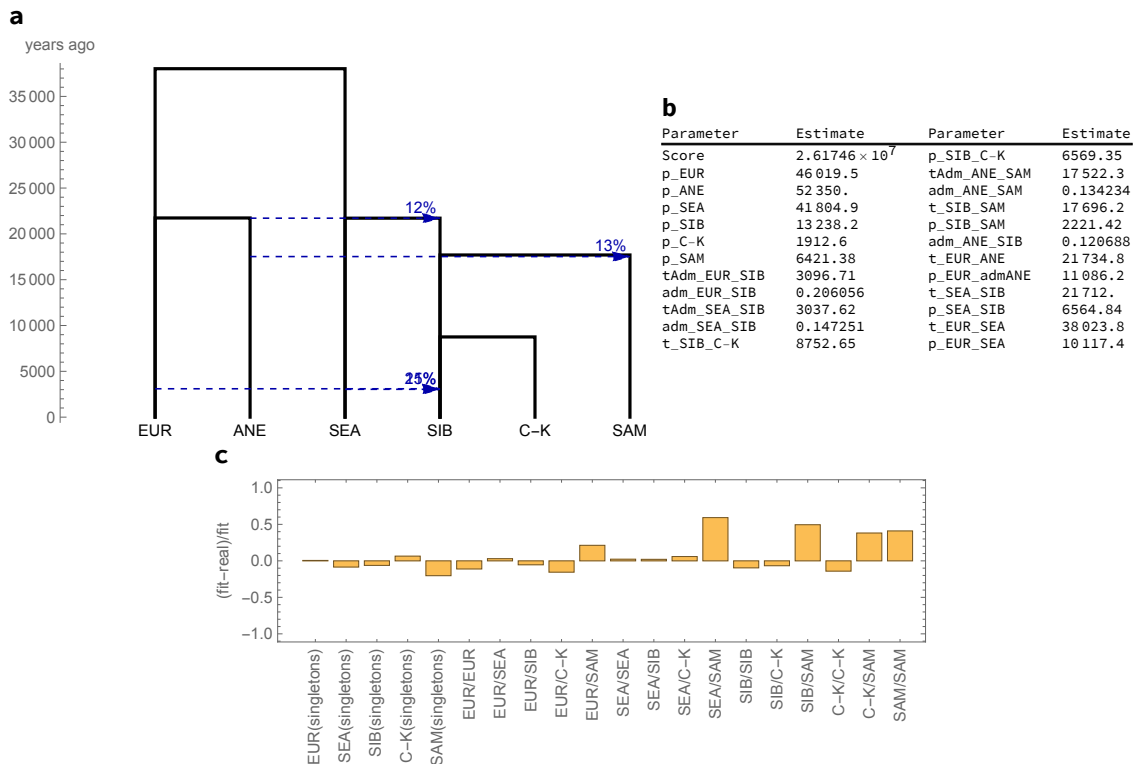
1282 In addition to Siberians, we also added populations from the Russian Far East (Koryak and
 1283 Itelmen) to the tree (Fig. S9.4). In contrast to the previous model, we now fix the time of the
 1284 ancient ANE contribution into the SIB/SAM ancestral branch, in order to reduce the number
 1285 of free parameters in the model, and since there is not much power to infer the times of
 1286 these deep admixture events. We here also added an admixture edge from SEA into SIB,
 1287 which improves the fit, but which apparently does not help much with the current
 1288 overestimation of the SAM/SEA sharing.

1289

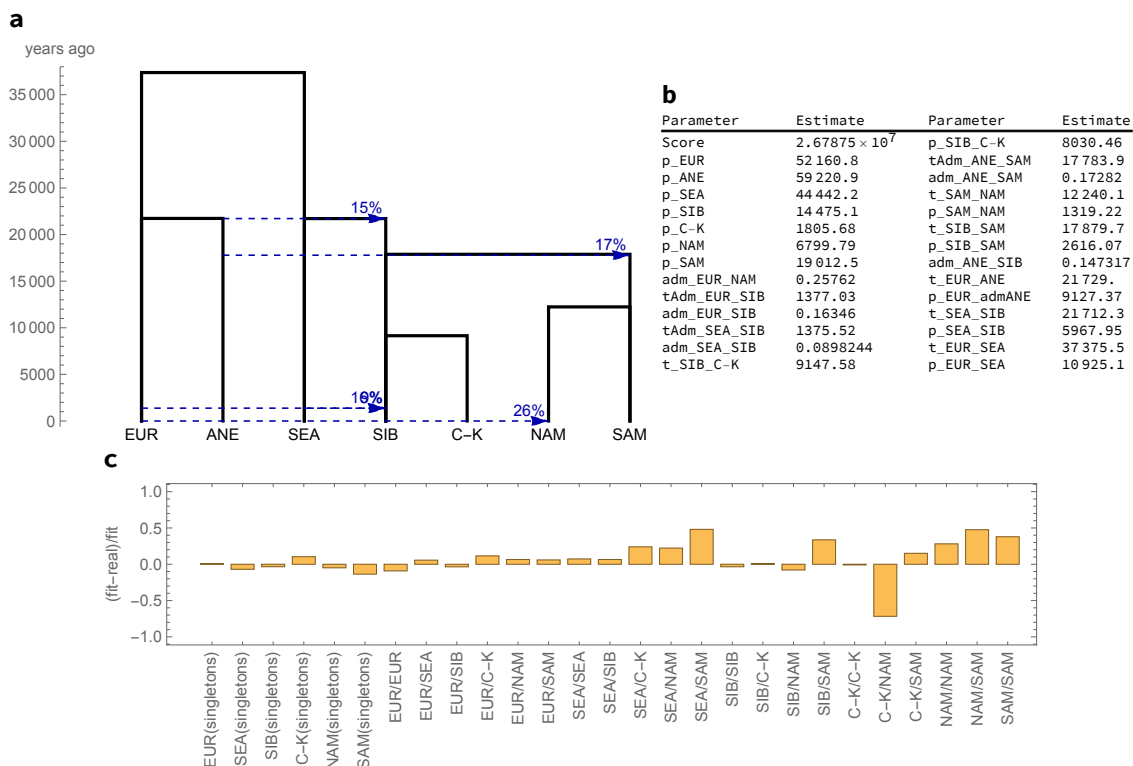
1290 Adding northern North Americans

1291 We next added Northern First Peoples (NAM) to the tree, which should be a sister clade to
 1292 the SAM, who – in contrast to Athabaskans – should not have any substantial Siberian
 1293 ancestry according to the *qpGraph* analysis, although they are expected to have European
 1294 colonial admixture. We therefore added NAM as a sister clade to SAM with additional EUR
 1295 admixture, arbitrarily fixed at 250 years ago (Fig. S9.5). The resulting tree shows a large

1296 underestimation of the C-K/NAM allele sharing, which must be due to the small levels of
 1297 First Peoples ancestry found in Chukotko-Kamchatkan speakers. As discussed in the
 1298 *qpGraph* section (section 10), we believe this ancestry came into Kamchatka through
 1299 bidirectional admixture with Yup'ik/Inuit branches, so we leave this underestimation for
 1300 now and first add the Yup'ik/Inuit (ESK) group to the tree.



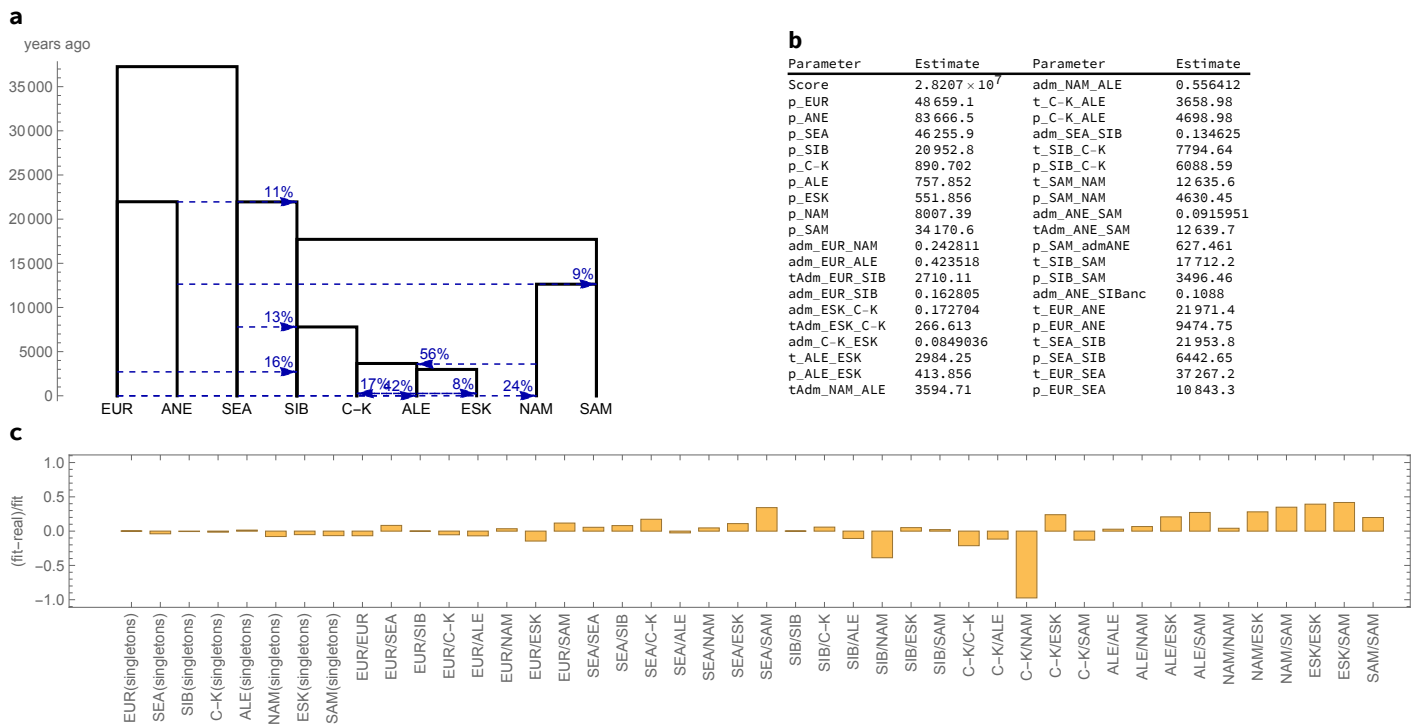
1301
 1302 **Fig. S9.4.** Adding Chukotko-Kamchatkan speakers (C-K) onto the EUR/SEA/SIB/SAM tree.



1303
 1304 **Fig. S9.5.** Adding Northern First Peoples (NAM) onto the EUR/SEA/SIB/C-K/SAM tree.

1305 **Adding Eskimo-Aleut-speaking populations to the tree**

1306 We next added several Eskimo-Aleut-speaking populations onto the tree, grouped into two
 1307 populations: ALE (Aleuts) and ESK (Yup'ik from Chukotka and Greenlandic Inuit). We added
 1308 them as a clade, which in turn is cladal with Chukotko-Kamchatkan speakers, with additional
 1309 Native American ancestry from NAM. We also added the ESK/C-K bidirectional admixture
 1310 event (Fig. S9.6). This model fits overall well, with one exception: The model largely
 1311 underestimates NAM/C-K sharing and to a much lesser extent SIB/NAM. This may suggest
 1312 some Asian gene flow from C-K, ALE or ESK into NAM, potentially through Athabaskans (see
 1313 below).



1314 **Fig. S9.6.** Adding Eskimo-Aleut speakers (ALE and ESK) onto the EUR/SEA/SIB/C-K/NAM/SAM tree, as a sister
 1315 group to C-K with additional Native American ancestry, and a bidirectional gene flow between C-K and ESK.
 1316

1317

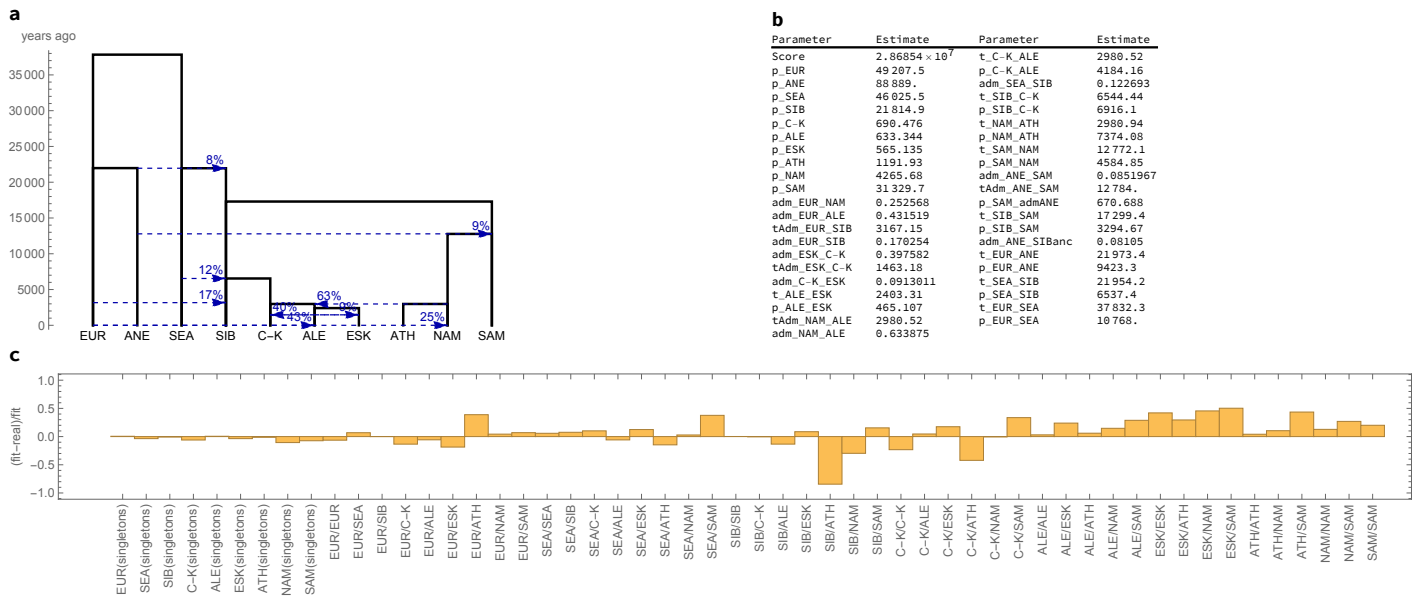
1318 **Adding Athabaskans**

1319 Finally, we added the Athabaskan meta-population to the tree (Dakelh and Chipewyans).
 1320 We first modeled them as a sister clade to NAM (Fig. S9.7).

1321 The model substantially underestimates the SIB/ATH allele sharing, suggesting some
 1322 Asian gene flow into Athabaskans, as consistent with other analyses and previous
 1323 publications (Reich et al. 2012, Raghavan et al. 2014b, 2015, Moreno-Mayar et al. 2018). We
 1324 tested three different models with Asian gene flow into Athabaskans (distinguished by the
 1325 topology on the Asian side) that emerged as best-fitting in our *qpGraph* analysis (Fig. S10.3):

1326 Model_1 (C-K, (ATH, (ESK, ALE))): The source that contributed to Athabaskans split
 1327 off the common ancestral branch of ESK and ALE after its split from the common ancestral
 1328 branch with C-K.

1329 Model_2 (ATH, (C-K, (ESK, ALE))): The source that contributed to Athabaskans split
 1330 off the common ancestor of C-K, ESK and ALE and is therefore an outgroup to those three
 1331 populations.



1332

1333 **Fig. S9.7.** Adding Athabaskans onto the EUR/SEA/SIB/C-K/ALE/ESK/NAM/SAM tree, as a sister group to NAM.
1334 The model underestimates SIB/ATH and C-K/ATH allele sharing.

1335

1336 Model_3 ((C-K, ATH), (ESK, ALE)): The Athabaskan source split off the branch leading
1337 to present-day C-K *after* its split from the common ancestor with ESK and ALE. This is the
1338 model proposed in (Moreno-Mayar et al. 2018).

1339 We first used “rarecoal maxl” to numerically optimize each model, and then used
1340 “rarecoal mcmc” to refine the estimates, using Markov Chain Monte Carlo to search for a
1341 local optimum. This is computationally more costly, but ensures that the optimum has been
1342 reached. The composite likelihood of the three refined competing models are:

1343

Model	Composite log-likelihood	Difference
Model_1	-28,682,166	0
Model_2	-28,682,227	-61
Model_3 (Moreno-Mayar et al. 2018)	-28,682,509	-343

1344

1345 The highest log-likelihood is achieved by Model_1 (C-K, (ATH, (ESK, ALE))) shown in
1346 Fig. S9.8. This model is consistent with the topology inferred by *qpGraph* (Fig. S10.5), but it
1347 underestimates allele sharing between NAM and SIB, suggesting some additional gene flow
1348 from ATH into NAM (consistent with *qpAdm* and PCA results, see Fig. 1, Extended Data Figs.
1349 2-4, Tables S5.3, S5.4). To test this, we ran the three models proposed above with an
1350 additional ATH->NAM gene flow.

1351

Model	Composite log-likelihood	Difference
Model_1_ATHadmNAM	-28,680,495	0
Model_2_ATHadmNAM	-28,680,861	-366
Model_3_ATHadmNAM	-28,681,925	-1,430

1352

1371

1372 **Correcting the composite likelihood for linkage correlations**

1373 *Rarecoal* uses a composite likelihood approach, which simply computes the total likelihood
1374 of the data given a model as the product of probabilities across all sites. This approach
1375 neglects linkage among sites, which does not affect the maximum likelihood parameter
1376 estimates. However, composite likelihoods cannot be used to compute posterior
1377 distributions or assess significance of model comparisons.

1378 We can solve this issue by correcting the composite likelihood by a factor that reflects the
1379 *effective* number of independent sites, which is much smaller than the true number of sites
1380 analyzed. To estimate the reduction factor of the likelihood, we first use a simple Block-
1381 Jackknife procedure to estimate the sampling variance of the joint allele frequency
1382 spectrum (Busing et al. 1999). Jackknife error estimation is built into the program
1383 “freqSum2histogram” from the rarecoal-tools repository used here
1384 (<https://github.com/stschiff/rarecoal-tools>), using the flag “-j”. This program generates a
1385 histogram of mutation patterns across the nine populations, which reports i) the number of
1386 times a given pattern is observed, ii) the frequency of that pattern, which is the number of
1387 observations divided by the total number of callable base pairs across the genome (here
1388 1,068,434,478), and iii) a Jackknife error estimate of that frequency, computed by
1389 chromosome-wise block Jackknife. Fig. S9.10 summarizes the error estimates as a function
1390 of the frequency of each pattern (up to total allele count 4).

1391 Under a true independent sites model without genetic linkage, the errors should follow a
1392 simple Poisson error model (the dashed line in Fig. S9.10), which predicts a square-root
1393 relationship between the error and the frequency of an observation. Specifically, the
1394 relationship between errors Δx and frequency x should be:

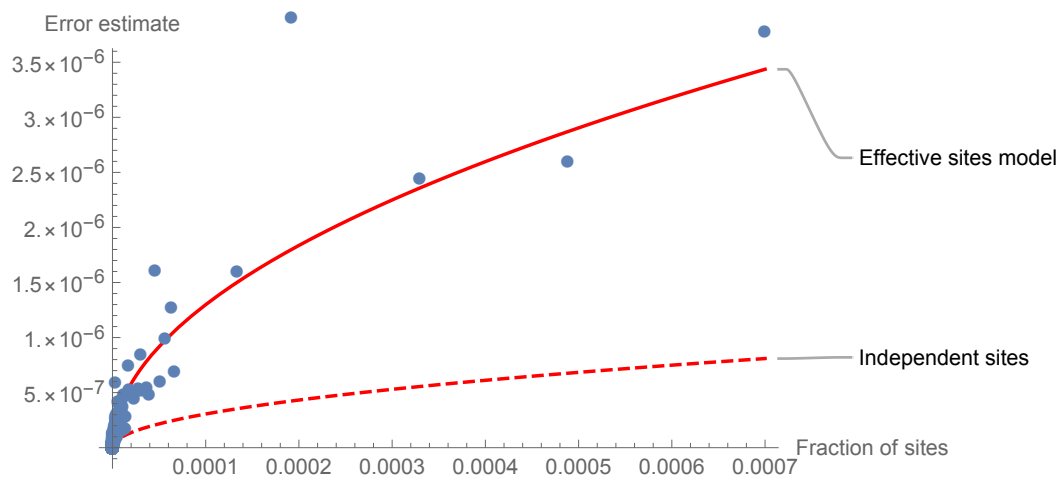
1395
$$\Delta x = \sqrt{\frac{x}{N}}$$

1396 where N is the number of callable sites.

1397 As can be seen, the true error estimates are much higher than under the
1398 independent sites assumption, which naturally reflects genetic linkage. We fitted an
1399 “Effective sites” model to the observed errors (the solid line in Fig. S9.10), by simply
1400 reducing the total number of callable sites by a factor α . Specifically, we fit the function

1401
$$\Delta x = \sqrt{\frac{x}{\alpha N}}$$

1402 inferring the parameter α by a simple least-square fit. We estimate $\alpha = 0.055$, which
1403 means that the inferred effective number of sites is about 18 times smaller than the true
1404 number of sites. This effective sites correction is not used in the maximum likelihood
1405 estimates above, but only in MCMC runs below and in model comparisons where indicated.



1406

1407

1408

Fig. S9.10. Fitting an effective sites error model to the joint site frequency spectrum for 9 populations (EUR, SEA, SIB, C-K, ALE, ESK, ATH, NAM, SAM).

1409

1410

1411

1412

1413

1414

Since the composite log-likelihood is a sum across all sites, a model with reduced effective number of sites simply results in a log-likelihood that is reduced by the same factor. Hence, the log-likelihood differences are also reduced by that same factor. We can therefore correct the likelihood differences for the three competing models discussed above (here without the ATH->NAM gene flow):

1415

Model	Composite log-likelihood difference	Corrected log-likelihood difference
Model_1	0	0
Model_2	-61	-3.3
Model_3 (Moreno-Mayar et al. 2018)	-343	-18.9

1416

1417

1418

1419

which shows that Model_2 is $e^{3.3} = 27.1$ times less likely than Model_1, and Model_3 is $e^{18.9} = 1.6 \times 10^8$ times less likely than Model_1, which gives significant support for Model_1, according to the arguments on significance in section 10.2.

1420

1421

1422

1423

We built into the program “rarecoal mcmc” an option implementing such an “effective sites” correction for reducing the total composite likelihood and hence widening the sampled posterior distribution. The resulting parameter estimates with and without that “effective sites” correction are shown in Fig. S9.11.

1424

1425

1426

1427

1428

1429

1430

1431

1432

1433

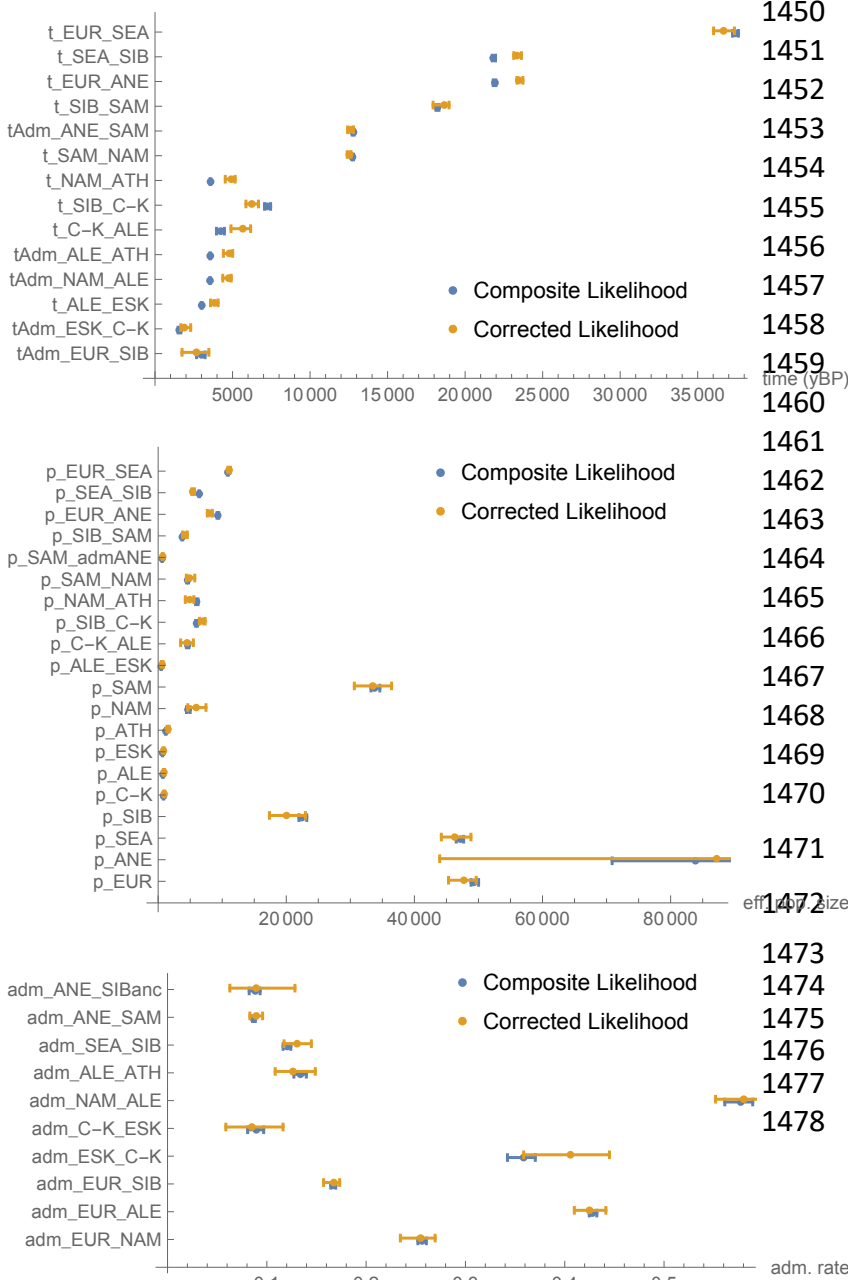
1434

Overall, the parameter estimates with and without correction overlap as expected, with some exceptions in particular for split times estimates (first panel in Fig. S9.11), where the inference based on the corrected likelihood yields older estimates for the most recent split times among the ALE, ESK and C-K branches, as well as for admixture times within these branches. Specifically, parameter estimates for $t_{\text{NAM_ATH}}$, $t_{\text{C-K_ALE}}$, $t_{\text{ALE_ESK}}$ as well as admixture times $t_{\text{Adm_NAM_ALE}}$ and $t_{\text{Adm_ALE_ATH}}$ are about 1,000 years older with the corrected likelihood compared to the composite likelihood, while $t_{\text{SIB_C-K}}$ is around 1,000 years younger compared to the composite likelihood estimate. We believe two factors might contribute to this discrepancy. First, the maximum likelihood estimate might represent a local optimum, whereas the broader parameter space exploration using the effective sites MCMC finds the global optimum which has older split times in this sub-

1435 tree. Second, these earlier split times might reflect differences in parameter space due to
 1436 constraints imposed by the model topologies. In particular, the model topology itself
 1437 imposes ordering constraints on split- and admixture time parameters. The joint posterior
 1438 distribution therefore could have subtle topological features which might cause the MCMC
 1439 to explore different regions of the parameter space despite slightly sub-optimal likelihoods
 1440 but larger probability areas.

1441 Overall, we believe the corrected likelihood Bayesian calculation yields realistic
 1442 posterior credibility intervals for parameters, and we use the median estimates of those
 1443 intervals for plotting our final model in Fig. 2. We summarize the maximum likelihood
 1444 estimates, as well as the corrected likelihood marginal posterior percentiles in Table S9.2.
 1445 The final model was calibrated using a mutation rate of 1.25×10^{-8} per basepair per
 1446 generation, and a generation time of 29 years. The resulting model appears to be overall
 1447 consistent with archaeology, with two small noteworthy issues. First, the ancient Anzick
 1448 genome (12,600 calBP) (Rasmussen et al. 2014) has a substantially higher affinity to the

1449 SAM than to the NAM branch.
 1450 To allow for this, the NAM/SAM
 1451 split time needs to be sufficiently
 1452 older than Anzick's age, which in
 1453 our estimate is barely the case.
 1454 We believe this can in principle
 1455 be fixed by using the Anzick
 1456 genome as a calibration point. A
 1457 related issue poses our estimate
 1458 of the ANE->SAM admixture
 1459 edge, which is estimated to be
 1460 too recent to allow for the older
 1461 NAM/SAM split necessary to fit
 1462 Anzick. We believe these
 1463 discrepancies are tolerable, but
 1464 acknowledge room for
 1465 improvement by using directly
 1466 dated ancient samples to further
 1467 constrain the model fits, which
 1468 however will also further
 1469 increase the already substantial
 1470 model complexity.



1471
 1472
 1473 **Fig. S9.11.** Posterior credibility
 1474 estimation for all parameters of the
 1475 final model shown in Fig. S9.8 with
 1476 and without the “effective sites”
 1477 correction of the likelihood.
 1478

	Parameter	Maximum composite likelihood estimate	2.5% posterior percentile, corrected likelihood	50% posterior percentile, corrected likelihood	97.5% posterior percentile, corrected likelihood
Split Times (ya)	t_ALE_ESK	3,032	3,580	3,835	4,066
	t_C-K_ALE	4,144	4,901	5,662	6,165
	t_SIB_C-K	7,161	5,865	6,241	6,674
	t_NAM_ATH	3,568	4,533	4,924	5,168
	t_SAM_NAM	12,714	12,396	12,549	12,639
	t_SIB_SAM	18,171	17,935	18,654	18,962
	t_EUR_ANE	21,949	23,346	23,463	23,727
	t_SEA_SIB	21,760	23,136	23,349	23,633
	t_EUR_SEA	37,323	36,024	36,668	37,370
Admixture Times (ya)	tAdm_EUR_SIB	3,045	1,742	2,671	3,470
	tAdm_ESK_C-K	1,622	1,668	1,886	2,299
	tAdm_NAM_ALE	3,550	4,371	4,752	4,914
	tAdm_ALE_ATH	3,558	4,410	4,799	5,005
	tAdm_ANE_SAM	12,799	12,423	12,618	12,800
Admixture Rates (%)	adm_EUR_NAM	26%	23%	25%	27%
	adm_EUR_ALE	43%	41%	42%	44%
	adm_EUR_SIB	17%	16%	17%	17%
	adm_ESK_C-K	37%	36%	41%	45%
	adm_C-K_ESK	9%	6%	8%	12%
	adm_NAM_ALE	58%	55%	58%	62%
	adm_ALE_ATH	13%	11%	13%	15%
	adm_SEA_SIB	12%	12%	13%	14%
	adm_ANE_SAM	9%	8%	9%	10%
adm_ANE_SIBanc	9%	6%	9%	13%	
Population Sizes	p_EUR	49,046	45,330	47,722	49,648
	p_ANE	84,473	43,952	87,184	179,202
	p_SEA	47,526	44,208	46,288	48,824
	p_SIB	22,542	17,375	20,031	22,986
	p_C-K	818	863	936	1,042
	p_ALE	752	818	918	1,014
	p_ESK	670	759	841	937
	p_ATH	1,196	1,409	1,538	1,716
	p_NAM	4,547	4,631	5,944	7,464
	p_SAM	33,988	30,625	33,516	36,439
	p_ALE_ESK	474	499	613	770
	p_C-K_ALE	4,581	3,510	4,512	5,501
	p_SIB_C-K	6,046	6,441	6,975	7,326
	p_NAM_ATH	6,008	4,242	4,906	5,564
	p_SAM_NAM	4,590	4,403	4,899	5,715
	p_SAM_admANE	626	654	720	776
	p_SIB_SAM	3,751	3,830	4,118	4,546
	p_EUR_ANE	9,358	7,678	8,058	8,465
	p_SEA_SIB	6,436	5,254	5,380	5,664
	p_EUR_SEA	10,861	10,896	11,093	11,297

1479 **Table S9.2.** Parameter estimates for the final model using default scaling with a mutation rate of 1.25×10^{-8}
1480 per generation per basepair, and a generation time of 29 years. Maximum likelihood estimates are based on
1481 the composite likelihood, while posterior distributions are computed for a corrected likelihood as described
1482 above.
1483

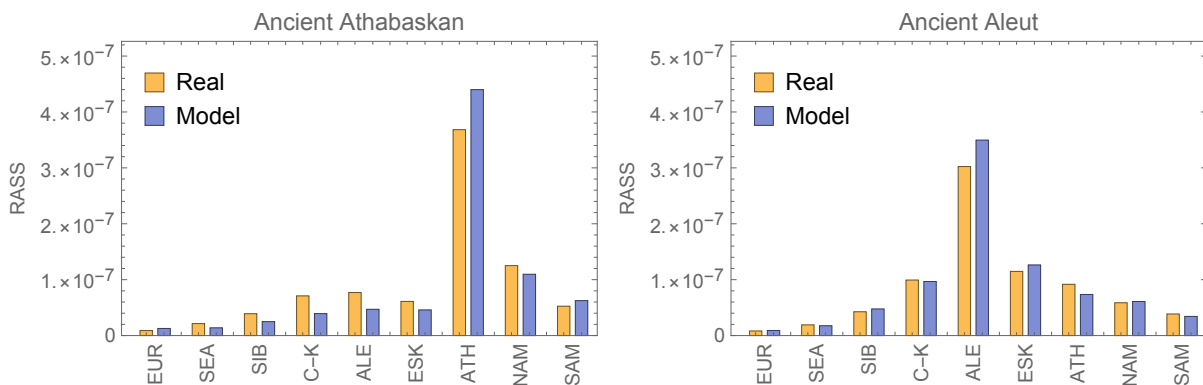
1484 **Adding ancient genomes**

1485 Onto the final tree estimated from present-day sequences only, we added the genomes of
1486 three ancient individuals with whole-genome shotgun data: The ancient Saqqaq genome
1487 published in Rasmussen et al. 2010, an ancient Aleut individual, and an ancient Athabaskan
1488 individual, both sequenced within this study. For all three samples, we made a Majority call
1489 with a minimum coverage of 3 at all variable sites in our “SGDP/Raghavan et al.” dataset
1490 (see details in section 8). Given previous results from *qpGraph* (see section 10), we tested a
1491 limited number of branching positions for these ancient individuals.

1492 For the ancient Aleut, we tested a branching position onto the modern Aleut branch
1493 at 600 ya (the median C14 date for that sample) and before colonial admixture at 250 ya.
1494 For the ancient Athabaskan, we tested a branching position onto the modern Athabaskan
1495 branch at 780 ya (its median C14 date). In both cases we did not attempt to estimate a more
1496 precise split time between the ancient sample and its corresponding modern branch given
1497 the limited information available from a single ancient sample, in particular with pseudo-
1498 haploid genotyping calls, which provide no information on private drift within the ancient
1499 branch.

1500 To evaluate those branching positions, we compared rare allele sharing statistics
1501 between the ancient individual and each of our modern populations with those estimated
1502 from a model with the ancient genome added to the final model (Fig. S9.12). Note that the
1503 Paleo-Eskimo admixture proportion in Athabaskans, as well as the Native American / PPE
1504 mixture proportions for Aleuts are taken from the final model estimates obtained without
1505 any ancient genomes (Table S9.2).

1506



1507

1508 **Fig. S9.12.** Mapping the ancient Athabaskan and ancient Aleut samples onto the tree.

1509

1510 In both cases, the model and real data agree very well. By far the highest allele
1511 sharing between ancient and modern populations is seen with the modern Athabaskan and
1512 the modern Aleut branch, respectively, strongly suggesting that these ancient samples are
1513 direct ancestors of the respective modern populations. However, in the case of the ancient
1514 Athabaskan, the allele sharing with C-K and ALE is higher than predicted under our model,
1515 suggesting that the ancient Athabaskan has even higher proportions of Paleo-Eskimo
1516 ancestry than does modern Athabaskans, which may be due to population structure within
1517 the Athabaskan population, or a dilution through subsequent admixture of non-Athabaskan
1518 First Peoples into the present-day Athabaskan population. This result is supported by our
1519 extensive admixture modeling using the *qpAdm* approach and by PCA (Fig. 1, Extended Data

1520 Figs. 2-4).

1521 In the case of the 3,900-year-old ancient Saqqaq genome (Rasmussen et al. 2010),
 1522 we tested four different locations on the tree to merge its branch with the best-fitting
 1523 modern phylogeny (Fig. S9.8). The first position, called ALE_beforeATHadm, is a position on
 1524 the ancestral branch leading to present-day Eskimo-Aleuts, but *before* admixture from that
 1525 branch into Athabaskans. The next position, called ALE_afterATHadm, is also on the
 1526 ancestral branch leading to Eskimo-Aleuts, but *after* admixture from that branch into
 1527 Athabaskans. The third position, called C-K_beforeALEsplit, is a position on the ancestral
 1528 branch leading to ALE, ESK and C-K. The final position, called C-K_afterALEsplit, is a position
 1529 on the branch leading to present-day C-K, after its split from the Eskimo-Aleut branch. The
 1530 four positions correspond to four different topologies within the PPE clade, as indicated in
 1531 Table S9.3:

1532

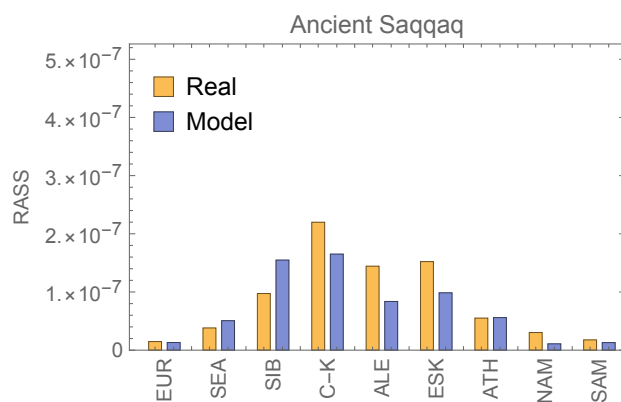
Saqqaq branch point	PPE clade topology	Split time	Log-likelihood	Log-likelihood difference	Corrected log-likelihood difference
ALE_beforeATHadm	(C-K, (P-E, (ATH, E-A)))	5,104 ya	-93,800	-277	-15
ALE_afterATHadm	(C-K, (ATH, (P-E, E-A)))	4,756 ya	-93,523	0	0
C-K_beforeALEsplit	(P-E, (C-K, (ATH, E-A)))	5,800 ya	-94,559	-1,036	-57
C-K_afterALEsplit	((C-K, P-E), (ATH, E-A))	5,220 ya	-94,375	-852	-47

1533 **Table S9.3.** Tested models for Saqqaq to branch onto the final maximum likelihood tree of 9 populations.

1534

1535 The winning position is the position on the branch leading to Eskimo-Aleuts, but
 1536 after the admixture into Athabaskans, corresponding to the topology (C-K, (ATH, (P-E, E-A))),
 1537 which is also the most likely topology obtained using the *qpGraph* method (section 10). All
 1538 model comparisons are significant, since the corrected log-likelihood differences are above
 1539 3 (see arguments from section 10.2).

1540 The comparison of RASS between the model and data for the winning topology is
 1541 shown in Fig. S9.13. The model captures the salient feature of the RASS statistics, which is
 1542 the high level of rare allele sharing between C-K and the ancient Saqqaq individual.
 1543 However, the model also underestimates RASS between Saqqaq and each population in the
 1544 PPE clade, i.e. Eskimo-Aleuts and Chukotko-Kamchatkans, which is difficult to explain, but
 1545 could be due to additional gene flow between Saqqaq descendants and ancestors of extant
 1546 populations that we currently do not model.



1547

1548 **Fig. S9.13.** Mapping the ancient Saqqaq individual onto the 9 population tree.

1549

1550 *References (for this section)*

- 1551 Busing, F. M. T. A., Meijer, E. & Van Der Leeden, R. Delete-M Jackknife for Unequal M. *Statistics and*
1552 *Computing* **9**, 3–8 (1999).
- 1553 Fenner, J. N. Cross-cultural estimation of the human generation interval for use in genetics-based population
1554 divergence studies. *Am. J. Phys. Anthropol.* **128**, 415–423 (2005).
- 1555 Haak, W. *et al.* Massive migration from the steppe was a source for Indo-European languages in Europe.
1556 *Nature* **522**, 207–211 (2015).
- 1557 Mallick, S. *et al.* The Simons Genome Diversity Project: 300 genomes from 142 diverse populations. *Nature*
1558 **538**, 201–206 (2016).
- 1559 Moreno-Mayar, J. V. *et al.* Terminal Pleistocene Alaskan genome reveals first founding population of Native
1560 Americans. *Nature* **553**, 203–207 (2018).
- 1561 Patterson, N. *et al.* Ancient admixture in human history. *Genetics* **192**, 1065–1093 (2012).
- 1562 Raghavan, M. *et al.* Upper Palaeolithic Siberian genome reveals dual ancestry of Native Americans. *Nature* **505**,
1563 87–91 (2014a).
- 1564 Raghavan, M. *et al.* The genetic prehistory of the New World Arctic. *Science* **345**, 1255832 (2014b).
- 1565 Raghavan, M. *et al.* Genomic evidence for the Pleistocene and recent population history of Native Americans.
1566 *Science* **349**, 1–20 (2015).
- 1567 Rasmussen, M. *et al.* Ancient human genome sequence of an extinct Palaeo-Eskimo. *Nature* **463**, 757–762
1568 (2010).
- 1569 Rasmussen, M. *et al.* The genome of a Late Pleistocene human from a Clovis burial site in western Montana.
1570 *Nature* **506**, 225–229 (2014).
- 1571 Reich, D. *et al.* Reconstructing Native American population history. *Nature* **488**, 370–374 (2012).
- 1572 Scally, A. & Durbin, R. Revising the human mutation rate: implications for understanding human evolution.
1573 *Nat. Rev. Genet.* **13**, 745–753 (2012).
- 1574 Schiffels, S. *et al.* Iron Age and Anglo-Saxon genomes from East England reveal British migration history. *Nat.*
1575 *Commun.* **7**, 10408 (2016).
- 1576

1577 **Supplementary Information section 10**

1578 **Admixture graph modeling using *qpGraph***

1579

1580 **10.1 Generating a basic model for present-day populations**

1581 dataset: *transitions and transversions*;

1582 populations: *selected present-day populations*.

1583 To investigate the phylogenetic relationship between relevant populations for this study, we
1584 tested models which fit observed f_4 -statistics using autosomal markers present in the 1240K
1585 capture panel¹. The f_4 -statistic measures correlations between allele frequency differences
1586 of two pairs of groups². Given a graph topology with population splits, genetic drift and
1587 admixture edges, the algorithm implemented in the *qpGraph* program infers branch lengths
1588 and mixture proportions that minimize the difference between the observed and expected
1589 f_4 -statistics.

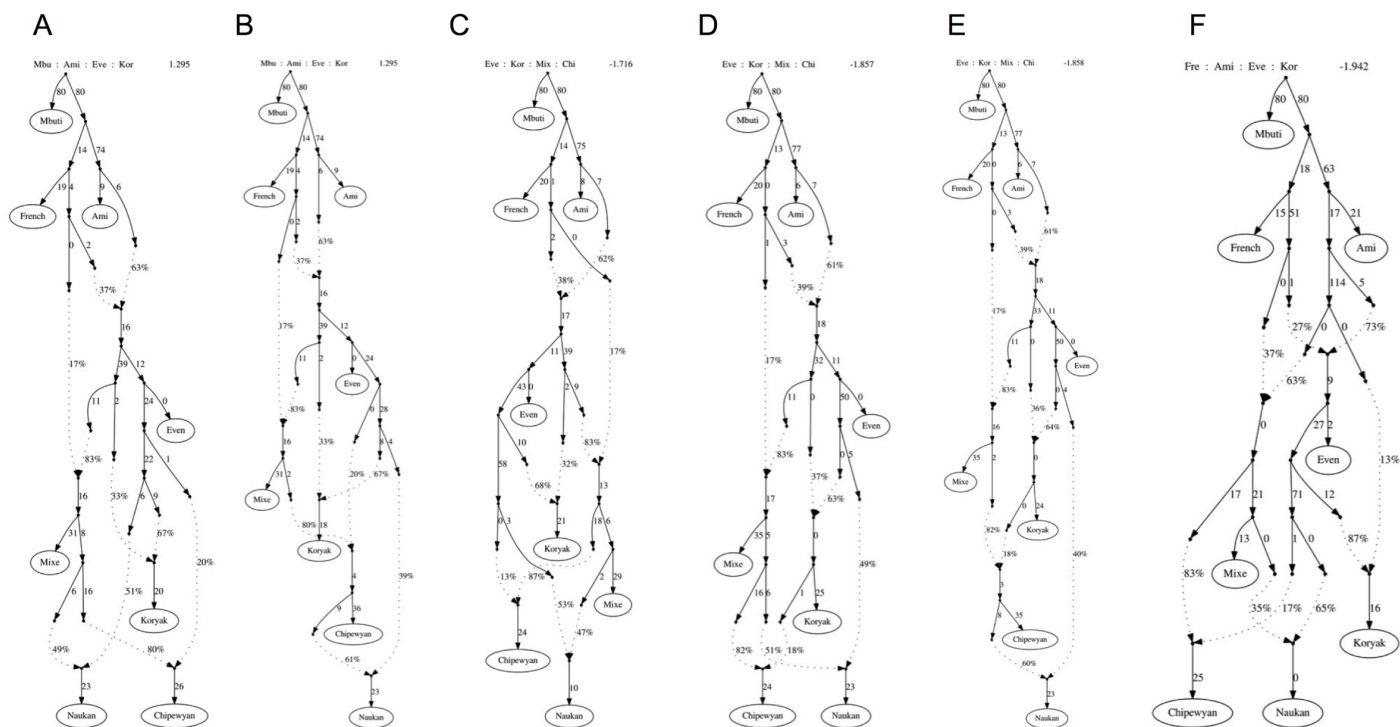
1590 For the analysis, we used whole genome sequence data from the Simons Genome
1591 Diversity Project³ and added additional 35 genomes published by Raghavan et al.⁴.
1592 Genotype calls for the autosomal part of the 1240K panel were extracted, and SNPs with
1593 >10% missing rate were removed, leaving 1,062,979 SNPs for the analysis (Supplementary
1594 Table 5). *qpGraph* analyses were performed in the “useallsnps: NO” mode. We first
1595 performed a comprehensive search for tree topologies fitting the data. For this, we selected
1596 the following populations: Mbuti, French, Ami, Mixe, Even, Yup'ik Naukan, Koryak, and
1597 Chipewyan to represent each of the 7 relevant meta-populations (AFR, EUR, SEA, SAM, SIB,
1598 E-A, C-K, and ATH, see Table S10.1). To perform an extensive search for possible population
1599 relationships, we began with a simple tree of three populations (Mbuti, (French, Ami)) and
1600 iteratively added one population to the tree in the following order: Mixe, Even, Koryak,
1601 Chipewyan, Yup'ik Naukan. More specifically, the added population was modeled either as a
1602 sister branch of an existing one or as a mixture of two branches. We tested all branches and
1603 branch pairs and kept all fitting models (having absolute Z-scores of the worst-fitting f_4 -
1604 statistic < 3) at each step. A total of 2,932 models were tested this way, and at the end of
1605 our search, we found 108 graphs that fit all observed f_4 -statistics within three standard error
1606 intervals ($|Z\text{-score}| < 3$) and 14 graphs that fit all observed f_4 -statistics within two standard
1607 error intervals ($|Z\text{-score}| < 2$). Six best-fitting graphs are shown in Fig. S10.1.

1608 The fitting graphs share several key features. The most important feature is that
1609 Mixe, Even, Koryak, Chipewyan and Yup'ik Naukan are all modeled as a mixture of western
1610 and eastern Eurasian branches, and none of them forms a sister branch with each other: i.e.
1611 at least one additional gene flow is required to add each population to the graph (Fig.
1612 S10.1). For example, Koryak cannot be a sister group to Even because of its excessive affinity
1613 to Mixe. Also, Chipewyan cannot be modeled as a sister group of Mixe and requires a gene
1614 flow from a Siberian source, e.g. either Koryak- or Even-related branch. Finally, Yup'ik
1615 Naukan is well modeled as a mixture of Koryak- and Chipewyan-related branches, or as a
1616 mixture of Koryak- and Mixe-related ones (Fig. S10.1). All possible topologies within the
1617 proto-Paleo-Eskimo (PPE) clade appear among the best-fitting models shown in Fig. S10.1:
1618 (PPE_{ATH}, (PPE_{C-K}, PPE_{E-A})) (Fig. S10.1a,b); (PPE_{C-K}, (PPE_{ATH}, PPE_{E-A})) (Fig. S10.1c,f); (PPE_{E-A},
1619 (PPE_{ATH}, PPE_{C-K})) (Fig. S10.1d,e). The abbreviations PPE_{ATH}, PPE_{C-K}, and PPE_{E-A} denote the
1620 sources of proto-Paleo-Eskimo-related ancestry in Chukotko-Kamchatkan (C-K), Athabaskan
1621 (ATH), and Eskimo-Aleut speakers (E-A), respectively. However, the latter two graphs (Fig.

1622 S10.1d,e) contain 0-length branches within the PPE clade, i.e. there is a trifurcation.
 1623 Notably, to account for excessive affinity between Koryak and Mixe, the former population
 1624 is in all cases modelled as having admixture from a source related to Native Americans, but
 1625 prior to the West Eurasian gene flow into them. For convenience, we term this source
 1626 “proto-American”. We also tested whether the models generated here fit the data for
 1627 composite meta-populations (Table S10.1) used for *Rarecoal* modeling (section 9). All
 1628 topologies shown in Fig. S10.1 fit the data ($|Z\text{-scores}| < 3$) for the AFR, EUR, SEA, SAM, C-K,
 1629 E-A, and ATH meta-populations.
 1630

Abb.	Full Name	Populations	Nr. of samples
AFR	Africans	Bantu Herero, Bantu Kenya, Bantu Tswana, Biaka, Dinka, Esan, Gambian, Jul'hoan North, Khomani San, Luhya, Luo, Mandenka, Masai, Mbuti, Mende, Somali, Yoruba	45
EUR	Europeans	Basque, Bergamo, Bulgarian, Crete, Czech, English, Estonian, French, Greek, Hungarian, Orcadian, Polish, Sardinian, Spanish, Tuscan	32
ANE	Paleolithic Siberian hunter-gatherers	Mal'ta (MA1) (Raghavan et al. 2014)	1
WHG	West European hunter-gatherers	Loschbour (Lazaridis et al. 2014)	1
SEA	Southeast Asians	Ami, Atayal, Dai, Kinh, Lahu, Miao, She	15
SIB	Core Siberians	Altaiian, Buryat, Ket, Nivkh, Even, Mansi, Tubalar, Ulchi, Yakut	22
C-K	Chukotko-Kamchatkan speakers	Itelmen, Koryak	3
E-A	Eskimo-Aleut speakers	East and West Greenlandic Inuit, Yup'ik	7
E-A anc.	ancient Aleuts and Neo-Eskimos	Aleuts (this study)	6
		Ekven (this study)	16
		Uelen (this study)	3
ATH	Northern Athabaskan speakers	Dakelh, Chipewyan	4
ATH anc.	ancient Athabaskans	Tochak McGrath (this study)	2
USR	ancient Beringian	Upward Sun River 1 (USR1) (Moreno-Mayar et al. 2018)	1
NAM	Northern First Peoples (in some figures, “northern First Americans”)	Cree, Tsimshian	3
SAM	Southern First Peoples (in some figures, “southern First Americans”)	Aymara, Mixe, Mixtec, Piapoco, Quechua, Yukpa, Zapotec	13

1631 **Table S10.1.** A table listing all present-day and ancient (grey shading) individuals and groups used in the *qpGraph*
 1632 analysis. The present-day data is from the two sources: Raghavan *et al.*⁴ and the Simons Genome Diversity Project
 1633 data set³ as indicated in Supplementary Table 4. The sources of ancient data are indicated in the table.



1635 **Fig. S10.1.** Best-fitting models from an extensive search of population graphs. In most cases, Mixe receives two
 1636 gene flows from a French-related branch (interpreted as ancient North Eurasians, ANE). Yup'ik Naukan is
 1637 modeled as a mixture of proto-Paleo-Eskimos (PPE) and a Chipewyan-related branch, either before (a, c, d, f)
 1638 or after (b, e) the PPE gene flow into Chipewyan. Chipewyan is modeled as a mixture of a Native American
 1639 lineage and either PPE (a-c, f) or a Koryak-related lineage (d, e).

1640

1641 **10.2 Testing all possible topologies within the proto-Paleo-Eskimo clade**

1642 dataset: *transversions only*;

1643 populations: *present-day meta-populations; pseudo-haploid Saqqaq, ancient Aleuts, ancient*
 1644 *Neo-Eskimos or present-day Yup'ik or Inuit, present-day or ancient Athabaskans.*

1645 We added ancient populations (the Saqqaq Paleo-Eskimo, Aleutian Islanders, Old Bering Sea
 1646 population from the Ekven and Uelen burial grounds) onto the backbone meta-population
 1647 graph created in the previous section. To mitigate ancient DNA biases, all transition
 1648 polymorphisms were removed from the dataset, with 208,649 sites remaining. We found
 1649 that ancient Aleuts can be modelled as a roughly one to one mixture of First Peoples and a
 1650 Saqqaq-related lineage, but the Ekven, Uelen and present-day Yup'ik populations require an
 1651 additional pulse of admixture from a lineage related to C-K. This reflects the fact that all
 1652 these groups were/are located in Chukotka, where they could interact with local C-K groups.
 1653 We then constructed a series of more complex models including both ancient Aleuts and
 1654 present-day Yup'ik or the ancient Ekven/Uelen populations (E-A). Using this set of
 1655 populations, we tested all possible topologies within the PPE clade. We varied the following
 1656 parameters: the branching order of real/hypothetical populations (18 topologies, including
 1657 models with E-A admixture in ATH) and the lineages receiving the "proto-American" and
 1658 Native American gene flows. In total, 56 models were tested for each ancient/modern E-A
 1659 population (see model statistics in Table S10.2). Only the following 8 topologies of the PPE
 1660 clade fit the data: 1/ ((ATH, *C-K), (E-A, P-E)); 2/ (*(ATH, C-K), (E-A, P-E)); 3/ ((ATH, C-K), (E-A,
 1661 P-E)); 4/ (*C-K, (ATH, (E-A, P-E))); 5/ (C-K, (ATH, (E-A, P-E))); 6/ (ATH, (*C-K, (E-A, P-E))); 7/
 1662 (ATH, *(C-K, (E-A, P-E))); 8/ (ATH, (C-K, (E-A, P-E))), where an asterisk denotes the entry point

1663 of the “proto-American” gene flow. Note that here and in the following, topology notations
1664 involving ATH, C-K, E-A and P-E denote the PPE component in those populations (unless
1665 explicitly specified), not the First Peoples component nor the sum of admixed ancestries. In
1666 summary, E-A and P-E (Saqqaq) are always the closest sister-groups, and the branching
1667 order of the PPE source populations that contributed to Athabaskans and C-K remains
1668 ambiguous. Another observation is that models either lacking the “proto-American” gene
1669 flow into C-K, or with this admixture not exclusive to C-K, are not among the best-fitting
1670 ones (compare Z-scores for models 1, 2, 4, and 6 and for models 3, 5, 7, and 8 above, Table
1671 S10.2). Two fitting models of this type are shown in Fig. S10.2 (topologies 2 and 5 listed
1672 above).

1673 We suspected that the affinity between C-K and First Peoples, which resulted in the
1674 “proto-American” gene flow emerging as an outcome of the unsupervised branch-adding
1675 procedure, can be explained in a much simpler way, if we suppose that the C-K/E-A
1676 admixture was bidirectional allowing us to remove the “proto-American” gene flow. Out of
1677 18 topologies of this kind, 15 do not fit at all ($|Z\text{-scores}| > 4$ or > 5), while 3 fit with exactly
1678 the same Z-scores around 2 and the same log-likelihood values: ((ATH, C-K), (E-A, P-E));
1679 (ATH, (C-K, (E-A, P-E))); (C-K, (ATH, (E-A, P-E))) (see model statistics in Table S10.3). Present-
1680 day Inuit can also be incorporated into the graph instead of Yup’ik, Ekven or Uelen, but
1681 cannot be modelled without an additional pulse of European gene flow which plausibly
1682 reflects colonial admixture (Table S10.3).

1683 Finally, we replaced present-day Athabaskans (4 individuals) with ancient
1684 Athabaskans (2 individuals), and the impasse was resolved: only one among 6 fitting
1685 topologies has no trifurcations and has the lowest Z-score and the best log-likelihood value,
1686 and that is the topology (C-K, (ATH, (E-A, P-E))). The log-likelihood difference between this
1687 topology and the second-best topologies ((ATH, C-K), (E-A, P-E)) and (ATH, (C-K, (E-A, P-E)))
1688 ranges from 2 to 2.7, depending on the E-A population. Thus, the best-fitting model is from
1689 7.2 to 15.5 times more likely than the second-best models, however these likelihood
1690 differences are non-significant in the case of the transversion-only dataset. See model
1691 statistics in Table S10.4 and 3 best-fitting graphs with absolute Z-scores < 2 in Fig. S10.3.

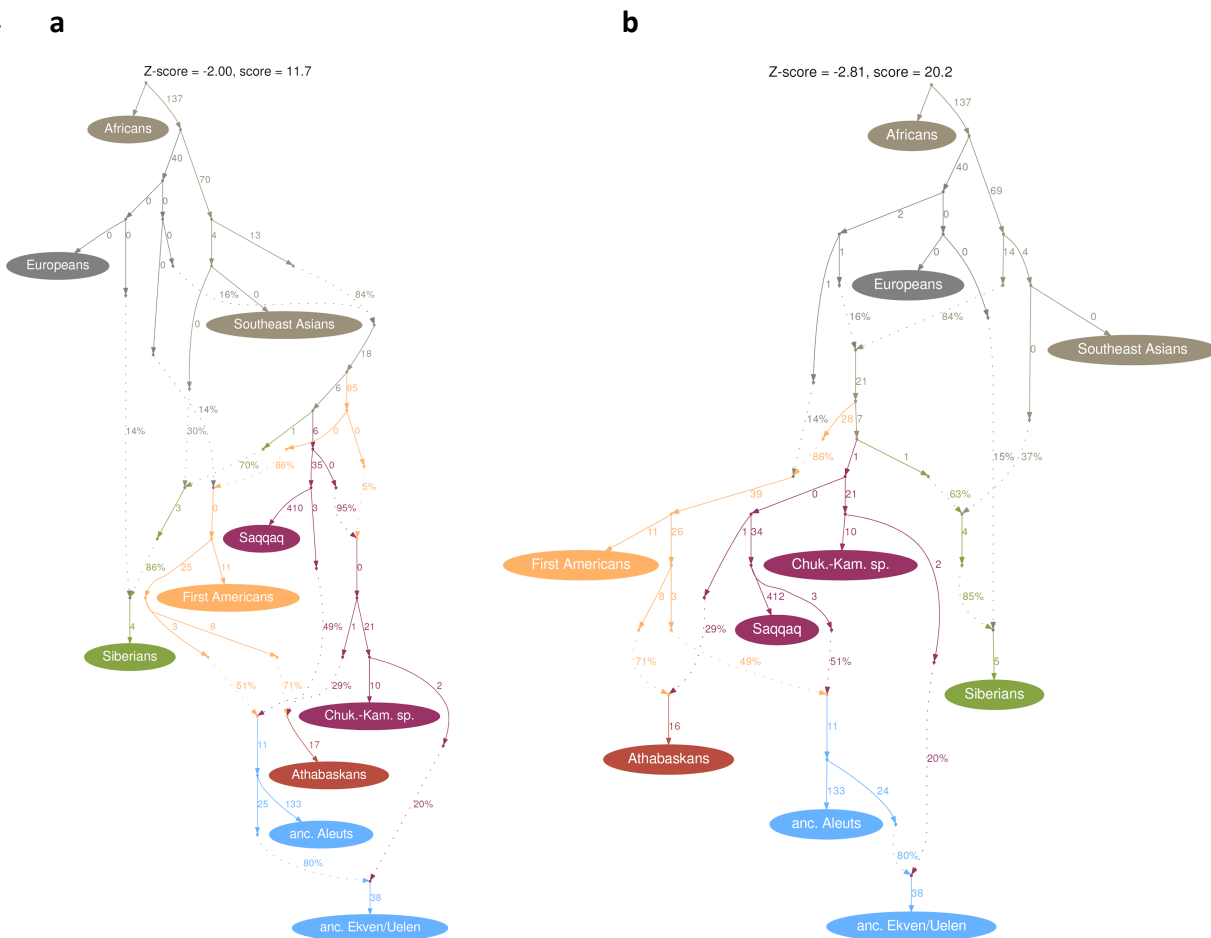
1692 Here and in the following, we generally consider likelihood ratios between
1693 competing models of 20 and higher (corresponding to log-likelihood differences of 3 and
1694 higher) to be “significant”, provided the two competing models have the same number of
1695 parameters and are applied to the same data. This can be derived using the Bayesian
1696 Information Criterion (BIC) for model comparisons, which is defined as $BIC = -2 \log L + C$,
1697 where C is a constant factor depending on sample size and number of model parameters,
1698 and L is the likelihood. A feature of BIC is the fact that it can be used to approximately
1699 compute the posterior probability of the model given the data, via
1700 $p(M|\text{data}) \sim \exp\left(-\frac{BIC}{2}\right) p(M) = L p(M)$, where $p(M)$ is the prior probability of the model.
1701 Using this, and using flat priors, it follows that deciding between two models $M1$ and $M2$
1702 with the same number of parameters and applied to the same data, we can use the
1703 likelihood ratio directly as an estimate of the ratio of posterior probabilities. It follows that a
1704 likelihood ratio of 20 or higher corresponds to one model being 20 times more likely (or
1705 higher) than the other model, which renders the posterior probability for one model being
1706 below 0.05 and the other above 0.95, which we consider to be significant support for one
1707 model over the other.

1708 A similar pattern as seen above for the transversion-only dataset is observed for the

1709 full dataset including transitions, but with generally poorer fits: the lowest absolute Z-score
 1710 equals 2.87 (Table S10.5). In this case, however, the model (C-K, (ATH, (E-A, P-E))) is from 39
 1711 to 202 times more likely than second-best models ((ATH, C-K), (E-A, P-E)) and (ATH, (C-K, (E-
 1712 A, P-E))), which according to the arguments above can be considered significant. According
 1713 to the best models, a low-level C-K admixture of up to 15-20% is characteristic for all Old
 1714 Bering Sea, Yup'ik and Inuit groups studied here, but not for Aleuts. E-A admixture is
 1715 inferred in all C-K groups: low levels up to 10% in Koryak and Itelmen, and a higher level (Fig.
 1716 1a, Extended Data Figs. 2-4 and 8, section 5) in Chukchi, omitted from the C-K meta-
 1717 population here. The topology favored by this analysis is not only a significantly better fit
 1718 than the other two including the ((ATH, C-K), (E-A, P-E)) topology favored by Moreno-Mayar
 1719 et al. (2018), but is also the “simplest” one from the archaeological point of view, as
 1720 detailed in the Discussion. The topology favored by Moreno-Mayar et al. (2018) - ((ATH, C-
 1721 K), (E-A, P-E)) - is among the best supported, however it results in a trifurcation (ATH, C-K,
 1722 (E-A, P-E)) and has a significantly worse log-likelihood (Tables S10.4, S10.5).

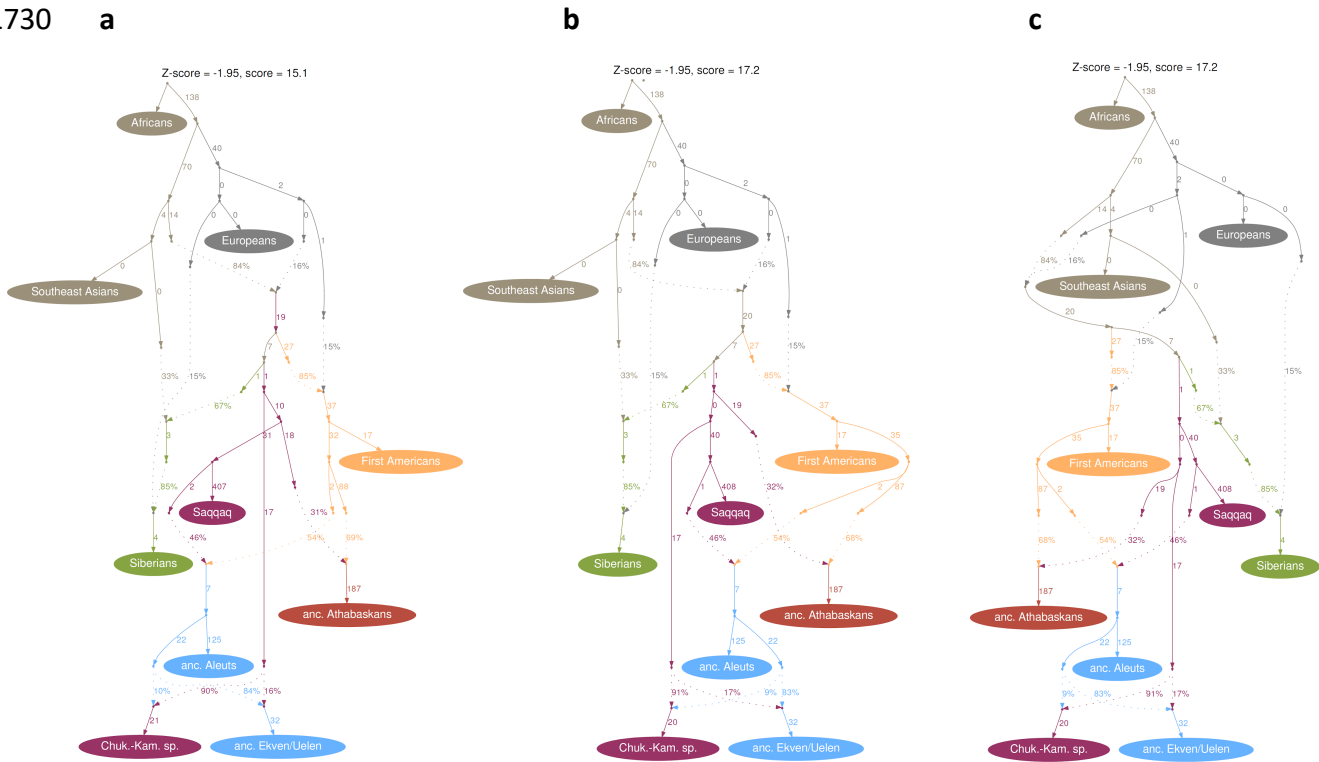
1723

1724



1725 **Fig. S10.2.** Two fitting admixture graphs (based on the transition-free dataset) with unidirectional C-K to E-K
 1726 gene flow, for other fitting topologies see Table S10.2. **a**, topology (*(ATH, C-K), (E-A, P-E)); **b**, topology (C-K,
 1727 (ATH, (E-A, P-E))). The asterisk in the topology notation stands for the entry point of the “proto-American”
 1728 gene flow.
 1729

1730



1731

1732 **Fig. S10.3.** Three best-fitting admixture graphs (based on the transition-free dataset) including ancient
 1733 Athabaskans and a bidirectional C-K to E-A gene flow, for other fitting topologies see Table S10.4. **a**, topology
 1734 (C-K, (ATH, (E-A, P-E))) having the highest likelihood and, the only fitting topology with no 0-length edges at
 1735 key positions in the PPE clade; **b**, topology (ATH, (C-K, (E-A, P-E))); **c**, topology ((ATH, C-K), (E-A, P-E)). While the
 1736 likelihood differences of these models are not significant, they are significant when using the full dataset
 1737 including transitions, although all models fit worse in that case (see text).

1738

1739 **10.3 Improving the West Eurasian and Native American sub-graphs**

1740 dataset: *transversions only*;

1741 populations: *present-day meta-populations including Northern First Peoples; pseudo-haploid*
 1742 *Saqqaq, ancient Aleuts, ancient Neo-Eskimos (Ekven+Uelen), ancient Athabaskans, Mal'ta*
 1743 *(MA1), Loschbour, and the ancient Upward Sun River 1 individual.*

1744 Next, we attempted to construct a more realistic model and added further ancient
 1745 individuals onto the best-fitting graph including the merged Ekven+Uelen Old Bering Sea
 1746 population and ancient Athabaskans. First, we tested all 5 possible placements of the
 1747 Upward Sun River 1 individual (USR1, Moreno-Mayar et al. 2018) as an unadmixed branch
 1748 within the First Peoples clade (Table S10.6). As demonstrated by Moreno-Mayar et al.
 1749 (2018), USR1 occupies the most basal position within the clade, and this topology is by far
 1750 the most supported. In parallel, we attempted constructing a more realistic model for
 1751 present-day Europeans as a mixture of three sources (Lazaridis et al. 2014): western hunter-
 1752 gatherers (WHG, represented by the Loschbour individual, Lazaridis et al. 2014); Siberian
 1753 Paleolithic hunter-gatherers of European origin, also known as ancient North Eurasians (the
 1754 Mal'ta 1 individual a.k.a. MA1, Raghavan et al. 2014); and early European farmers (EEF) with
 1755 substantial basal Eurasian ancestry (Haak et al. 2015, Lazaridis et al. 2016), here represented
 1756 by a ghost basal Eurasian branch. The Mal'ta-related gene flow was mediated by Yamnaya
 1757 steppe pastoralists and followed the initial WHG-EEF admixture event (Allentoft et al. 2015,

1758 Haak et al. 2015). We constructed our models accordingly: first, a group related to WHG
1759 admixed with the basal Eurasian branch; second, a Mal'ta-related West Eurasian lineage
1760 contributed to First Peoples, Siberians/PPE, and Europeans.

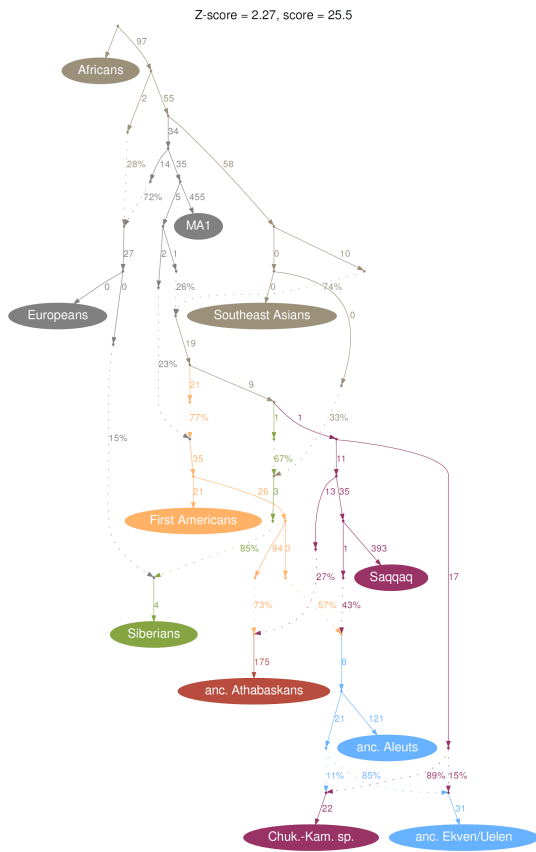
1761 Initially we tested simpler models, where Europeans = a West Eurasian lineage + a
1762 basal Eurasian lineage. On this graph we tested all possible split points of MA1 within the
1763 West Eurasian clade (Table S10.7). Although all Z-scores were the same, the topology ((EUR,
1764 SIB), (MA1, (NEA, SAM))) was the single most plausible one from the perspective that it
1765 resulted in the smallest number of 0-length edges at key positions within the West Eurasian
1766 clade, and at the same time the basal Eurasian contribution in present-day Europeans was
1767 not overestimated (Fig. S10.4a). SIB here stands for the recent European admixture source
1768 in present-day Siberians, NEA and SAM - for Mal'ta-related admixture sources in northeast
1769 Asians (a group uniting Siberians, PPE, and Native Americans) and in Native Americans,
1770 respectively. Then we added WHG (Loschbour) onto the best graph from the previous step,
1771 switched to the 3-component model for Europeans described above, and tried to derive the
1772 gene flow into Europeans from all possible branches within the Mal'ta clade (Table S10.7).
1773 The topology ((WHG, (EUR<, SIB)), <(MA1, (NEA, SAM))) was probably the best one: it
1774 resulted in the smallest number of 0-length edges at key positions within the West Eurasian
1775 clade, and at the same time the basal Eurasian contribution in present-day Europeans was
1776 not overestimated (Fig. S10.4b). The "<" signs here show the direction of the Mal'ta-related
1777 gene flow in Europeans: from the (MA1, (NEA, SAM)) clade into EUR. We acknowledge that
1778 the model for Europeans should be even more complex and include Early European farmers
1779 and Yamnaya pastoralists or related herder groups explicitly. The latter population can be
1780 modelled as a roughly 50%-50% mixture of Mal'ta-related eastern hunter-gatherers (EHG)
1781 and Iranian farmers or related Caucasian hunter-gatherers (CHG) (Lazaridis et al. 2016). But
1782 in order to keep the number of groups in our final model (presented below) reasonably
1783 small, we preferred the simplified version that is anyway much more complex than the
1784 initial version including unadmixed Europeans (Fig. S10.3).

1785 Next, we combined in the same model the updated West Eurasian clade with the
1786 updated Native American clade including the USR1 individual (associated with a major basal
1787 Native American population, termed Ancient Beringians (Moreno-Mayar et al 2018)), and
1788 again tried to derive the gene flow into Europeans from all possible branches within the
1789 Mal'ta clade (Table S10.8). The same best topology was recovered as in the previous search:
1790 ((WHG, (EUR<, SIB)), <(MA1, (NEA, SAM))). We further tested whether any USR1-related
1791 gene flow into Athabaskans improves the model fit. USR1 is associated with the Denali
1792 complex (Potter et al. 2014), which was replaced by the Northern Archaic tradition ca. 6000
1793 calBP (Potter 2010). The Northern Archaic tradition likely includes ancestors of Na-Dene
1794 speakers given its geographic distribution and continuity with the recent past (Workman
1795 1978). We tested various entry points for the USR1-related gene flow: into the common
1796 ancestor of ATH and the Native American source population of E-A, into ATH only, and into
1797 E-A ancestors only, and combined these topologies with 5 possible topologies of the Mal'ta-
1798 related gene flow into EUR. All models had 0-length edges at key positions in the Native
1799 American clade, or 0% admixture from the USR1 lineage in other lineages, or the model-
1800 fitting process failed (Table S10.8). Hence, we conclude that the gene flow from the USR1
1801 branch into the Northern North American clade is unlikely to improve the model fit. This
1802 suggests Ancient Beringians were replaced by Northern Native Americans (including Na-
1803 Dene) around 6000 calBP in interior Alaska.

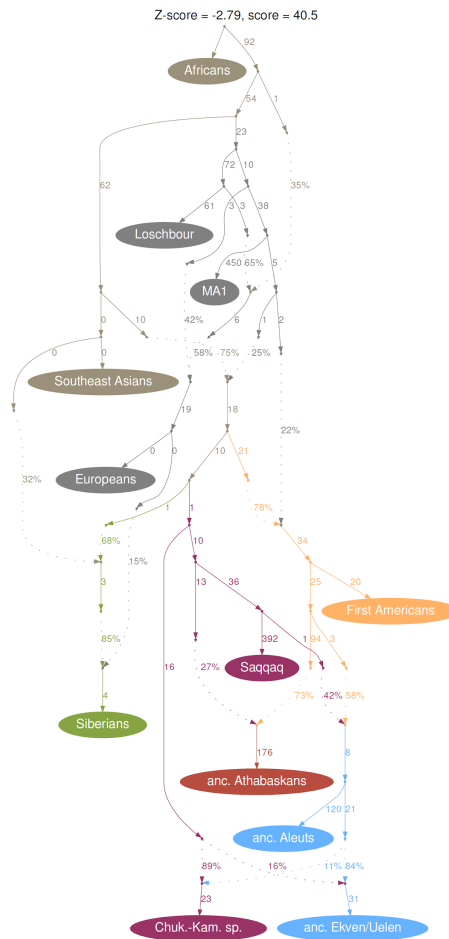
1804

1805

a



b



1806

1807 **Fig. S10.4.** Best-fitting admixture graphs (based on the transition-free dataset) including a two-component (a)
 1808 or a three-component (b) model for Europeans.

1809

1810 We next included into the model other representatives of the Northern North
 1811 American clade (a.k.a. Northern First Peoples or NAM) (Raghavan et al. 2015, Lindo et al.
 1812 2017, Scheib et al. 2018) besides Athabaskans: two Cree and one Tsimshian individual. This
 1813 NAM branch required a recent European admixture and was placed at all possible positions
 1814 within the Native American clade. Each topology was combined initially with the best 2-
 1815 component model for Europeans, and also with three best-fitting 3-component models
 1816 tested previously (Table S10.9). The best-fitting model of the latter class has a $|Z\text{-score}|$ of
 1817 3.12, has no 0-length edges at key positions within the Native American, West Eurasian, and
 1818 PPE clades, and the basal Eurasian contribution into Europeans stands at 34% (Fig. S10.5).
 1819 Thus, the main part of the modeling process was finished. We believe that the Z-score of
 1820 3.12, although being higher than the commonly accepted threshold of 3, is a reasonably low
 1821 score for such a complex model composed of 14 groups: present-day composite meta-
 1822 populations and ancient individuals. The best model fits the data with only two outlying f_4 -
 1823 statistics with $|Z\text{-scores}| > 3$ (Table S10.10):

1824 a) f_4 (Southern First Peoples, USR1; ancient Aleuts, MA1), with the observed value larger
 1825 than the expected value, Z-score = 3.123;

1826 b) f_4 (Southern First Peoples, USR1; Ekven+Uelen, MA1), with the observed value larger than
 1827 the expected value, Z-score = 3.034.

1828 These deviations might reflect elevated Mal'ta-related ancestry in the USR1
1829 individual as compared to Southern First Peoples. To keep this complex graph as simple as
1830 possible, we avoided modeling separate Mal'ta-related gene flows into all relevant groups
1831 since that would add 7 admixture events on top of 11 modelled currently.

1832 Finally, we re-tested three by far best-fitting alternative topologies in the PPE clade
1833 (Table S10.4, Fig. S10.3) on the background of this complex model (Table S10.11). The
1834 topology (ATH, (C-K, (E-A, P-E))) (here again referring to the PPE components in those
1835 groups) resulted in a 0-length edge (a trifurcation), and the other two topologies showed no
1836 0-length edges. The topology (C-K, (ATH, (E-A, P-E))) as compared to the topology ((ATH, C-
1837 K), (E-A, P-E)) published by Moreno-Mayar et al. (2018) had a 5.7 times higher likelihood and
1838 a slightly lower number of outlying f_4 -statistics with absolute Z-scores > 2 , 137 vs. 138
1839 statistics (Table S10.11). A similar result was observed for the full dataset with transitions
1840 included: the topology (C-K, (ATH, (E-A, P-E))) as compared to the topology ((ATH, C-K), (E-A,
1841 P-E)) had a 9.4 times higher likelihood and a lower number of outlying f_4 -statistics with
1842 absolute Z-scores > 2 , 322 vs. 340 statistics (Table S10.11). The likelihood differences
1843 observed are suggestive, but not significant, and thus do not allow us to confidently pick
1844 one model. However, significant likelihood differences were observed for the simpler graph
1845 and the full dataset including transitions (see section 10.2). *Rarecoal*, another demographic
1846 modeling method we used, also provides better resolution (see section 9).

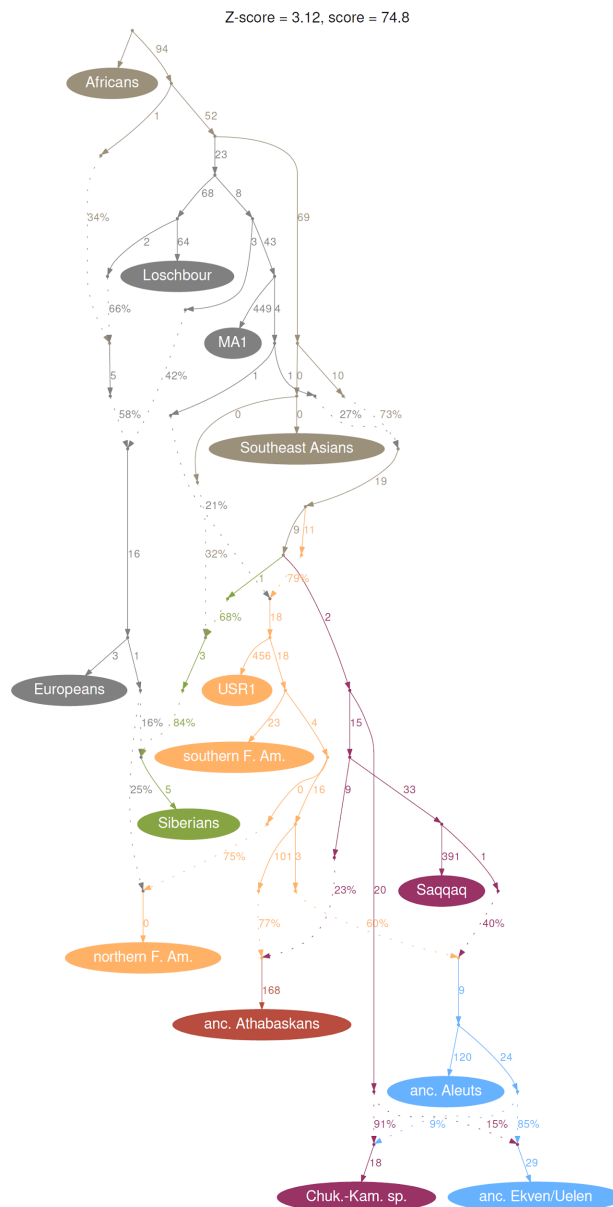
1847

1848 **10.4 Testing all possible combinations of populations at key branches**

1849 dataset: *transversions only*;

1850 populations: *separate present-day populations; pseudo-haploid Saqqaq, ancient Aleuts,*
1851 *ancient Neo-Eskimos (Ekven, Uelen), ancient Athabaskans, Mal'ta (MA1), Loschbour, ancient*
1852 *Upward Sun River 1 individual.*

1853 To explore the best model further, instead of meta-populations we tested all possible
1854 combinations of separate populations. First, we returned to a simple model without the
1855 MA1, Loschbour, USR1, and NAM clades (Z-score = 1.95, Table S10.4, Fig. S10.3a) and tested
1856 separate populations in the merged SGDP+Raghavan et al.+ancient dataset (Supplementary
1857 Table 4) composed of two or more individuals at the following five branches in the graph : E-
1858 A (3 populations: Ekven, Uelen, Yup'ik; present-day Inuit cannot be simply integrated into
1859 this model since they require an additional pulse of recent European admixture); EUR (16
1860 populations); SAM (7 populations, excluding Mayans and Mixtec having low-level European
1861 and/or African admixture); SEA (8 populations); SIB (10 populations, including an Ust'-Belaya
1862 Angara individual I7760 having the West Siberian genetic profile (section 4), abbreviated as
1863 UBS). To replace populations that were removed due to the minimum size requirement of 2
1864 individuals, we considered some additional populations (Table S10.12) that were not
1865 included into the original meta-populations as defined in Table S10.1. Among 26,880 models
1866 tested, just 7% were non-fitting ($|Z\text{-score}| > 3$), and for one model the algorithm failed.
1867 Absolute Z-scores down to 0.91 were observed (2.19 on average among all models), and in 7
1868 graphs no 0-length edges were found (4.9 on average among all models). See Table S10.12
1869 for a full list of tested models and summary statistics. Since the simple topology is fitting for
1870 almost all combinations of populations, it is unlikely that the observed result depends on
1871 the composition of meta-populations.



1872

1873

1874

1875

Fig. S10.5. The best-fitting admixture graph (based on the transition-free dataset) featuring a three-component model for Europeans and a complex American clade including the ancient USSR1 individual and present-day Northern First Peoples (NAM).

1876

1877

1878

1879

1880

1881

1882

1883

1884

1885

Second, we attempted an even more exhaustive testing of population combinations at 6 branches for the most complex model (Z-score = 3.12, Fig. S10.5). We relaxed the population size requirement of 2 or more individuals and took the following populations (Table S10.13): E-A (3 populations: Ekven, Uelen, Yup'ik); EUR (19 populations); SAM (13 populations, including the Clovis ancient individual); NAM (2 populations); SEA (9 populations); SIB (10 populations, including the Ust'-Belaya Angara ancient individual I7760). Among 133,380 models tested, 12% had a $|Z\text{-score}| < 4$. Absolute Z-scores down to 2.98 were observed, and 4.8% of graphs had no 0-length edges at key positions within the EUR, PPE, and Native American clades.

1886

1887

1888

We also re-tested three by far best-fitting alternative topologies in the PPE clade (Table S10.4, Fig. S10.3) on the background of this complex model with separate populations. First, we took 1,831 population combinations that yielded absolute Z-scores <

1889 3.5 for the (C-K, (ATH, (E-A, P-E))) topology (Table S10.13) and tested the three topologies
1890 (Table S10.11). The topology (ATH, (C-K, (E-A, P-E))) was the worst one according to all
1891 metrics, and it also had the lowest likelihood among the three best meta-population-based
1892 models (Table S10.11), therefore we excluded it from further testing. Then we tested
1893 133,380 population combinations for the topologies (C-K, (ATH, (E-A, P-E))) and ((ATH, C-K),
1894 (E-A, P-E))). We find that both topologies are favored by some combinations of populations,
1895 with the topology (C-K, (ATH, (E-A, P-E))) winning more often in terms of absolute Z-scores
1896 and higher likelihoods than the topology ((ATH, C-K), (E-A, P-E)) (Table S10.14). Although the
1897 distributions of likelihoods over 133,380 population combinations are largely overlapping
1898 (Table S10.14), median likelihood of the topology (C-K, (ATH, (E-A, P-E))) is 58.5 higher than
1899 that of the topology ((ATH, C-K), (E-A, P-E)), a significant difference according to our
1900 arguments from section 10.2. On average, the topology ((ATH, C-K), (E-A, P-E)) also yields
1901 more 0-length edges within the PPE clade (2.3 vs. 1.5 edges), which in particular includes
1902 many cases with a trifurcation of the form (ATH, C-K, (E-A, P-E)), and also yields a larger
1903 number of outlying f_4 -statistics with absolute Z-scores > 2 (409 vs. 379 statistics).

1904 Overall, the outcome of the model testing with separate populations is the same as
1905 that of the meta-population approach, which arguably has a higher resolution due to larger
1906 number of individuals per populations, and may be less prone to overfitting. Thus, we favor
1907 the topology (C-K, (ATH, (E-A, P-E))) over the alternative ((C-K, ATH), (E-A, P-E)), although the
1908 difficulty of distinguishing between the two topologies may also reflect the possibility of a
1909 near-trifurcation of the three groups C-K, ATH, and (E-A, P-E).

1910 To obtain an independent hypothesis test for the PPE topology, we performed
1911 demographic modeling with *Rarecoal* (section 9), as well as exhaustive testing of population
1912 triplets and quadruplets using *qpWave* and *qpAdm* with various outgroup sets (section 5).

1913

1914 *References (for this section)*

- 1915 Allentoft, M. E. *et al.* Population genomics of Bronze Age Eurasia. *Nature* **522**, 167–172.
1916 Haak, W. *et al.* Massive migration from the steppe was a source for Indo-European languages in Europe. *Nature*
1917 **522**, 207–211 (2015).
1918 Lazaridis, I. *et al.* Ancient human genomes suggest three ancestral populations for present-day Europeans. *Nature*
1919 **513**, 409–413 (2014).
1920 Lazaridis, I. *et al.* Genomic Insights into the Origin of Farming in the Ancient Near East. *Nature* **536**, 419–424
1921 (2016).
1922 Lindo, J. *et al.* Ancient individuals from the North American Northwest Coast reveal 10,000 years of regional
1923 genetic continuity. *Proc. Natl. Acad. Sci. U. S. A.* **114**, 4093–4098 (2017).
1924 Moreno-Mayar, J. V. *et al.* Terminal Pleistocene Alaskan genome reveals first founding population of Native
1925 Americans. *Nature* **553**, 203–207 (2018).
1926 Potter, B. A. Archaeological patterning in Northeast Asia and Northwest North America: an examination of the
1927 Dene-Yeniseian hypothesis. *The Dene-Yeniseian Connection*, ed. Kari, J., Potter, B. A. *Anthropological Papers*
1928 *of the University of Alaska: New Series* **5**, 138–167 (2010).
1929 Potter, B. A. *et al.* New insights into Eastern Beringian mortuary behavior: a terminal Pleistocene double infant
1930 burial at Upward Sun River. *Proc. Natl. Acad. Sci. U. S. A.* **111**, :17060–17065 (2014).
1931 Raghavan, M. *et al.* Upper Palaeolithic Siberian genome reveals dual ancestry of Native Americans. *Nature* **505**,
1932 87–91 (2014).
1933 Raghavan, M. *et al.* Genomic evidence for the Pleistocene and recent population history of Native Americans.
1934 *Science* **349**, 1–20 (2015).
1935 Scheib, C. L. *et al.* Ancient human parallel lineages within North America contributed to a coastal expansion.
1936 *Science* **360**, 1024–1027 (2018).
1937 Workman, W. B. The Prehistory of the Aishihik-Kluane area, southwest Yukon Territory. *National Museum of Man*,
1938 *Mercury Series* No. 74 (1978).

1939 **Supplementary Information section 11**

1940 **Additional results on Aleutian population history**

1941

1942 A controversial chapter of American Arctic prehistory concerns Aleuts (Balter 2012). The
1943 Aleutian Islands were settled much earlier than the American Arctic, about 9,000 calBP
1944 (Hatfield 2010), and discontinuities in the Aleutian archaeological record were observed at
1945 ~4,500 calBP (Knecht and Davis 2001, Hatfield 2010, Davis et al. 2016) and at ~800 – 900
1946 calBP (Brenner Coltrain et al. 2006, Hatfield 2010). The first discontinuity was associated
1947 with Paleo-Eskimo influence, which is consistent with the final model presented in this
1948 study, and the latter with Neo-Eskimo influence, although the extent of technological
1949 interactions, and the role of genetic continuity vs. population replacement is debated
1950 (Brenner Coltrain et al. 2006, Smith et al. 2009, Misarti and Maschner et al. 2015). Three
1951 burial sites in the eastern Aleutian Islands received most attention so far: the Chaluka
1952 midden site on the Umnak Island was associated with an early population (3,600 – 300
1953 calBP) with a dolichocranic morphology, inhumation burials (Hrdlička 1945, Brenner Coltrain
1954 et al. 2006) and a predominance of mtDNA haplogroup A2a (Smith et al. 2009). Other sites,
1955 at the Kagamil and Ship Rock Islands, were associated with a later population (800 – 900
1956 calBP and later), a brachycranial morphology, mummification burials (Hrdlička 1945, Brenner
1957 Coltrain et al. 2006) and a predominance of mtDNA haplogroup D2a (Smith et al. 2009). The
1958 former population has been historically termed Paleo-Aleut, and the latter Neo-Aleut.

1959 We carried out a small-scale sampling of ancient genomes from all three sites
1960 (Extended Data Table 1). Radiocarbon dates obtained for these individuals in a previous
1961 study (Brenner Coltrain et al. 2006) were recalibrated using a more appropriate marine
1962 reservoir correction (Misarti and Maschner 2015) resulting in the following median dates:
1963 2,050 – 530 calBP for Paleo-Aleuts and 580 – 280 calBP for Neo-Aleuts (Supplementary
1964 Table 2, Supplementary Information section 2). Among 11 ancient Aleuts subjected to in-
1965 solution target enrichment of more than 1.2 million SNPs using a protocol by Fu *et al.*
1966 (2015), 4 Neo-Aleuts and 2 Paleo-Aleuts passed the 70% missing rate cut-offs that we
1967 applied in order to permit high-density SNP analyses and were incorporated into both the
1968 HumanOrigins and Illumina SNP array datasets (Supplementary Table 4). In addition, one
1969 Paleo-Aleut individual dated to 700 – 310 calBP (IDs I0719 and 378620, the latter used by
1970 Brenner Coltrain et al. 2006) was sequenced with the shotgun approach at 2.3x coverage
1971 (with filtered reads). Due to low coverage of both the enrichment and shotgun data, only
1972 pseudo-haploid SNP calls were generated for ancient Aleuts, hence these samples were
1973 used for *qpWave/qpAdm*, *PCA*, *ADMIXTURE*, *ALDER*, and rare allele sharing analyses only.

1974 Analyzing these data, we found that four Neo-Aleut samples with median dates
1975 between 580 – 340 calBP and two Paleo-Aleut samples dated to 1260 – 870 and 700 – 310
1976 calBP are indistinguishable. In particular, in both the HumanOrigins and Illumina datasets,
1977 the Paleo- and Neo-Aleuts were indistinguishable according to *PCA* (Fig. 1a, Extended Data
1978 Fig. 2, section 4) and *ADMIXTURE* patterns (Extended Data Fig. 8), showing that the Neo-
1979 Aleuts arose directly from the Paleo-Aleuts and contradicting suggestions – based on
1980 morphology (Hrdlička 1945) and mitochondrial DNA haplogroup frequency changes (Smith
1981 et al. 2009) – that the transition between Paleo- and Neo-Aleuts was driven by a new
1982 migration into the islands from the outside. Pooling the six ancient Aleuts together for
1983 *qpWave/qpAdm* and *qpGraph* analyses (sections 5 and 10), we find that both groups have a
1984 strong Neo-Eskimo genetic affiliation, and in this respect are similar to present-day Aleuts.

1985 In addition, the single Paleo-Aleut genome (I0719) that we generated was placed into the
 1986 Aleut branch with high certainty using *Rarecoal* (Fig. 2b, section 9).

1987 We also used this first data from the Aleutian Islands prior to European colonization
 1988 to test a claim by Raghavan *et al.* (2015) of a genetic affinity between Papuans and Aleuts.
 1989 The original study attempted to account for the substantial amounts of recent European
 1990 ancestry in the present-day Aleutian individuals analyzed by identifying and excluding
 1991 segments of the genomes that could be reliably called as European in ancestry. However,
 1992 this procedure could in principle have introduced bias that affected the original reported
 1993 signal that had a significance level of $Z=2$ to $Z=3$ (because the ancestry inference is not
 1994 perfect and may selectively exclude segments of non-colonial ancestry with greater or lesser
 1995 affinity to Papuans). We thus used *D*-statistics to test whether there was evidence of an
 1996 excess affinity to Papuans in the ancient Aleuts, using a variety of subsets of the data, but
 1997 find no evidence of an excess affinity to Papuans ($Z < 2$) (Table S11.1). These results suggest
 1998 that an excess affinity to Australo-Melanesians is exclusively found in South America and
 1999 primarily observed in Amazonian populations (Skoglund *et al.* 2015).

2000

2001 **Table S11.1.** Aleutian ancient DNA shows no evidence of Papuan-related gene flow hypothesized by Raghavan
 2002 *et al.* (2015) on the basis of present-day European-admixed Aleuts. The following *D*-statistics were calculated:
 2003 $D(A, B; X, Y)$, where A=Yoruba or Dai; B=Papuans, Australians, or Onge; X=Mixe; Y=Neo-Aleuts, Paleo-Aleuts,
 2004 Ancient Aleuts combined, or Surui. Z-scores are color-coded: $Z > 3$ in red, and $2 < Z < 3$ in yellow.

dataset	treatment	pop A, pop B	pop X	pop Y							
				ancient Aleuts				ancient Aleuts			
				Neo-Aleut	Paleo-Aleut	combined	Surui	Neo-Aleut	Paleo-Aleut	combined	Surui
				Z-scores				informative SNPs			
HumanOrigins (Lazaridis <i>et al.</i> 2014)	normal	Yoruba, Australian	Mixe	0.7	1.63	1.43	1.67	272,013	275,100	306,158	314,186
		Yoruba, Papuan		0.65	1.46	1.31	2.88	274,210	277,200	308,606	316,685
		Yoruba, Onge		0.85	1.32	1.41	3.87	273,679	276,757	308,026	316,118
		Dai, Australian		-1.34	-0.91	-1.21	1.08	262,660	265,765	295,150	302,843
		Dai, Papuan		-1.51	-1.28	-1.52	2.29	267,002	270,010	300,081	307,977
	Dai, Onge	-1.54		-1.78	-1.79	3.26	265,435	268,527	298,351	306,289	
	no transitions	Yoruba, Australian		-0.18	0.76	0.06	0.85	50,109	51,071	56,733	58,428
		Yoruba, Papuan		-0.34	1.18	-0.03	2.11	50,487	51,441	57,158	58,866
		Yoruba, Onge		0.15	1.29	0.83	3	50,415	51,366	57,073	58,770
		Dai, Australian		-1.53	-1.29	-1.69	0.72	48,383	49,290	54,706	56,306
Dai, Papuan		-1.74	-1.03	-1.93	2.05	49,161	50,067	55,601	57,250		
Dai, Onge	-1.43	-1.11	-1.24	3.08	48,864	49,762	55,263	56,918			
genomes (Mallick <i>et al.</i> 2016)	normal	Yoruba.DG, Australian.DG	2.01	2.68	2.37	3.65	433,909	405,920	494,182	506,885	
		Yoruba.DG, Papuan.DG	1.56	1.9	1.86	4.06	459,513	428,834	523,154	536,078	
		Yoruba.DG, Onge.DG	2	2.01	2.25	3.27	432,997	405,045	493,166	506,158	
		Dai.DG, Australian.DG	-1.28	-0.92	-1.24	2.13	442,560	413,584	503,073	516,854	
		Dai.DG, Papuan.DG	-1.96	-2.02	-2.09	2.68	460,213	429,322	523,311	536,979	
	Dai.DG, Onge.DG	-1.35	-1.65	-1.45	1.59	441,305	412,384	501,610	515,733		
	no transitions	Yoruba.DG, Australian.DG	0.8	1.3	0.95	1.62	84,512	79,527	97,011	101,213	
		Yoruba.DG, Papuan.DG	0.76	1.58	1.05	2.66	89,441	83,985	102,642	107,037	
		Yoruba.DG, Onge.DG	1.65	2.81	2.59	2.05	84,355	79,368	96,826	101,115	
		Dai.DG, Australian.DG	-1.75	-2.11	-2.2	1.06	86,131	80,979	98,740	103,131	
Dai.DG, Papuan.DG		-1.94	-2.13	-2.36	2.18	89,599	84,130	102,768	107,298		
Dai.DG, Onge.DG	-0.88	-0.56	-0.6	1.38	85,861	80,703	98,441	102,861			

2006

2007 *References (for this section)*

2008 Balter, M. The peopling of the Aleutians. *Science* **335**, 158–161 (2012).
 2009 Brenner Coltrain, J. B., Hayes, M.G. & O'Rourke D.H. Hrdlička's Aleutian population-replacement hypothesis. A
 2010 radiometric evaluation. *Curr. Anthropol.* **47**, 537–548 (2006).
 2011 Davis, R., Knecht, R. & Rogers, J. First Maritime Cultures of the Aleutians. *The Oxford Handbook of the Prehistoric*
 2012 *Arctic*, ed. Friesen, T. M., Mason, O. K. New York: Oxford University Press. 279–302 (2016).
 2013 Fu, Q. *et al.* An early modern human from Romania with a recent Neanderthal ancestor. *Nature* **524**, 216–219
 2014 (2015).
 2015 Hatfield, V. L. Material culture across the Aleutian archipelago. *Hum. Biol.* **82**, 525–556 (2010).

- 2016 Hrdlička, A. *The Aleutian and Commander Islands and their inhabitants*. Philadelphia: Wistar Institute of
2017 Anatomy and Biology (1945).
- 2018 Knecht, R. A. & Davis, R. S. A prehistoric sequence for the eastern Aleutians. *Archaeology in the Aleut zone of*
2019 *Alaska: Some recent research*, ed. Dumond, D. *University of Oregon Anthropological Papers* **58**, 269–288
2020 (2001).
- 2021 Misarti, N. & Maschner, H. D. G. The Paleo-Aleut to Neo-Aleut transition revisited. *J. Anthropol. Archaeol.* **37**,
2022 67–84 (2015).
- 2023 Raghavan, M. *et al.* Genomic evidence for the Pleistocene and recent population history of Native Americans.
2024 *Science* **349**, 1–20 (2015).
- 2025 Skoglund, P. *et al.* Genetic evidence for two founding populations of the Americas. *Nature* **525**, 104–108
2026 (2015).
- 2027 Smith, S. *et al.* Inferring population continuity versus replacement with aDNA: A cautionary tale from the
2028 Aleutian Islands. *Hum. Biol.* **81**, 19–38 (2009).
- 2029

2030 **Supplementary Information section 12**

2031 **Dating admixture events using *ALDER***

2032

2033 We have dated the Paleo-Eskimo admixture event in Na-Dene speakers using the
2034 *GLOBETROTTER* method (section 7). In addition, we applied a different linkage
2035 disequilibrium (LD)-based method, *ALDER*, that relies on allele frequency data at SNP sites
2036 and can accommodate pseudo-haploid ancient data (Loh et al. 2013). Although a single-
2037 pulse admixture model implemented in *ALDER* is likely to be an oversimplification, it can still
2038 provide a reasonable time frame for the admixture events. *ALDER v.1.03* works in the
2039 following way (Loh et al. 2013): 1/ builds a weighted LD-decay curve given a test population
2040 and a pair of reference populations related to the admixture partners; 2/ estimates a
2041 jackknife-based p -value and Z-score by leaving out each chromosome in turn and refitting
2042 the decay curve; 3/ determines the distance to which LD in the test population is
2043 significantly correlated with LD in either reference A or reference B; 4/ to minimize signal
2044 from shared demographic history, data from SNP pairs at distances smaller than this
2045 correlation threshold are ignored; 4/ computes additional LD curves and associated p -values
2046 and Z-scores, substituting either reference A or B by the test population. If the test
2047 population is admixed between populations related to references A and B, the one-
2048 reference curves are expected to pick up the same LD decay signal. If the test population is
2049 not admixed but has experienced a shared bottleneck with one of the reference groups, an
2050 LD decay curve is unlikely to emerge. Thus, if the two-reference test and both one-reference
2051 tests yield Z-scores > 2 , the *ALDER* test is considered successful. This test procedure is
2052 intended to be conservative (Loh et al. 2013).

2053 In Table S12.1 *ALDER* results for present-day and ancient E-A groups are
2054 summarized. Outcomes of two-reference tests that yielded p -values < 0.05 (Z-scores > 2) are
2055 shown. Target groups composed of 4 or more individuals were suitable for this analysis.
2056 Various First Peoples (SAM or NAM) and Saqqaq were used as surrogates for the admixture
2057 partners. Given the strong support we have obtained for the *qpGraph* and *qpAdm* models
2058 “E-A = FAM + P-E” (sections 5 and 10), we expected similar models to be supported by
2059 *ALDER*. On the other hand, the additional pulse of C-K admixture in Yup’ik and Inuit
2060 ancestors is expected to compromise the *ALDER* results: populations with complicated
2061 histories (e.g., multiple waves of admixture) often have different estimates of admixture
2062 dates with one- and two-reference LD-decay curves (Loh et al. 2013).

2063 Here we consider the *ALDER* results population by population (HumanOrigins
2064 dataset, Table S12.1). First, for Iñupiat, a relatively large present-day population of 15
2065 individuals without noticeable colonial European admixture and having a low level of C-K
2066 admixture (judging by the overall PPE ancestry proportion, see section 5), most *ALDER*
2067 admixture tests were successful (16 of 22 tests with different FAM references), and a
2068 further 5 tests were nearly successful (Z-scores for a one-reference test with a FAM group $>$
2069 1.84). Upper and lower boundaries of the SD interval around the admixture date were
2070 averaged across all FAM surrogates, and thus the admixture date probably falls between
2071 2,700 and 4,400 years ago (ya, values rounded to the nearest century, see Table S12.1). This
2072 is a broad range, but it fits two important archaeological constraints: the arrival of P-E to
2073 Alaska ca. 5,000 calBP and the emergence of Chukotkan Neo-Eskimos in the archaeological
2074 record ca. 2,200 calBP in the form of the Old Bering Sea culture (Mason et al. 2016). We
2075 expect that the formative admixture event that gave rise to Eskimo-Aleut speakers

2076 happened at least few centuries before the back-migration of Yup'ik and Inuit ancestors to
2077 Chukotka, thus the estimate of 2,700 ya and earlier seems realistic.

2078 Ancient Aleuts are expected to yield “cleaner” results because of the absence of the
2079 C-K gene flow (section 10), however this group is composed of just 6 pseudo-haploid non-
2080 contemporaneous samples (Supplementary Table 2). Although 8 FAM surrogates resulted in
2081 two-reference p -values < 0.05 , all one-reference pre-tests (ancient Aleuts + FAM as
2082 references) failed (Table S12.1), probably due to lack of power. Reassuringly, admixture
2083 dates averaged across these 8 tests are similar to those obtained for Iñupiat: 2,700 ya to
2084 4,900 ya. For calculating these dates, we introduced an offset of 600 ya by averaging the
2085 calibrated radiocarbon dates obtained for the 6 ancient Aleut individuals analyzed here
2086 (Supplementary Table 2) and rounding to the nearest hundredth. The admixture dates
2087 estimated for the ancient Ekven population (16 ind.) were roughly 400 years older (Table
2088 S12.1). For this population, we introduced an offset of 1000 ya by averaging the calibrated
2089 radiocarbon dates obtained for the 16 ancient individuals buried at Ekven and analyzed here
2090 (Supplementary Table 2) and rounding to the nearest hundredth. The admixture dates
2091 estimated for two present-day Yup'ik groups (9 and 15 ind.) were even older than those for
2092 Ekven (Table S12.1). The results for the Yup'ik and Ekven groups were most probably
2093 confounded by a high proportion of PPE ancestry contributed by the second (C-K) gene flow
2094 (Extended Data Fig. 8, sections 5, 8, and 10).

2095

2096 *References (for this section)*

2097 Loh, P. R. *et al.* Inferring admixture histories of human populations using linkage disequilibrium. *Genetics* **193**,
2098 1233–1254 (2013).

2099 Mason, O. K. The Old Bering Sea florescence about Bering Strait. *The Oxford Handbook of the Prehistoric Arctic*,
2100 ed. Friesen, T. M., Mason, O. K. New York: Oxford University Press. 417–442 (2016).

2101

2102 **Supplementary Information section 13**

2103 **Overview of the Dene-Yeniseian linguistic hypothesis**

2104 by Edward J. Vajda

2105

2106 The Dene-Yeniseian language hypothesis is considered here in light of the demonstrated
2107 Paleo-Eskimo genetic contribution to modern Tlingit, Eyak and Athabaskan speakers dated
2108 to ~4,400-5,000 ya and shared more distantly with Siberians at a time depth of ~6,200 ya
2109 (Table S9.2). The timing of this genetic link and plausible archaeological patterning
2110 described below provide the first evidence apart from linguistics that realistically supports
2111 the Dene-Yeniseian language hypothesis. Given that Paleo-Eskimo-related ancestry is
2112 likewise found in populations speaking Eskimo-Aleut and Chukotko-Kamchatkan languages,
2113 the Paleo-Eskimo linguistic legacy could instead be associated with the origins of either of
2114 these families rather than with Dene-Yeniseian. However, because the accumulated Dene-
2115 Yeniseian and internal Na-Dene comparative linguistic evidence correlates so plausibly with
2116 the coalescence dates of the Paleo-Eskimo genetic loci shared by populations speaking
2117 precisely these languages, it is useful to elaborate further on the potential significance of
2118 these results for situating the Dene-Yeniseian language family in space and time – questions
2119 left without clear answers in Kari and Potter (2010) and the genetic results of this paper.

2120 The Dene-Yeniseian hypothesis posits that the Ket language spoken near the Yenisei
2121 River in Central Siberia is related to the widespread Na-Dene language family in North
2122 America. Na-Dene comprises Tlingit and the recently extinct Eyak in Alaska along with over
2123 thirty Athabaskan languages spoken from the western North American Subarctic to pockets
2124 in California (Hupa), Oregon (Tolowa) and the American Southwest (Navajo, Apache) (Krauss
2125 1976). The severely endangered Ket is the sole survivor of Siberia's once widespread
2126 Yeniseian language family, whose ancient presence in the region predates the expansion of
2127 reindeer breeders and other pastoralists in North and Inner Asia (Dul'zon 1959, 1962, Vajda
2128 2001, 2009, Werner 2005). Dene-Yeniseian as a linguistic hypothesis dates back to at least
2129 1923, when Italian linguist Alfredo Trombetti linked Athabaskan and Tlingit with Ket on the
2130 basis of a few similar-sounding words (Trombetti 1923). In the past two decades new
2131 evidence supporting the connection has been published in the form of shared
2132 morphological systems and lexical cognates showing interlocking sound correspondences
2133 (Ruhlen 1998, Vajda 2001, Werner 2004, Vajda 2010a, 2010b). However, Dene-Yeniseian
2134 cannot be accepted as a proven language family until the evidence of lexical and
2135 morphological correspondences between Yeniseian and Na-Dene is significantly expanded
2136 and tested by further critical analysis. It will also be essential to determine the potential
2137 relationship between Yeniseian and Old World languages and families such as Sino-Tibetan,
2138 North Caucasian, and the Burushaski isolate of northern Pakistan – all of which have been
2139 proposed at various times in the past as relatives of Yeniseian, and sometimes also of Na-
2140 Dene (G. Starostin 2010). While parallel research from genetics, archaeology and folklore
2141 studies cannot prove a language connection (only comparative linguistic analysis can
2142 accomplish that), interdisciplinary archaeological and genetic studies can demonstrate in
2143 important ways the plausibility or implausibility of such a connection, as well as situating
2144 populations in space and time.

2145 The timing of the Dene-Yeniseian language split could shed important light on Native
2146 American as well as North Asian prehistory. In attempting to reconcile the apparent
2147 closeness of Yeniseian and Na-Dene grammatical homologies with what at the time was

2148 assumed to be a much greater genetic distance between Ket and Na-Dene speakers, Potter
2149 (2010) discussed a number of possible scenarios for the Dene-Yeniseian connection,
2150 including: 1) a Late Pleistocene separation connected with the Paleo-Indian migrations into
2151 the Americas, with an extraordinary slow rate of linguistic change; 2) a separation involving
2152 a back migration of Yeniseians from Beringia; and 3) an Early to Mid-Holocene separation
2153 connected with the entrance into Alaska around 5,000 calBP by the population associated
2154 with the Arctic Small Tool tradition (ASTt) (see also Dumond 2010). The first two scenarios
2155 are unlikely based on results from this paper, while the third becomes more plausible (see
2156 below).

2157 In contrast to the ability of archaeologists to radiocarbon-date their finds, or
2158 geneticists to calibrate the time separating two related populations, there is no universally
2159 accepted method to reliably and precisely compute the time of separation of languages
2160 known to be genealogically related. All proposed methods of dating prehistoric language
2161 splits have been criticized (Campbell 2013:447-492). McMahon & McMahon (2005: 177-
2162 204) distinguish between methods of establishing relatedness or degrees of relatedness
2163 between languages (lexicostatistics) from the use of such data to assign precise dates for
2164 prehistoric language splits based on an assumed regular rate of linguistic change
2165 (glottochronology), which in fact does not exist across languages or even in a single
2166 language over time. While rejecting glottochronology, McMahon & McMahon (2005:204)
2167 support the value of gathering and comparing lexicostatistic data, which then can
2168 sometimes be useful for purposes of dating when combined with facts from other
2169 disciplines such as archaeology and genetics. Several types of evidence can potentially be
2170 combined with evidence of shared vocabulary and grammatical homologies to help narrow
2171 the range of plausible separation dates between related languages. For Dene-Yeniseian, all
2172 of them suggest a split roughly between 9,000 and 7,000±500 ya. The shallower end is
2173 favored by the detailed morphological homologies shared by the two families (Nichols
2174 2010). The deeper end, which is suggested by the more meager number of shared lexical
2175 cognates, would still be far too shallow to match a connection with the earliest Paleo-Indian
2176 migrations during the Late Pleistocene. However, this range does provide a realistic
2177 temporal parallel for the migration of ASTt ancestors from North Asia into the Americas
2178 about 5,000 calBP. If this population consisted of Pre-Proto-Na-Dene speakers, then the split
2179 with their Yeniseian-speaking cousins in south-central Siberia would necessarily have been
2180 earlier.

2181 Most previous calculations by historical linguists place the timeline for the internal
2182 diversification of Na-Dene languages between 6,000 and 3,500 ya. All Athabaskan
2183 languages, whether spoken in Alaska, Canada, California, or Arizona, share over 70%
2184 cognates in basic vocabulary, the number becoming higher if the list includes words
2185 associated with northern boreal forest lifeways, such as 'birch', 'wolverine', etc. Krauss
2186 (1976:330) showed that all Athabaskan languages share 33% of basic vocabulary from the
2187 100-word Swadesh List with Eyak. Athabaskan-Eyak, in turn, is clearly more distantly related
2188 to the Tlingit dialect cluster spoken in the southeast Alaskan coast and parts of interior
2189 Yukon Territory (Heggarty & Renfrew 2014:1236). Using a variety of lexicostatistic methods
2190 and reliable data, Krauss (1976:333) estimated a time depth for Proto-Athabaskan of
2191 2,400±500 years and for Athabaskan-Eyak of 3,400±500 years. Estimates for the earlier
2192 breakup of Tlingit and Athabaskan-Eyak range from 6,000 (Mülenbernd & Rama 2017) or
2193 5,000 years (Swadesh 1958) to as shallow as 3,500 years (Kaufman & Golla 2000), with an
2194 estimate of 4,500 years by Krauss (1980:11-13). The deeper dates would be favored by the
2195 known conservatism of Na-Dene languages and also by the fact that the phylogenetic

2196 relationship between Athabaskan-Eyak-Tlingit (Na-Dene) was universally accepted only in
2197 the past decade, despite being suspected for over a century (Campbell 2011). The late
2198 acceptance date derives mainly from the fact that before Leer (2010), the evidence for
2199 Athabaskan-Eyak-Tlingit in the form of shared finite verb structure significantly outweighed
2200 the expected parallel lexical evidence, making it unclear whether language mixing rather
2201 than genetic inheritance was involved in the historical similarities between these languages.

2202 The relatedness between Athabaskan languages, despite their far-flung geography, is
2203 close enough that it has never been in doubt (Campbell 1997). This suggests a rapid spread
2204 from a common source, most likely somewhere in Northwestern Canada near the current
2205 border between British Columbia and Alaska or in adjacent parts of Interior Alaska. Another
2206 support for a recent dispersal is the high rate of mutual intelligibility between
2207 geographically distant Athabaskan languages (Krauss 1976). Some scholars posit a time
2208 depth for Proto-Athabaskan as shallow as 2,000 ya (Kaufman & Golla 2000), though a date
2209 closer to 3,000 is more likely given the resistance to borrowing observed with all of these
2210 languages. A time depth of at least 2,500 years for Athabaskan, following the estimate in
2211 Krauss (1976), would concur with the westward spread of the Taltheilei Culture beginning
2212 2,750 calBP, which has been previously linked with the spread of Athabaskan speakers
2213 (Potter 2010, Kari 2010).

2214 The interior Alaskan and northwestern Canadian portions of the Athabaskan range
2215 show no clear archaeological evidence of prehistoric population replacement during the
2216 past ~6000 years (Potter 2010, Kari 2010). For this reason, Kari (2010) posits that the
2217 Athabaskans have lived in interior northwestern North America for at least that span of
2218 time. Kari cites the near complete absence of substrate place names in the Northern
2219 Athabaskan areas as evidence for their ancient occupation of these areas. However, the
2220 Navajo and Apache areas of the American Southwest likewise have virtually no toponymic
2221 substrate from the languages previously spoken there, yet the Athabaskan presence in this
2222 area dates no farther back than 1,200 calBP. This reflects a strong Athabaskan avoidance of
2223 borrowing place names rather than ancient occupancy. In any event, such a degree of
2224 linguistic conservatism, whereby geographically distant languages maintain mutual
2225 intelligibility over a span of ~6000 years, would be unique and unprecedented. After
2226 adjusting for the conservatism of Na-Dene languages, retention rates for vocabulary and
2227 grammatical structures would appear to support a time depth of 5,000±500 years for the
2228 ancestral Athabaskan-Eyak-Tlingit language (i.e., Proto-Na-Dene). This coheres well with the
2229 possibility that the language ancestral to Na-Dene could have been introduced around 5,000
2230 ya into Alaska by North Asian immigrants associated with the later development and spread
2231 of the ASTt. Also probably connected with these “Paleo-Eskimos” is the spread of other
2232 elements of North Asian material culture and folklore (Alekseenko 1995; Berezkin 2015) to
2233 the Na-Dene.

2234 Like the Athabaskan family, Yeniseian languages are obviously related genealogically.
2235 Ket and its now extinct relatives (Yugh, Kott, Assan, Arin, and Pumpokol) were recognized as
2236 closely related more than 150 years ago (Vajda 2001). Studies of substrate toponyms (Vajda
2237 2018b) show that the known Yeniseian daughter branches (except the Ket-Yugh sub-branch)
2238 had already diversified by 2,000 ya, when Turkic and Uralic-speaking pastoralists started
2239 displacing them in most of their southern and western territory, acquiring Ket-related river
2240 names and other substrate linguistic elements in the process. If the main sub-branching
2241 existed 2,000 years ago, the family is clearly older. The high rate of shared cognates in basic
2242 vocabulary (over 70%) between Ket and Kott, which belong to different primary branches of

2243 the family, suggest that Proto-Yeniseian must be at least 2,500 to 3,000 years, if not older,
2244 which would roughly match the more plausible estimates of time depth for Athabaskan. It is
2245 possible to reconstruct Proto-Yeniseian vocabulary (Starostin 1995) and many aspects of
2246 grammatical structure (Vajda 2013; Vajda 2017) with a high degree of confidence. If Para-
2247 Yeniseian linguistic relatives once existed in other parts of North Asia, the influx of pastoral
2248 tribes from the south must have obliterated them during the past 3,000 years, leaving no
2249 observable traces. Taking into account the probability of language extinction, the breakup of
2250 the earliest Proto-Yeniseian language, one predating the form reconstructable on the basis
2251 of Ket and Kott, could conceivably have begun earlier than 3,000 ya.

2252 All Na-Dene languages share innovations demonstrating their equidistance from
2253 Yeniseian, whose split from the language ancestral to Na-Dene must be older than Proto-
2254 Na-Dene itself. To cite one particularly vivid example, Pre-Proto-Na-Dene restructured three
2255 of its inherited Dene-Yeniseian verb prefixes into the so-called classifier complex, for which
2256 the family is well known. All three component prefixes have cognates in Yeniseian but did
2257 not develop the characteristic function of transitivity increase and decrease found in all Na-
2258 Dene languages (Vajda 2016, 2017, 2018a). Contrary to Holton and Sicoli (2014), there is no
2259 linguistic evidence indicating a back migration into Asia of Yeniseian speakers from Beringia
2260 after Na-Dene had already begun to diversify.

2261 The evidence supporting Dene-Yeniseian so far appears asymmetrically stronger in
2262 the realm of shared morphology than in the lexicon (Nichols 2010). The number and
2263 specificity of homologies in verb structure on their own would seem to preclude a
2264 separation earlier than the Mid-Holocene. Given the low number of lexical cognates, the
2265 time depth of Dene-Yeniseian may be twice that of Na-Dene. So far, the number of
2266 proposed Dene-Yeniseian cognates, even if all of them are valid, is less than half the number
2267 shared between Tlingit and Athabaskan-Eyak. If the Dene-Yeniseian linguistic link is fully
2268 demonstrable, however, substantially more abundant evidence of lexical cognates should
2269 be expected to emerge as the sound correspondences shared between the two families are
2270 fully worked out, favoring a shallower time depth range in line with the morphological
2271 evidence. This would repeat the historiography of Athabaskan-Eyak-Tlingit comparative
2272 linguistic studies, whereby the family's striking parallels in verb morphology were
2273 successfully identified well in advance of the accumulation of a large enough body of
2274 cognates in basic vocabulary to support a full range of systematic sound correspondences
2275 between Tlingit and Athabaskan-Eyak and fully demonstrate the Na-Dene family.

2276 Though linguistic science can only rarely offer precise dates for prehistoric language
2277 splits, few linguists would claim it is not possible to distinguish a split that occurred two or
2278 three thousand years ago from one that is at least six or seven thousand years old. The
2279 evidence that can be brought to bear on the possible time depth of the lexical and
2280 grammatical homologies shared by Yeniseian and Na-Dene all point roughly to an Early to
2281 Mid-Holocene date of 9,000 to 7,000 ya as a plausible time depth for the breakup of Dene-
2282 Yeniseian. A separation date significantly earlier than 9,000 ya would be incompatible with
2283 generally accepted facts about language change, while a date significantly more recent than
2284 7,000 ya is contradicted by the fact that Na-Dene itself shows evidence of internal
2285 diversification that likely began at least 4,500 ya (Krauss 1976). Both the grammatical and
2286 lexical comparative data indicate that the Dene-Yeniseian connection is significantly deeper
2287 than Proto-Na-Dene but still detectable using the Comparative Method. The accumulated
2288 linguistic and genetic evidence preclude the possibility that the Dene-Yeniseian connection
2289 dates back to the original peopling of the Americas from a common Beringian population, or

2290 that the Yeniseians derive from a recent back migration from Alaska across Bering Strait.
2291 Rather, the connection of Dene-Yeniseian with the ASTt migration, first suggested explicitly
2292 by Dumond (2010) and Potter (2010), appears increasingly plausible. These early
2293 suggestions assumed a congruence between language, material culture, and genetics, and
2294 did not consider more complex admixture models.

2295 However, the language(s) of a prehistoric population can never be identified based
2296 on DNA studies alone, and pairing genetic and linguistic data to hypothesize about the
2297 language of the founding ASTt population yields at least four additional possibilities. The
2298 ASTt / Paleo-Eskimo people could have spoken a language that disappeared leaving no living
2299 descendants. A second possibility is that the material culture known as ASTt, along with
2300 related Siberian Neolithic groups, could reflect multiple populations speaking different
2301 languages, including Proto-Eskimo-Aleut, Proto-Na-Dene, Proto-Chukotko-Kamchatkan, and
2302 perhaps others. It is also possible that the Paleo-Eskimos spoke only Proto-Eskimo-Aleut and
2303 were responsible for introducing that family into the Americas five millennia ago. Eskimo-
2304 Aleut consists of a branch containing the closely related Eskimoan languages (Yup'ik,
2305 Iñiupiaq, etc.), probably separated at a depth of less than 2,500 years, and a more divergent
2306 Aleut branch. Krauss (1980:7) roughly estimates the split between Eskimoan and Aleut at
2307 about 4,000 ya, which, even with the inexactness of linguistic time depth estimations, would
2308 still roughly fit the scenario that the original Paleo-Eskimo founding population may have in
2309 fact spoken Proto-Eskimo-Aleut (Fortescue 2017). The Eskimo-Aleut family is less likely to
2310 descend from a language brought into North America during the Pleistocene than from a
2311 language brought from Asia after 5,000 ya, given the many typological, areal, and possibly
2312 deep genetic affinities it shares with Uralic, Yukaghir and other North Asian families that
2313 have long been noted by linguists (Fortescue 1998, 2017). The fourth possibility is that the
2314 ASTt population, which also shows a close genetic link to present-day Chukchi and Koryak
2315 peoples in the Russian Far East, could have spoken a language belonging to the Chukotko-
2316 Kamchatkan family, but which subsequently disappeared in North America, leaving living
2317 relatives only on the Asian side of Bering Strait. Within Chukotko-Kamchatkan, the Itelmen
2318 branch is quite divergent from the family's other branch, which contains Chukchi and Koryak
2319 – languages so similar that they could almost be regarded as dialects of a single language
2320 (Comrie 1981: 240). Estimating the age of this family as a whole, however, is hindered by
2321 the probability that the Itelmen and Chukchi-Koryak sub-branches mixed with different
2322 neighbor languages (Fortescue 1998: 210-213). The same could be argued for estimating the
2323 Aleut split with Eskimoan, as Aleut also shows possible signs of substrate admixture or at
2324 least of rapid phonological and morphological change (Fortescue 1998: 35-37), which could
2325 make the split appear older than it actually is. Chukotko-Kamchatkan and Eskimo-Aleut are
2326 both regarded as first-order families, not relatable to one another using the Comparative
2327 Method. A fully convincing demonstration of the Dene-Yeniseian linguistic hypothesis,
2328 however, would favor the scenario whereby Paleo-Eskimos brought a language directly
2329 ancestral to Proto-Na-Dene into Alaska, whether or not this was the only language spoken
2330 by bearers of the culture known as ASTt. The genetic link through Paleo-Eskimos between
2331 present-day Siberians (including Kets) and the population ancestral to Na-Dene speaking
2332 peoples appears to be the only physical connection between the two groups that falls within
2333 a time depth known to be recoverable by the Comparative Method.

2334 Table S14.1 below summarizes a plausible prehistoric scenario for the existence of a
2335 Dene-Yeniseian language link involving the Paleo-Eskimo arrival into Alaska 5,000 calBP
2336 from an earlier source in the Syalakh Culture (6,500 to 5,200 calBP) spreading eastward
2337 from Siberia.

2339 **Table S14.1. Chronology of Dene-Yeniseian linguistic diversification**

~5,900-6,700 ya – breakup of the Dene-Yeniseian proto-language in central-eastern Siberia (based on the coalescence date of Paleo-Eskimo ancestry shared between contemporary Siberians and Na-Dene-speaking populations, see Table S9.2); speakers of the language ancestral to Proto-Yeniseian remained in Siberia, where diversification of the known Yeniseian daughter languages is unlikely to predate 4,000 ya (based on lexicostatistic estimates).

~5,000 ya – language ancestral to Proto-Na-Dene, and possibly also the language ancestral to Eskimo-Aleut, brought into Alaska by Paleo-Eskimos (indexed by archaeological data).

after 5,000 ya – split between Tlingit and Athabaskan-Eyak (indexed by the coalescence date of Paleo-Eskimo genetic ancestry shared by contemporary Na-Dene peoples, see Table S9.2).

~3,400 to 3,000 ya – split between Eyak and Athabaskan (based on lexicostatistic estimates).

~2,700 to 2,200 ya – beginning of diversification and spread of Athabaskan languages (based on lexicostatistic estimates).

2340 Despite the shared Paleo-Eskimo genetic component in their speaker populations,
2341 the Dene-Yeniseian, Eskimo-Aleut, and Chukotko-Kamchatkan language families are not
2342 relatable to one another using the Comparative Method. Various deep connections have
2343 been proposed between Eskimo-Aleut, Uralic, and sometimes Yukaghiric and other Eurasian
2344 families (Fortescue 1998; see Campbell and Poser 2008 for a critique); however, even if any
2345 of these hypotheses are valid, the linguistic unity in question would greatly predate the
2346 spread of Middle Holocene cultures as well as the coalescence dates of the Paleo-Eskimo
2347 genetic ancestry shared by their speakers.

2348

2349 *References (for this section)*

- 2350 Alekseenko, E. A. K izucheniju mifologicheskikh paralelej medvezh'emu kul'tu ketov [Mythological parallels to
2351 the Ket Bear Cult]. *Sistemnye Issledovanija Vzaimosvjazi Drevnikh Kul'turr Sibiri i Severnoj Ameriki. Vypusk*
2352 *2: Dukhovnaja Kul'tura*. St. Petersburg: RAN, 22-46. (1995).
- 2353 Berezkin, Y. Sibirskij fol'klor i proiskhozhdenie na-dene [Siberian folklore and Na-Dene origins]. *Arkheologija,*
2354 *Ėtnografija i Antropologija Evrazii* **43.1**: 122-134. (2015)
- 2355 Campbell, L. *American Indian Languages: The Historical Linguistics of Native America*. Oxford: Oxford
2356 University Press (1997).
- 2357 Campbell, L. Review of "The Dene-Yeniseian Connection". *International Journal of American Linguistics* **77.3**,
2358 445-451 (2011).
- 2359 Campbell, L. *Historical Linguistics: An Introduction* (3rd edition). Cambridge, Mass.: MIT Press (2013).
- 2360 Campbell, L. & Poser, W. *Language Classification: History and Method*. Cambridge: Cambridge University Press.
2361 (2008).
- 2362 Comrie, B. *The Languages of the Soviet Union*. Cambridge: Cambridge University Press. (1981).
- 2363 Dul'zon, A. P. Ketskie toponimy Zapadnoj Sibiri [Ket toponyms of Western Siberia]. *Uchenye Zapiski Tomskogo*
2364 *Gosudarstvennogo Pedagogicheskogo Instituta [Scholarly Proceedings of Tomsk State Pedagogical*
2365 *Institute]* **18**, 91–111 (1959).
- 2366 Dul'zon, A. P. Byloe rasselenie ketov po dannym toponimiki [The former settlement of the Kets according to

- 2367 the facts of toponymy]. *Voprosy Geografii* **68**, 50–84 (1962).
- 2368 Dumond, D. The Dene arrival in Alaska. *The Dene-Yeniseian Connection*, ed. Kari, J., Potter, B. *Anthropological*
- 2369 *Papers of the University of Alaska: New Series* **5**, 335-346 (2010).
- 2370 Fortescue, M. *Language Relations Across Bering Strait: Reappraising the Archaeological and Linguistic*
- 2371 *Evidence*. London & New York: Cassell (1998).
- 2372 Fortescue, M. The relationship of Nivkh to Chukotko-Kamchatkan revisited. *Lingua* **121**: 1359-1376 (2011)
- 2373 Fortescue, M. Correlating Palaeo-Siberian language populations: Recent advances in the Uralo-Siberian
- 2374 Hypothesis. *Man in India*: **97.1**, 47-68 (2017).
- 2375 Golla, V. *California Indian Languages*. Berkeley, Los Angeles, London: University of California Press (2011).
- 2376 Heggarty, P, & Renfrew, C. The Americas: languages. *Cambridge World Prehistory*. Cambridge: Cambridge
- 2377 University Press, 1326-1353 (2014).
- 2378 Holton G, & Sicoli, M. 2014. Linguistic phylogenies support back-migration from Beringia to Asia. *PLoS ONE* **9.3**:
- 2379 e91722. doi:10.1371/journal.pone.0091722
- 2380 Kari, J. The concept of geolinguistic conservatism in Na-Dene prehistory. *The Dene-Yeniseian Connection*, ed.
- 2381 Kari, J., Potter, B. *Anthropological Papers of the University of Alaska: New Series* **5**, 194-222. (2010).
- 2382 Kari, J, & Potter, B. (Eds.). *The Dene-Yeniseian Connection. Anthropological Papers of the University of Alaska:*
- 2383 *New Series* **5**. Fairbanks, AK: ANLC (2010).
- 2384 Kaufman, T., & Golla, V. Language groupings in the New World: their reliability and usability in cross-
- 2385 disciplinary studies. *America Past, America Present: Genes and Languages in the Americas and Beyond*, ed.
- 2386 Renfrew, C. Cambridge: Macdonald Institute for Archaeological Research, 47-57 (2000).
- 2387 Krauss, M. Na-Dene. *Native Languages of the Americas*, vol. 1, ed. Sebeok, T. A. New York & London: Plenum
- 2388 Press, 283-358 (1976).
- 2389 Krauss, M. *Alaska Native Languages: Past, Present and Future*. Fairbanks, AK: ANLC (1980).
- 2390 Krauss, M. Athabaskan tone. *Athabaskan Prosody*, ed. Hargus, S., Rice, K, Amsterdam & New York: John
- 2391 Benjamins, 55-136 (2005).
- 2392 Leer, J. *Comparative Athabaskan Lexicon*: www.uaf.edu/anla/collections/ca/cal/ (2006).
- 2393 Leer, J. The palatal series in Athabaskan-Eyak-Tlingit with an overview of the basic sound correspondences. *The*
- 2394 *Dene-Yeniseian Connection*, ed. Kari, J., Potter, B. *Anthropological Papers of the University of Alaska: New*
- 2395 *Series* **5**, 168-193 (2010).
- 2396 McMahon, A, & McMahon, R. *Language Classification by Numbers*. Oxford: Oxford University Press (2005).
- 2397 Mühlenbernd, R., & Rama, T. What phoneme networks tell us about the age of language families. *Journal of*
- 2398 *Language Evolution* **2**, 67-76. (2017).
- 2399 Nichols, J. Proving Dene-Yeniseian genealogical relatedness. *The Dene-Yeniseian Connection*, ed. Kari, J.,
- 2400 Potter, B. *Anthropological Papers of the University of Alaska: New Series* **5**, 299-309 (2010).
- 2401 Pevnov, A. M. The problem of the localization of the Tungus-Manchu homeland. *Recent advances in Tungusic*
- 2402 *linguistics*, ed. A. Malchukov, Whaley, L. Wiesbaden: Harrassowitz, 17-40. (2012).
- 2403 Potter, B. Archaeological patterning in northeast Asia and northwest North America: an examination of the
- 2404 Dene-Yeniseian Hypothesis. *The Dene-Yeniseian Connection*, ed. Kari, J., Potter, B. *Anthropological Papers*
- 2405 *of the University of Alaska: New Series* **5**, 138-167 (2010).
- 2406 Ruhlen, M. The origin of the Na-Dene. *Proc. Natl. Acad. Sci. USA* **95**, 13994–13996 (1998).
- 2407 Starostin, G. Dene-Yeniseian and Dene-Caucasian: pronouns and other thoughts. *Working Papers in*
- 2408 *Athabaskan Languages* **8**. Fairbanks, AK: ANLC, 107-117 (2010).
- 2409 Starostin, S. A. Sravnitel'nyj slovar' enisejskikh jazykov [A comparative vocabulary of Yeniseian languages].
- 2410 *Ketskij Sbornik* vol. 4, Moscow: Vostochnaja Literatura, 176-315 (1995).
- 2411 Swadesh, M. Some new glottochronological dates for Amerindian linguistic groupings. *Proceedings of the 32nd*
- 2412 *International Congress of Americanists* 670-674 (1958).
- 2413 Trombetti, A. *Elementi di Glottologia*. Bologna: Nicola Zanichelli. pp. 486, 511 (1923).
- 2414 Vajda, E. *Yeniseian Peoples and Languages: A History of their Study with an Annotated Bibliography and a*
- 2415 *Source Guide*. Surrey, England: Curzon Press (2001).
- 2416 Vajda, E. Loanwords in Ket. *The Typology of Loanwords*, ed. Haspelmath, M., Tadmor, U. Oxford: Oxford
- 2417 University Press, 125–139 (2009).
- 2418 Vajda, E. Siberian link with Na-Dene languages. *The Dene-Yeniseian Connection*, ed. Kari, J., Potter,
- 2419 B. *Anthropological Papers of the University of Alaska: New Series* **5**, 33–99 (2010a).
- 2420 Vajda E. Yeniseian, Na-Dene, and historical linguistics. *The Dene-Yeniseian Connection*, ed. Kari, J., Potter, B.
- 2421 *Anthropological Papers of the University of Alaska: New Series* **5**, 100–118 (2010b).
- 2422 Vajda, E. Vestigial possessive morphology in Na-Dene and Yeniseian. *Working Papers in Athabaskan (Dene)*
- 2423 *Languages 2012*. (Alaska Native Language Center Working Papers No. 11). Fairbanks: ANLC, 79-91 (2013).
- 2424 Vajda, E. Dene-Yeniseian. *Oxford Research Encyclopedia of Linguistics*. Oxford Online (2016).

- 2425 Vajda, E. Patterns of innovation and retention in templatic polysynthesis. *Handbook of Polysynthesis*, ed.
2426 Fortescue, M, Mithun, M., Evans, N. Oxford: Oxford University Press, 363-391 (2017).
2427 Vajda, E. Dene-Yeniseian: progress and unanswered questions. *Diachronica* 35.2: 277-295 (2018a).
2428 Vajda, E. Yeniseian and Athapaskan toponyms. *Language and Toponymy in Alaska and Beyond*. (2018b).
2429 Werner, H. *Zur jenseits-indianischen Urverwandtschaft [Yeniseian and Native American Relatedness]*.
2430 Wiesbaden: Harrassowitz (2004).
2431 Werner, H. *Die Jenisej-Sprachen des 18. Jahrhunderts [Yeniseian Languages of the 18th Century]*. Wiesbaden:
2432 Harrassowitz (2005).
2433

2434 **Supplementary Discussion**

2435 The time and place of the Eskimo-Aleut founder admixture event remains uncertain. Under
2436 our demographic model, the admixture event that is shared by all members of this lineage
2437 was dated by two independent methods, *ALDER* and *Rarecoal*, at 2,700-4,900 ya and 4,400-
2438 4,900 ya, respectively (Fig. 2b, Supplementary Information section 12), and involved a
2439 substantial (~55-62%) genetic contribution from a Northern First Peoples population distantly
2440 related to Athabaskans (Fig. 2). There is no clear archaeological evidence for a Native
2441 American back-migration to Chukotka^{1,2}, increasing the weight of evidence that this
2442 admixture event occurred in Alaska. Indeed, the Alaskan Peninsula and Kodiak Archipelago
2443 have long been suggested as a source of influences shaping the Neo-Eskimo material
2444 culture^{3,4} (Fig. 3b). Some of the earliest maritime adaptations in Beringia and America are
2445 encountered in this region associated with the Ocean Bay tradition (~6,800 – 4,500 calBP)^{5,6}.
2446 Around 4,000 calBP, the Ocean Bay tradition was succeeded by the Early Kachemak tradition,
2447 which is seen as a dramatic departure from the preceding phase, with some archaeological
2448 evidence for contacts with the Paleo-Eskimo Arctic Small Tool tradition⁶. Given the new
2449 genetic results, it seems possible that this cultural discontinuity is associated with the
2450 emergence of the ancestral Eskimo-Aleut population. Early Paleo-Eskimo people used marine
2451 resources on a seasonal basis only, depended for the most part on hunting caribou and
2452 muskox, and lacked sophisticated hunting gear that allowed the later Inuit to become
2453 specialized in whaling⁷. It is conceivable that a transfer of cultural traits and gene flow
2454 between Paleo-Eskimos and First Peoples happened simultaneously.

2455 An important further clue is given by our finding that the ancestors of Inuit/Yup'ik
2456 experienced bidirectional gene flow with Chukotko-Kamchatkan ancestors, while Aleuts did
2457 not. This is consistent with a scenario of PPE/First Peoples admixture in Alaska, and a
2458 subsequent migration of Aleut ancestors into the Aleutian Islands (Fig. 3b), which might
2459 have occurred around 4,000 calBP according to known discontinuities in the Aleutian
2460 archaeological record (the onset of the Margaret Bay phase, which saw an influx of ASTt and
2461 Kodiak elements⁸). Conversely, ancestors of Inuit and Yup'ik migrated back to Chukotka,
2462 where around 2,200 calBP they established the earliest culture securely assigned
2463 archaeologically and genetically to Neo-Eskimos⁹, i.e. the Old Bering Sea culture^{10,11},
2464 admixed with local populations, most likely in interior Chukotka, and re-expanded from
2465 there to Alaska and later throughout the American Arctic. The Thule expansion was likely
2466 driven by innovations in hunting and the food surplus created by whaling. The oldest Old
2467 Bering Sea individual in this study was dated to ~1,500-1,900 calBP, which also overlaps our
2468 estimated time of the bidirectional admixture between Inuit/Yup'ik ancestors and
2469 Chukotko-Kamchatkan-speaking groups (~1,700-2,300 ya).

2470 A succession of western Alaskan cultures, namely the Old Whaling, Choris, Norton,
2471 and Ipiutak (with the earliest dates around 3,100, 2,700, 2,500, and 1,700 calBP,
2472 respectively), combined cultural influences from earlier local Paleo-Eskimo sources as well
2473 as sources in Chukotka and southwestern Alaska^{3,12}. Parallels between these cultures and
2474 subsequent Neo-Eskimos are notable³, and they might represent partial links between the
2475 founding population at 4,800 ya and the Old Bering Sea culture at 2,200 calBP (Fig. 3b). The
2476 location and source populations for early Eskimo-Aleuts will likely be resolved if future
2477 analyses can include samples from these western Alaskan traditions, as well from the Ocean
2478 Bay and Kachemak traditions in southwestern Alaska.

2479 The descendants of the proto-Paleo-Eskimo lineage speak widely different

2480 languages, belonging to the Chukotko-Kamchatkan, Eskimo-Aleut, and Na-Dene families.
 2481 Based on lexicostatistical studies of languages surviving in the 20th century, the time depth
 2482 of the former two families is likely shallow, and the Na-Dene family is probably much older,
 2483 on the order of 5,000 years (Supplementary Information section 13). Thus, while the
 2484 linguistic affiliation of Paleo-Eskimos is impossible to determine from genetic data, the
 2485 finding that the most diverse linguistic group whose speakers carry large proportions of PPE
 2486 ancestry is Na-Dene and that Na-Dene linguistic variation may reach back to the Paleo-
 2487 Eskimo period suggests that proto-Na-Dene may have been spoken by a Paleo-Eskimo
 2488 population. A Siberian linguistic connection was proposed for the Na-Dene family under the
 2489 Dene-Yeniseian hypothesis^{13,14}. This hypothetical language macrofamily unites Na-Dene
 2490 languages and Ket, the only surviving remnant of the Yeniseian family, once widespread in
 2491 South and Central Siberia^{15,16}. Although the Dene-Yeniseian family is not universally
 2492 accepted among historical linguists^{17,18}, and correlations between linguistic and genetic
 2493 histories are far from perfect, evidence of a genetic connection between Siberian and Na-
 2494 Dene populations mediated by Paleo-Eskimos suggests that future research should further
 2495 explore Dene-Yeniseian as a genealogical family¹⁴ or as part of a wider clade¹⁸.

2496 *References (for this section)*

- 2497 1. Potter, B. A. Archaeological patterning in Northeast Asia and Northwest North America: an examination of
 2498 the Dene-Yeniseian hypothesis. *The Dene-Yeniseian Connection*, ed. Kari, J., Potter, B. A. *Anthropological*
 2499 *Papers of the University of Alaska: New Series* 5, 138–167 (2010).
- 2500 2. Hoffecker, J. F. & Elias, S. A. *Human Ecology of Beringia*. New York: Columbia University Press (2007).
- 2501 3. Dumond, D. E. Norton hunters and fisherfolk. *The Oxford Handbook of the Prehistoric Arctic*, ed. Friesen, T.
 2502 M., Mason, O. K. New York: Oxford University Press. 395–416 (2016).
- 2503 4. Ackerman, R. E. Early maritime traditions in the Bering, Chukchi, and East Siberian seas. *Arctic Anthropol.*
 2504 35, 247–262 (1998).
- 2505 5. Fitzhugh, B. The origins and development of Arctic maritime adaptations in the Subarctic and Arctic
 2506 Pacific. *The Oxford Handbook of the Prehistoric Arctic*, ed. Friesen, T. M., Mason, O. K. New York: Oxford
 2507 University Press. 253–278 (2016).
- 2508 6. Steffian, A., Saltonstall, P. & Yarborough, L. F. Maritime economies of the central Gulf of Alaska after 4000
 2509 B.P. *The Oxford Handbook of the Prehistoric Arctic*, ed. Friesen, T. M., Mason, O. K. New York: Oxford
 2510 University Press. 303–322 (2016).
- 2511 7. Hoffecker J. F. *A Prehistory of the North: human settlement of the higher latitudes*. Rutgers University
 2512 Press (2004).
- 2513 8. Davis, R., Knecht, R. & Rogers, J. First Maritime Cultures of the Aleutians. *The Oxford Handbook of the*
 2514 *Prehistoric Arctic*, ed. Friesen, T. M., Mason, O. K. New York: Oxford University Press. 279–302 (2016).
- 2515 9. Raghavan, M. *et al.* The genetic prehistory of the New World Arctic. *Science* 345, 1255832 (2014).
- 2516 10. Mason, O. K. The Old Bering Sea florescence about Bering Strait. *The Oxford Handbook of the Prehistoric*
 2517 *Arctic*, ed. Friesen, T. M., Mason, O. K. New York: Oxford University Press. 417–442 (2016).
- 2518 11. Bronshtein, M. M., Dneprovsky, K. A. & Savintsky, A. B. Ancient Eskimo cultures of Chukotka. *The Oxford*
 2519 *Handbook of the Prehistoric Arctic*, ed. Friesen, T. M., Mason, O. K. New York: Oxford University Press.
 2520 469–488 (2016).
- 2521 12. Darwent, C. M. & Darwent, J. The enigmatic Choris and Old Whaling cultures of the Western Arctic. *The*
 2522 *Oxford Handbook of the Prehistoric Arctic*, ed. Friesen, T. M., Mason, O. K. New York: Oxford University
 2523 Press. 371–394 (2016).
- 2524 13. Ruhlen, M. The origin of the Na-Dene. *Proc. Natl. Acad. Sci. USA* 95, 13994–13996 (1998).
- 2525 14. Vajda, E. J. Siberian link with Na-Dene languages. *The Dene-Yeniseian Connection*, ed. Kari, J., Potter, B. A.
 2526 *Anthropological Papers of the University of Alaska: New Series* 5, 33–99 (2010).
- 2527 15. Dul'zon, A. P. Byloe rasselenie Ketov po dannym toponimiki [The former settlement of the Kets according
 2528 to the facts of toponymy]. *Voprosy Geografii* 68, 50–84 (1962).
- 2529 16. Vajda, E. J. Loanwords in Ket. *The Typology of Loanwords*, ed. Haspelmath, M., Tadmor, U. Oxford:
 2530 Oxford University Press, 125–139 (2009).
- 2531 17. Campbell, L. Review of 'The Dene-Yeniseian Connection', ed. by James Kari and Ben A. Potter. *Int. J. Am.*
 2532 *Linguistics* 77, 445–451 (2011).
- 2533 18. Starostin, G. Dene-Yeniseian: a critical assessment. *J. Language Relationship* 8, 117–138 (2012).